The Diverse Chemistry of Some Tungsten Nitrosyl Complexes

by

Diana Fabulyak

B.Sc., The University of British Columbia, 2014

A THESIS SUBMITTED IN PARTIAL FULFILLMENT OF

THE REQUIREMENTS FOR THE DEGREE OF

MASTER OF SCIENCE

in

THE FACULTY OF GRADUATE AND POSTDOCTORAL STUDIES

(Chemistry)

THE UNIVERSITY OF BRITISH COLUMBIA

(Vancouver)

March 2017

Abstract

The η^5-$C_5H_4{}^iPr$ ligand imparts unprecedented effects on the physical and chemical properties of (η^5-$C_5H_4{}^iPr$)W(NO)(CH_2CMe_3)(η^3-CH_2CHCMe_2) (**2.3**) and its precursors. Specifically, the reaction of (η^5-$C_5H_4{}^iPr$)W(NO)$(CO)_2$ (**2.1**) with PCl_5 results in the formation of the PCl_3 adduct of the (η^5-$C_5H_4{}^iPr$)W(NO)Cl_2 complex. Moreover, the subsequent metathesis reaction with the $Mg(CH_2CH{=}CMe_2)_2$ binary reagent occurs at the P-Cl bond of the adduct affording (η^5-$C_5H_4{}^iPr$)W(NO)($PCl_2CMe_2CH{=}CH_2$)Cl_2 (**2.4**). The investigation of the unique effects of the η^5-$C_5H_4{}^iPr$ ligand on the chemistry of tungsten-nitrosyl complexes has been extended to encompass (η^5-$C_5H_4{}^iPr$)W(NO)(H)(η^3-CH_2CHCMe_2) (**3.1**), (η^5-$C_5H_4{}^iPr$)W(NO)$(CH_2CMe_3)_2$ (**3.7**), and *trans*-(η^5-$C_5H_4{}^iPr$)W(NO)(H)(κ^2-$PPh_2C_6H_4$) (**3.9**). Results of these studies are summarized in following paragraphs.

Trapping reactions of the coordinatively unsaturated reactive intermediates, formed via intramolecular isomerization of **3.1**, using PMe_3 show a preferential isomerization to the η^1 intermediate (η^5-$C_5H_4{}^iPr$)W(NO)(H)(η^1-$CH_2CH{=}CMe_2$), isolable as its PMe_3 adduct. Increasing the temperature facilitates the intramolecular rearrangement to the desired η^2-alkene intermediate, but due to the thermal instability of the starting material, the C-H activation of alkanes cannot be carried out at very high temperatures.

The reaction of **3.7** with H_2 and PPh_3 shows instantaneous *cis* to *trans* isomerization of the generated ortho-metallated complex to form an inert *trans*-(η^5-$C_5H_4{}^iPr$)W(NO)(H)(κ^2-$PPh_2C_6H_4$) (**3.9**). In this case, the faster rate of *cis* to *trans* isomerization hinders the C-H activation potential of the ortho-metallated product.

In addition, results of the investigation of the multiple C-H activation chemistry of (η^5-C_5Me_5)W(NO)(CH_2CMe_3)$_2$ (**4.1**) are presented. Thermolysis of **4.1** in neat hydrocarbons results in elimination of neopentane and formation of the transient (η^5-C_5Me_5)W(NO)(=$CHCMe_3$) complex, which subsequently effects the multiple C-H activations of linear *n*-alkanes. The corresponding (η^5-C_5Me_5)W(NO)(H)(η^3-allyl) complexes obtained from the reactions with various *n*-alkanes have been isolated and characterized. These thermolysis reactions are accompanied by the generation of alkenes. Attempts to improve the production of olefins by varying different experimental factors have been investigated.

The preliminary results of the investigation of the C-C coupling reactivity of (η^5-C_5Me_5)W(NO)(H)(η^3-allyl) complexes with aldehydes and phenylacetylene are presented. Thermolysis reactions of (η^5-C_5Me_5)W(NO)(H)(η^3-allyl) complexes with aldehydes under aerobic conditions result in the formation of the corresponding coupled alcohol product. Also, thermolysis reactions of (η^5-C_5Me_5)W(NO)(H)(η^3-CH_2CHCMe_2) with phenylacetylene reveal incorporation of phenylacetylene molecules into the (η^5-C_5Me_5)W(NO) and (η^5-C_5Me_5)W(NO)(H)(η^3-CH_2CHCMe_2) fragments.

Preface

Some of the work presented in this thesis has resulted from collaboration with other researchers. Collection, solution, and refinement of the X-ray diffraction data for most solid-state molecular structures has been performed by Dr. Brian Patrick. The collection of data and solution of the solid-state molecular structure of **2.5** has been done by Dr. Rhett A. Baillie.

In Chapter 4, the theoretical investigation of the reactivity of **4.1** and its molybdenum analogue using *n*-pentane as a representative alkane substrate has been carried out by Dr. Guillaume P. Lefèvre. The detailed analysis of the olefin production by GC-FID analysis of octenes has been carried out by Monica V. Shree using the experimental method developed by Joseph M. Clarkson.

Table of Contents

List of Tables

List of Figures

List of Schemes

List of Abbreviations

Å	Angstrom; 10^{-10} m
anal	analysis
APT	attached proton test
ca	about (Latin circa)
calcd.	calculated
$^{13}C\{^{1}H\}$	carbon-13 proton-decoupled
cm	centimeters
cm^{-1}	wavenumbers
COSY	correlated spectroscopy
d	doublet (spectral); days (time)
D	deuterium, ^{2}H
dd	doublet of doublets
ddd	doublet of doublets of doublets
deg	degree
EA	elemental analysis
EI	electron impact
Et_2O	diethyl ether
EtOAc	ethyl acetate
eV	electronvolt
equiv.	equivalent
FT-IR	Fourier transform infrared
g	gram

^{1}H	hydrogen; proton
HMBC	heteronuclear multiple-bond correlation
HR	high resolution
HSQC	heteronuclear single quantum coherence
Hz	Hertz
*i*Pr	*iso*-propyl
IR	infrared
J	scalar coupling constant
L	litre
LR	low resolution
m	multiplet (spectral)
M	molarity; mol/L
M^{+}	parent molecular ion
MALDI	matrix-assisted laser desorption/ionization
Me	methyl; CH_3
MHz	Megahertz
min	minute
mL	millilitre
mmol	millimole
mol	mole
MS	mass spectrum
m/z	mass-to-charge ratio
NMR	nuclear magnetic resonance

nPr	*n*-propyl
o	ortho
^{31}P	phosphorus-31 proton-decoupled
Ph	phenyl; C_6H_5
ppm	parts per million
r.t.	room temperature
s	singlet (NMR), strong signal (IR), second (time)
sept	septet (spectral)
t	triplet (spectral), time
THF	tetrahydrofuran
TOF	time of flight
UV	Ultra Violet
º	degree (of angle or temperature)
β	beta
δ	chemical shift in ppm
η	hapticity
κ	kappa
π	pi orbital
σ	sigma orbital
σ*	sigma antibonding orbital
ν	stretching frequency

Acknowledgements

First I would like to thank Prof. Peter Legzdins for his support and guidance. Thank you for believing in me and teaching me many valuable science and life lessons. It is an honour to be a part of the Legzdins family.

Thank you to my parents Lyuba and Paul. Without your love, support and understanding none of this would have been possible.

I would like to thank current and past group members with whom I had a pleasure of working during my undergraduate and graduate studies. Special thanks to Monica V. Shree for always being there for me. I will forever cherish our memories together; you are my didi for life. Thank you to Taleah Levesque for helping me with the tedious editing process, and Aaron Holmes for good lunchtime laughs.

Thanks to the UBC Chemistry department facilities staff who helped me along the way. Particularly, Dr. Brian Patrick of the X-ray Crystallography facility for always trying to help me solve my research conundrums, Marshall Lapawa of the Mass Spectrometry facility for fun and educational chats, and Dr. Maria Ezhova of the NMR facility for helping with my NMR analyses.

Special thanks to The Dow Chemical Company for providing funding that made this work possible.

Dedication

This thesis is dedicated to my grandmother Evgenia.

Chapter 1: Introduction

1.1 Hydrocarbons

Alkanes are among the major components of natural gas and petroleum, yet they are not utilized to their full potential in synthesis as raw materials.[1] Instead, they are extensively exploited for their energy content by combustion.[2] The difficulty of expanding the range of alkane applications in the chemical industry is based on the inherent inertness of these compounds. The C-C and C-H bonds of alkanes are very strong with dissociation energies of 377-460 kJ mol^{-1}, they have low polarity and lack nucleophilic or electrophilic reactive sites, which makes them relatively unreactive.[3] Their old name "paraffins", from the Latin *parum affinis* (without affinity), describes perfectly the complications associated with exploiting alkanes as starting materials for synthesis of other valuable chemicals.[4] Addition of other functional groups to alkanes would offer essential reactive sites for their further transformation. One particularly appealing method of functionalization of alkanes is a conversion to olefins, which are traditionally produced from steam cracking of naphtha, light diesel and other oil by-products.[5,6] However, these processes are highly energy demanding, showing low selectivity to production of terminal olefins.

The use of transition metals for the activation and functionalization of alkanes is a fundamental area of research which explores potential applications of these molecules as starting materials. Additionally, utilization of transition metals can provide better control of selectivity that otherwise is hard to achieve under more forcing conditions.

1.2 C-H activation

The C-H bond activation by organometallic complexes is the first step toward the more ambitious goal of functionalization of unsaturated hydrocarbons. Labinger and Bercaw have divided C-H activation reactions into five different subtypes.[2] First is the oxidative addition process which involves electron donation from the C-H σ bond to the empty d_{z2} orbital, and the reinforcing back-donation interaction during which electron density from the tungsten d_{xz} or d_{yz} orbital is donated into the C-H σ* anti-bonding orbital (Figure 1.1). Both of these interactions weaken the C-H bond, resulting in its cleavage. This mode of reactivity is typical for complexes containing electron-rich transition metal centres. Both the hydrogen atom and the alkyl group in this reaction are incorporated on the metal resulting in an increase in the metal oxidation state by two.

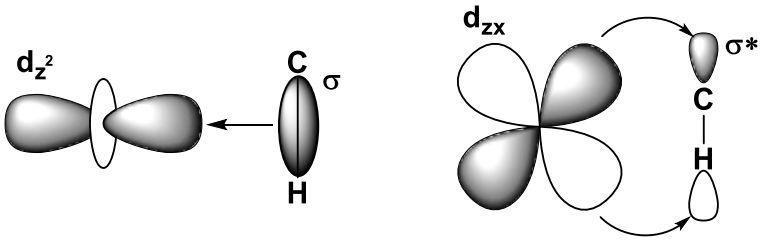

Figure 1.1. Orbital interactions involved in the oxidative addition of a C-H bond at the metal centre.

In 1982 two research groups reported the intramolecular C-H activation of saturated hydrocarbons by iridium complexes (Scheme 1.1).[7,8] Once irradiated with UV light, Bergman's iridium dihydride complex (η^5-C_5Me_5)Ir(H)$_2$(PMe_3) in cyclohexane loses H_2 and generates the

reactive 16e intermediate. Subsequently this complex effects the C-H activation of the substrate, and forms the corresponding (η^5-C_5Me_5)Ir(PMe_3)(H)(C_6H_{11}).[7] Similarly, Graham's (η^5-C_5Me_5)Ir$(CO)_2$ complex in neopentane loses CO upon UV light irradiation, and effects C-H activation of the substrate.[8]

Scheme 1.1. Examples of intramolecular C-H activation reported by a) Bergman and b) Graham

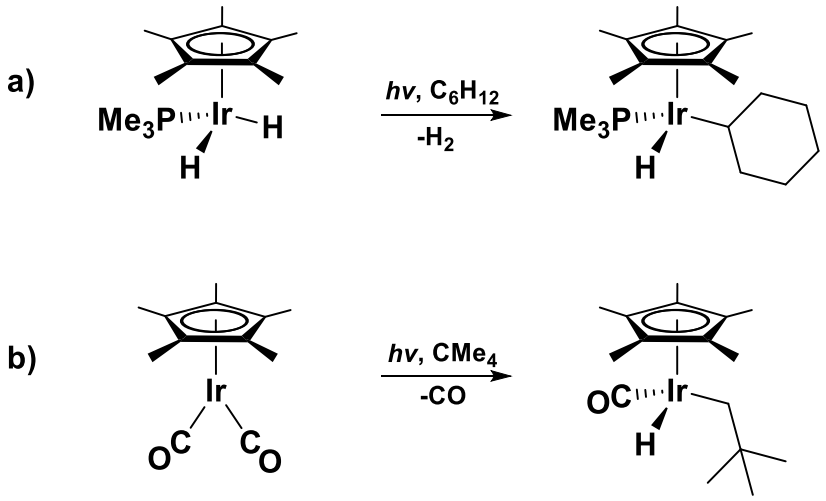

σ-bond metathesis is another type of C-H activation reaction typically exhibited by the electron-poor transition metals in groups 3-5 with d^0 electron configurations. These reactions proceed via a four-centred, four-electron transition state without any changes in the oxidation state of the metal centre in the overall transformation.[9] Metalloradical C-H activations are catalyzed by rhodium(II) porphyrin complexes which exist in a monomer-dimer equilibrium. The C-H activation of a substrate results in the attachment of two fragments of the bond to two separate monomeric complexes.[2] In 1,2-addition reactions the alkane is added across a metal-

heteroatom double bond.[2] Lastly, in electrophilic activations products of the C-H activation reaction are functionalized alkanes rather than new organometallic complexes.[2]

1.3 Alkane Functionalization: Dehydrogenation

Olefins are among the most important key building blocks in synthesis.[5,6] They have a broad spectrum of derivatives composing a vast majority of valuable chemicals used in different industries. Notably, ethylene is the most produced petrochemical in the world. It is also a starting material for 1,2-dichlorethane, ethylene oxide, and styrene which are used in the production of polymers valuable in the packaging, textile, and construction industries.[5,6]

The first stoichiometric homogeneous transfer dehydrogenation of cyclic alkanes was reported by Crabtree in 1979. In the presence of tert-butylethylene (TBE), which functions as a hydrogen acceptor, $[IrH_2(acetone)_2(PPh_3)_2][BF_4]$ dehydrogenates cyclopentane and cyclooctane (COA) to cyclopentadienyl (Cp) and cyclooctadienyl (COD) complexes, respectively (Scheme 1.2).[10] Similar iridium bis(trialkylphosphine) complexes have demonstrated catalytic acceptorless dehydrogenation of COA with turnover numbers (TON) below 100 due to thermal instability of the catalyst.[10]

Scheme 1.2. Stoichiometric transfer dehydrogenation of cyclic alkanes initiated by $[IrH_2(acetone)_2(PPh_3)_2][BF_4]$

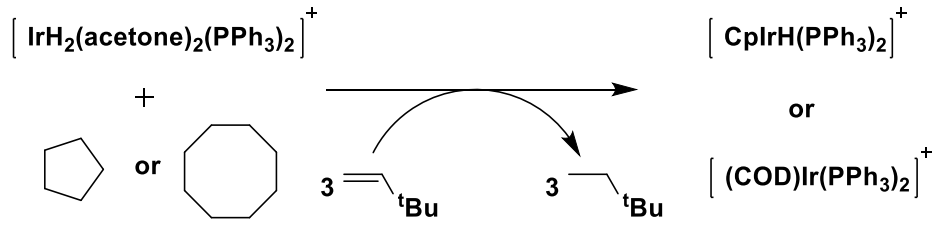

Dehydrogenation is inherently a highly endothermic reaction, and requires thermal stability of the catalyst to effect the desired transformation.[5] Pincer-ligated complexes have demonstrated good thermal stability due to the rigid tridentate binding mode of the ligand resulting in a strong M-C σ bond.

The first iridium pincer-ligated catalyst precursor for alkane dehydrogenation (^{tBu4}PCP)IrH_2 [^{R}PCP = κ^3-C_6H_3-2,6-$(CH_2PR_2)_2$] was introduced by Jensen and Kaska in 1996.[11] This complex has demonstrated a great thermal stability. It can effectively mediate homogeneous transfer dehydrogenation of COA in the presence of a small amount of TBE affording 82 turnovers per hour at 150 ºC.[11,12] The mechanism of transfer dehydrogenation by pincer-ligated iridium catalysts has been studied extensively by Goldman and coworkers.[11]

Scheme 1.3. Proposed mechanism of *n*-alkane/TBE transfer dehydrogenation by (^{tBu4}PCP)IrH$_2$

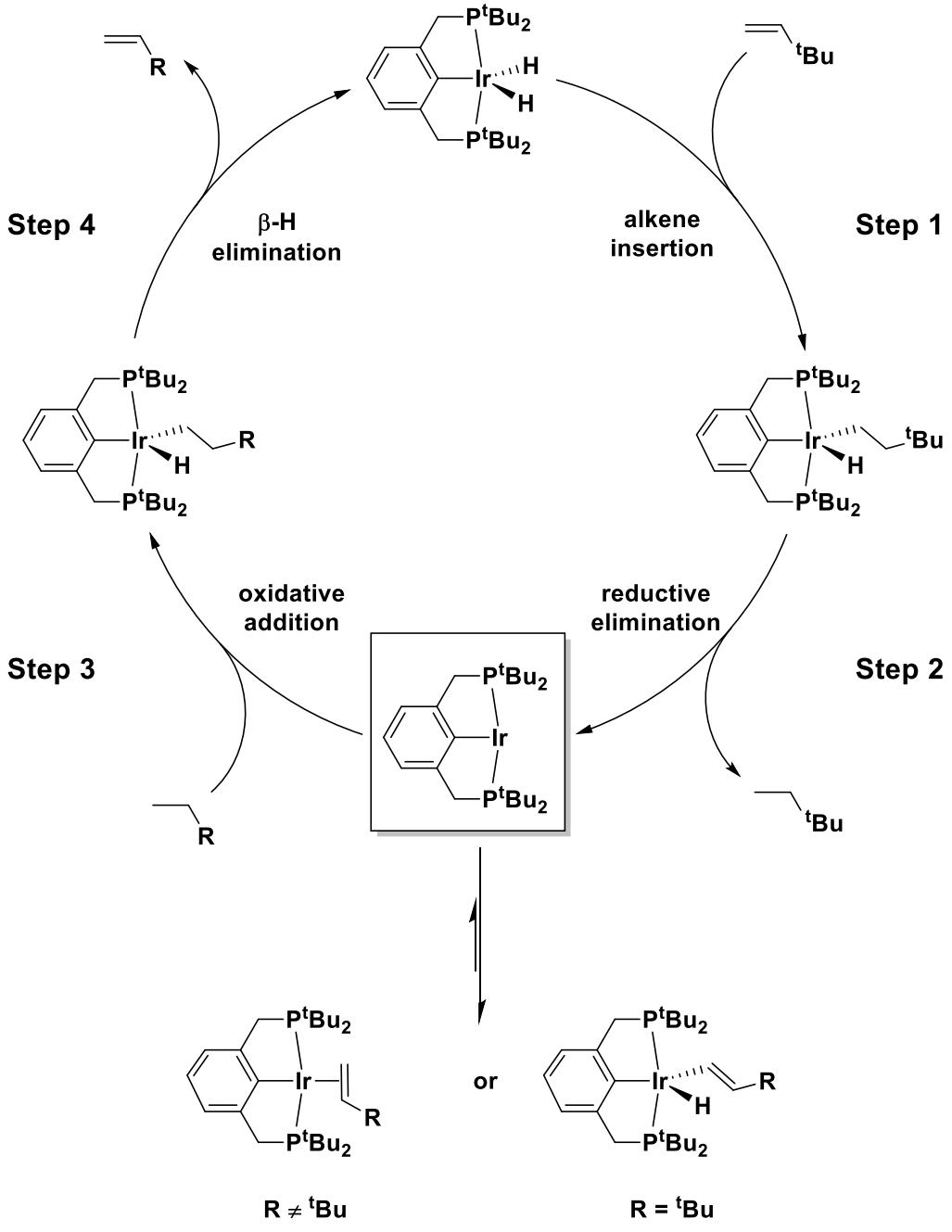

The mechanism of *n*-alkane/TBE transfer dehydrogenation is outlined in Scheme 1.3. The reactive 14e reactive species (^{tBu4}PCP)Ir is generated upon insertion of TBE into the Ir-H

bond of (^{tBu4}PCP)IrH_2 (step 1), and the subsequent reductive elimination of tert-butylethane (TBA) (step 2). Afterwards, (^{tBu4}PCP)Ir undergoes oxidative addition of the substrate (step 3) followed by the β-H elimination (step 4), which results in alkene release and the regeneration of the dihydride complex. The reactivity of the catalyst can be inhibited by the olefin binding to the coordinatively unsaturated (^{tBu4}PCP)Ir complex either by π-coordination (dehydrogenated product) or by C-H addition (TBE).[11]

A series of effective solid-phase catalysts with different (PCP)Ir motifs have been developed for heterogeneous transfer dehydrogenation of gas-phase alkanes in the presence of ethylene or propene as a hydrogen acceptor (Scheme 1.4).[13] Unlike other heterogeneous systems utilizing metal oxides on various support systems (e. g. dehydrogenation of propane over WO_x-VO_x/SiO_2 with TOF of 8.3 mmol/s/mol VO_x)[14], pincer-ligated iridium complexes are the first purely molecular solid-phase catalysts utilized for transfer dehydrogenation.[5] (^{iPr4}PCP)Ir(C_2H_4), in particular, demonstrates extremely high rates of dehydrogenation of *n*-pentane (over 1000 turnovers after 180 min per 1 mM of catalyst). These results are unprecedented even for solution-phase transfer dehydrogenation. These systems also show great selectivity for formation of terminal alkenes.

Scheme 1.4. Dehydrogenation of *n*-pentane by solid-phase molecular (^{iPr4}PCP)Ir(C_2H_4)

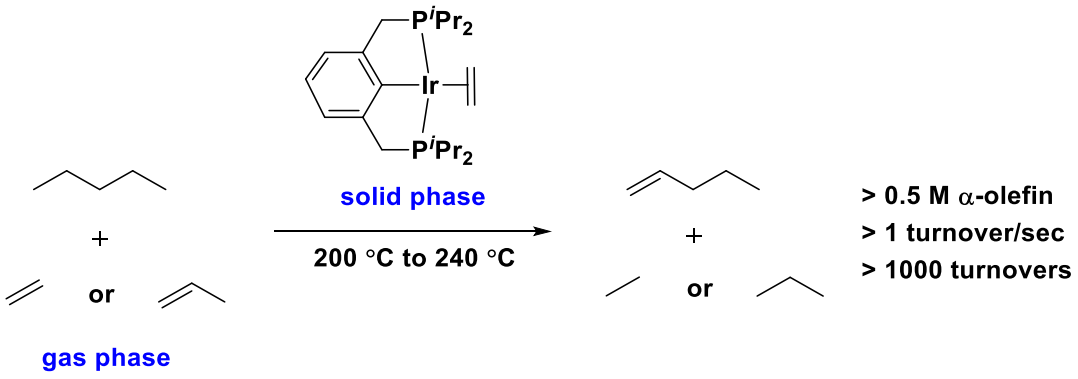

Alkylidene complexes have been also considered in dehydrogenation studies. Generation of transition metal alkylidene complexes via intramolecular elimination of neopentane was first reported by Schrock in 1974. Reaction of $Ta(CH_2{}^tBu)_3Cl_2$ with 2 equivalents of $LiCH_2{}^tBu$ generates an alkylidene complex namely $Ta{=}CH{}^tBu(CH_2{}^tBu)_3$.[15] The first reported example of intermolecular C-H activation of alkanes via addition across a metal-carbon bond of an alkylidene ligand has been demonstrated in our group using a reactive (η^5-C_5Me_5)W(NO)$(CH_2CMe_3)_2$ complex.[16] The chemistry of this system will be discussed in great detail later in the text.

Scheme 1.5. Synthesis and reactivity of (PNP)Ti=CH^{t}Bu(CH$_2{}^t$Bu)

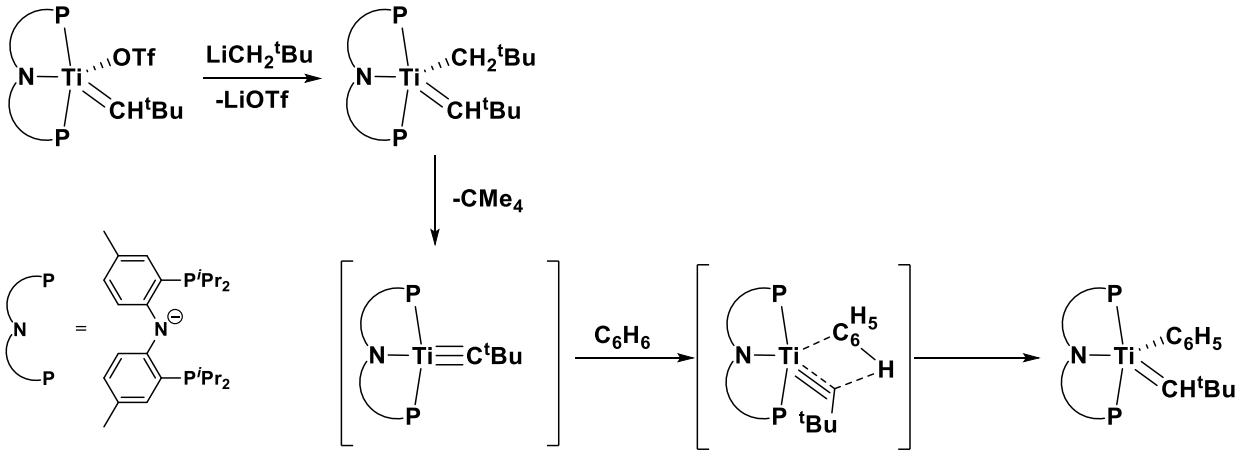

Mindiola and coworkers have utilized titanium complexes containing pincer and alkylidene moieties to effect C-H activation (Scheme 1.5).[17] Under mild conditions (PNP)Ti=CH^{t}Bu(CH$_2{}^t$Bu) (PNP$^-$ = *N*[2-P(CHMe$_2$)$_2$-4-methylphenyl]$_2^-$) undergoes elimination of neopentane generating the transient reactive titanium alkylidyne intermediate (PNP)Ti≡C^{t}Bu. This complex undergoes subsequent 1,2-CH bond addition of benzene across a triple bond forming (PNP)Ti=C^{t}Bu(C_6H_5). Based on kinetic, mechanistic, and theoretical studies, the C-H

activation of the substrate is a pseudo-first order reaction with respect to the organometallic reactant. The α-H abstraction from the neopentylidene complex is the rate-determining step.[18]

Scheme 1.6. Dehydrogenation of ethane by transient (PNP)Ti≡C^{t}Bu complex

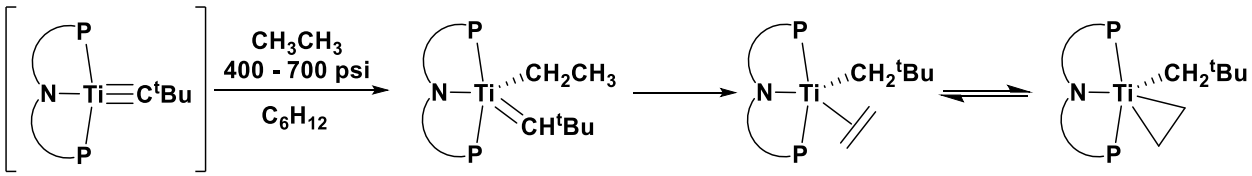

The C-H activation chemistry of this complex has been extended to sp^3 C-H activation of various substrates including methane.[19] The reaction of the titanium alkylidyne complex with ethane results in stepwise α-C-H bond activation followed by metal-mediated β-H migration forming the η^2-ethylene complex (PNP)Ti(η^2-H_2C=CH_2)($CH_2{}^t$Bu) (Scheme 1.6). In reactions of titanium-olefin complexes with C_2-C_8 alkanes, dehydrogenation of the substrate is observed along with the formation of (PNP)Ti(η^2-H_2C=CHR)($CH_2{}^t$Bu) type complexes with R = H, CH_2, CH_2CH_3, *n*-propyl, *n*-butyl, *n*-pentyl, and *n*-hexyl. Release of the dehydrogenated product occurs under thermolytic conditions with decomposition of the organometallic product or by exposing the η^2-olefin complex to oxidants (e.g. N_2O, N_3P, and $N_2Ctolyl_2$). At the present time this dehydrogenation of *n*-alkanes is stoichiometric.[20]

1.4 Legzdins Group C-H Activation Chemistry

1.4.1 Thermal C-H Activation of (η^5-C_5Me_5)W(NO)(η^3-allyl)(CH_2CMe_3) Complexes

C-H activation reactivity of the family of the 18-electron (η^5-C_5Me_5)W(NO)(CH_2CMe_3)(η^3-allyl) complexes (η^3-allyl = η^3-CH_2CHCMe_2, η^3-$CH_2CHCHMe$, and η^3-$CH_2CHCHPh$) has been extensively investigated in the Legzdins group.[21,22,23] Thermolysis of the reaction mixtures of these complexes in excess hydrocarbon substrate results in the formation of the 16-electron η^2-diene or/and η^2-allene intermediate complexes upon the loss of neopentane. The neopentyl ligand has been utilized as an alkyl group due to its propensity to undergo intramolecular α-H abstraction reactions. The intermediate complexes have never been detected using classic spectroscopic techniques, but their 18-electron PMe_3 adducts have been isolated and characterized. Another piece of evidence for this reaction pathway has been obtained using deuterium labelling studies, which reveal that upon activation of a C-D bond of the substrate, deuterium is incorporated into the η^2-allene or η^2-diene ligand (Scheme 1.7).[21]

Scheme 1.7. Thermal generation of the η^2-allene and η^2-diene intermediates and subsequent C-H activation of benzene-d_6

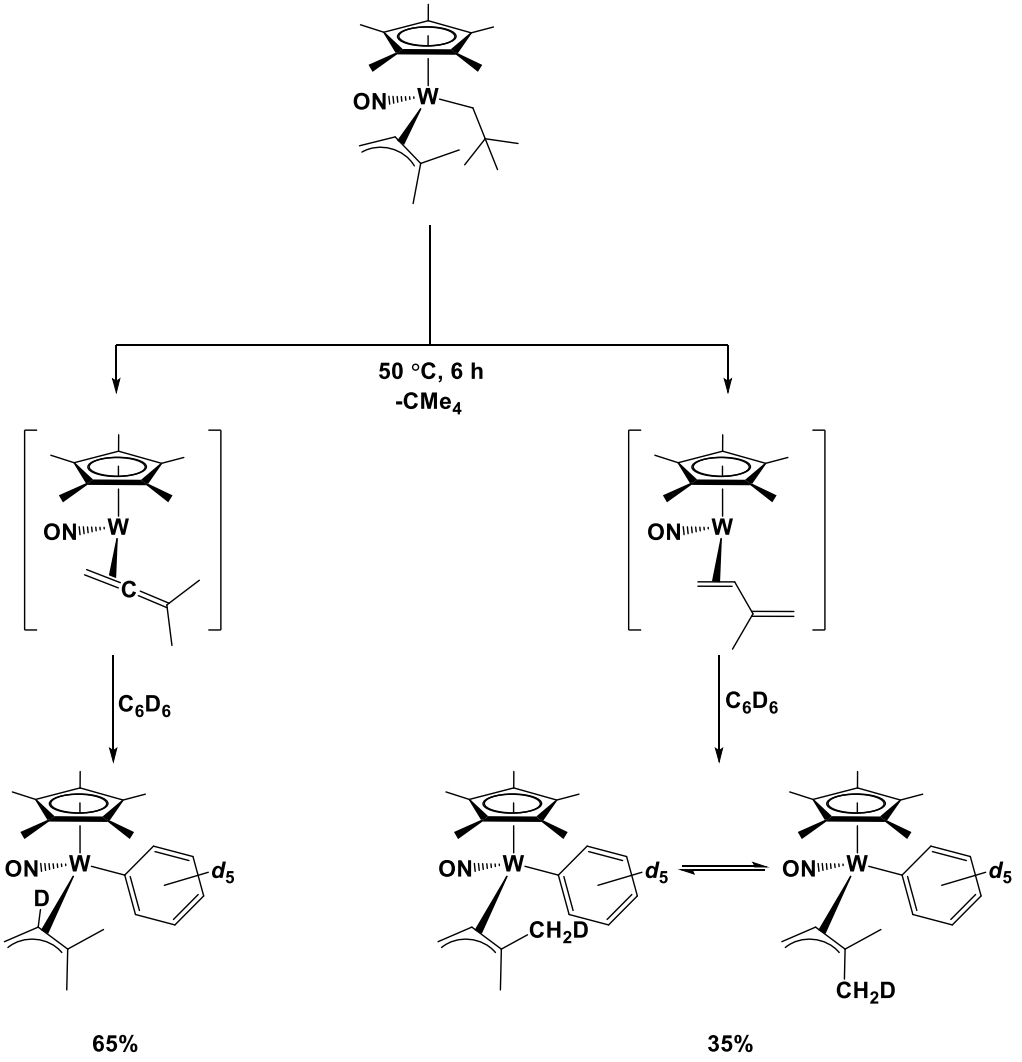

The η^2-allene and η^2-diene intermediates can effect C-H activations of R-H (R = alkyl, aryl) substrates in three different ways depending on the nature of the allyl ligand, the hydrocarbon substrate, the substituents on the cyclopentadienyl ligand, and the employed experimental conditions.[24] The first one is the single C-H bond activation, which affords η^1-hydrocarbyl- or η^1-aryl-η^3-allyl complexes. Thus, under ambient conditions (η^5-C_5Me_5)W(NO)(CH_2CMe_3)(η^3-$CH_2CHCHMe$) loses neopentane and forms the η^2-diene

intermediate complexes, which then effects the terminal C-H activation of *n*-pentane (Scheme 1.8).[24]

Scheme 1.8. Generation of the η^2-diene intermediate under ambient conditions, and subsequent multiple C-H activation of *n*-pentane

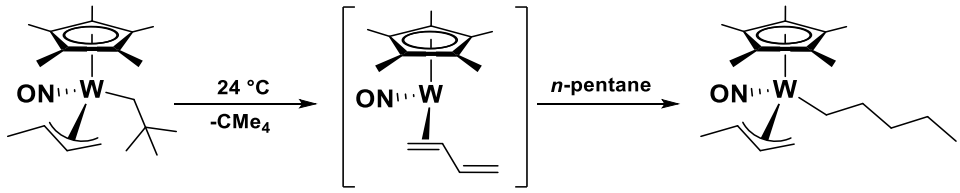

Alternatively, when this complex is exposed to arenes, the second mode of reactivity is observed. Following the single C-H bond activation of the substrate, an intramolecular exchange of the η^1-aryl ligand with the hydrogen on the η^3-allyl ligand occurs resulting in formation of the metal hydride complex (Scheme 1.9).[24] The last reaction pathway of thermal reactivity of the (η^5-C_5Me_5)W(NO)(CH_2CMe_3)(η^3-allyl) complexes involves multiple C-H bond activations of the substrate. For example, thermolysis of (η^5-C_5Me_5)W(NO)(CH_2CMe_3)(η^3-CH_2CHCMe_2) in *n*-pentane at 55 ºC for 6 h leads to the formation of the new (η^5-C_5Me_5)W(NO)(H)(η^3-C_5H_9) complex and loss of the original allyl ligand (Scheme 1.10).[22]

Scheme 1.9. C-H activation of benzene effected by the η^2-diene intermediate, and the subsequent aryl-hydrogen exchange

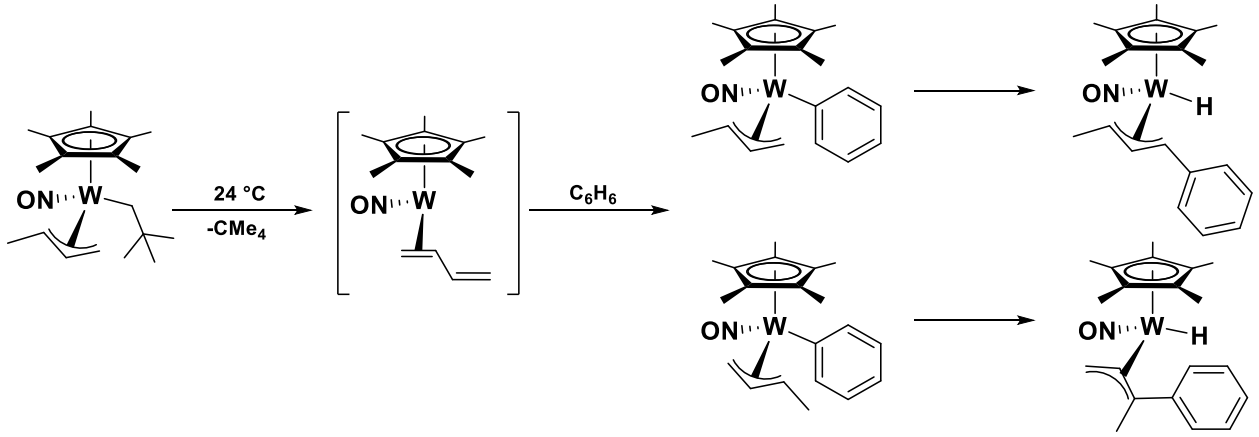

Scheme 1.10. Multiple C-H activation of *n*-pentane by (η^5-C_5Me_5)W(NO)(CH_2CMe_3)(η^3-CH_2CHCMe_2)

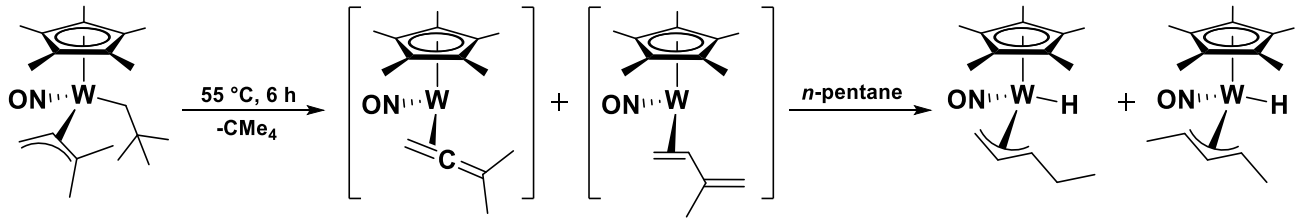

The C-D activation of C_6D_6 by (η^5-$C_5H_4{}^iPr$)W(NO)(CH_2CMe_3)(η^3-CH_2CHCMe_2) has also been investigated and compared to that exhibited by its η^5-C_5Me_5, η^5-C_5Me_4H, and η^5-$C_5Me_4{}^nPr$ analogues.[25] Kinetic analyses of the analogous C-D activations have established that the presence of the η^5-$C_5H_4{}^iPr$ ligand significantly increases the rate of the reaction, an outcome that can be attributed primarily to electronic factors.[25] In addition, mechanistic studies have established that in solution this complex loses neopentane under ambient conditions to generate exclusively the 16e η^2-diene intermediate complex, (η^5-$C_5H_4{}^iPr$)W(NO)(η^2-CH_2=CMeCH=CH_2),

which then effects the subsequent C-D activations. The 18e PMe_3 adducts of the η^2-diene intermediate have been isolated (Scheme 1.11).[25]

Nitric oxide is a strong π-acceptor ligand that contributes to the stabilization of metal centres in low oxidation states.[24] The strength of the N-O bond, reflected in its IR-stretching frequency, has been utilized for the comparison of electronic environments at the metal centres in complexes containing different cyclopentadienyl ligands.[25]

Scheme 1.11. Thermolysis of (η^5-$C_5H_4{}^iPr$)W(NO)(CH_2CMe_3)(η^3-CH_2CHCMe_2) in C_6D_6 in the presence of PMe_3

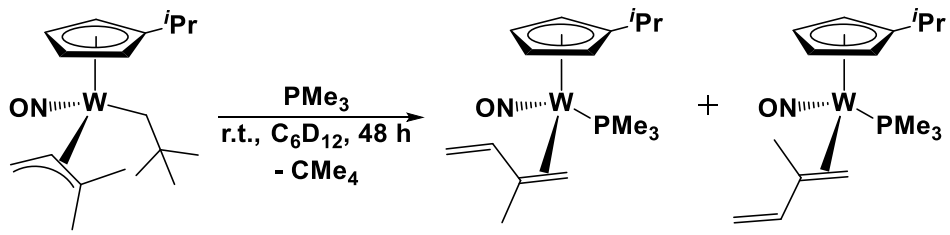

To put these results into perspective, it may be noted that the analogous (η^5-C_5Me_5)W(NO)(CH_2CMe_3)(η^3-CH_2CHCMe_2) complex forms both 16e η^2-allene and η^2-diene intermediates upon thermolysis.[21,25] Formation of the η^2-diene intermediate complex via loss of neopentane has a calculated activation barrier of 168.0 kJ mol^{-1} that is higher in energy than the activation barrier for the alternative allene pathway (147.8 kJ mol^{-1}).[26] Consistently, the 16e (η^5-C_5Me_5)W(NO)(η^2-CH_2=C=CMe_2) complex is the dominant intermediate for subsequent C-H activation reactions initiated by the η^5-C_5Me_5 system, and it has also been isolated as its 18e PMe_3 adduct.[21] Results of the trapping reaction involving (η^5-$C_5H_4{}^iPr$)W(NO)(CH_2CMe_3)(η^3-CH_2CHCMe_2) as well as the labeling studies with benzene-d_6 suggest that the η^5-$C_5H_4{}^iPr$ ligand

inverts the energy levels of the intermediate complexes such that the η^2-diene intermediate is now the principal species that effects the subsequent C-H activations.

1.4.2 Thermal C-H Activation Chemistry of $(\eta^5\text{-}C_5Me_5)W(NO)(CH_2CMe_3)_2$

Thermolysis of $(\eta^5\text{-}C_5Me_5)W(NO)(CH_2CMe_3)_2$ in neat hydrocarbons results in elimination of neopentane and formation of the transient $(\eta^5\text{-}C_5Me_5)W(NO)(=CHCMe_3)$ intermediate complex, which subsequently effects C-H activations of substrates. This intermediate is inferred based on trapping reactions with a Lewis base affording the $(\eta^5\text{-}C_5Me_5)W(NO)(=CHCMe_3)(PMe_3)$, and labelling reactions utilizing benzene-d_6 as a substrate.[16] This neopentylidene complex effects single C-H activations of tetramethylsilane, benzene, and substituted arenes; also multiple C-H activations of cyclohexane even in the presence of PMe_3 have been reported (Scheme 1.12). Interestingly, thermolysis of $(\eta^5\text{-}C_5Me_5)W(NO)(CH_2CMe_3)_2$ in neat methylcyclohexane results in multiple C-H activations of the substrate and formation of the $(\eta^5\text{-}C_5Me_5)W(NO)(H)(\eta^3\text{-}C_7H_{11})$ hydride complex. Similarly, thermolysis of $(\eta^5\text{-}C_5Me_5)W(NO)(CH_2CMe_3)_2$ in neat ethylcyclohexane affords $(\eta^5\text{-}C_5Me_5)W(NO)(H)(\eta^3\text{-}C_8H_{13})$.[27]

Scheme 1.12. Thermal chemistry of (η^5-C_5Me_5)W(NO)(=CHCMe$_3$) generated by thermolysis of (η^5-C_5Me_5)W(NO)(CH_2CMe_3)$_2$

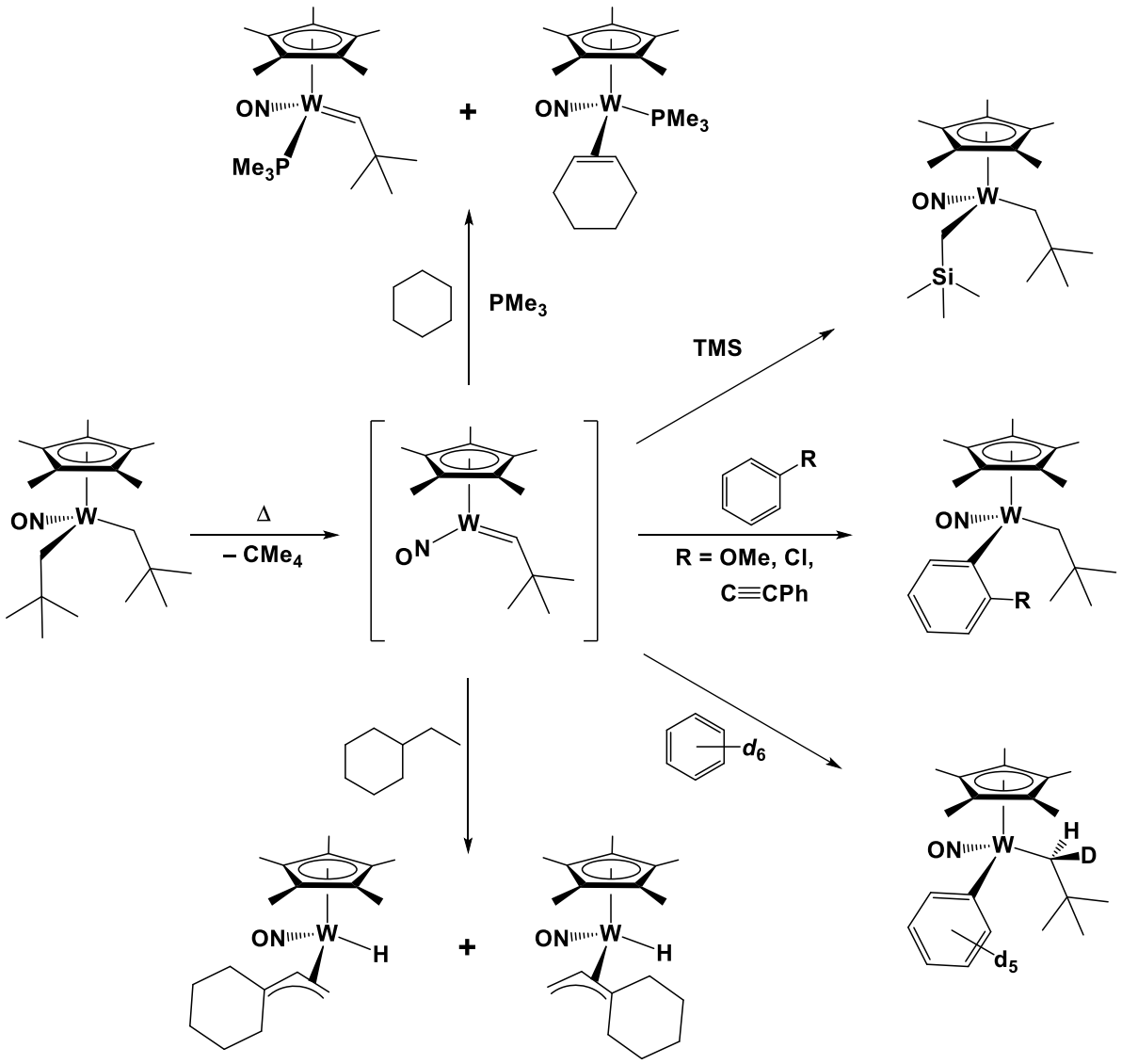

1.5 Scope of This Thesis

The first question addressed in this thesis is the effect of the η^5-$C_5H_4{}^iPr$ ligand on the chemical reactivity of various tungsten-nitrosyl complexes. Can the η^5-$C_5H_4{}^iPr$ ligand exert similar beneficial kinetic effects on the C-H activation reactivity in other tungsten-nitrosyl

systems? What other chemical differences can result from the substitution of η^5-C_5Me_5 with the η^5-$C_5H_4{}^iPr$ ligand? Is there a better, more efficient methodology for synthesis of (η^5-$C_5H_4{}^iPr$)W(NO)(CH_2CMe_3)(η^3-CH_2CHCMe_2), which has been shown to be outstanding in effecting the C-H activation of arenes?[25]

The second question addressed in this thesis is related to the thermal chemistry of the (η^5-C_5Me_5)W(NO)(CH_2CMe_3)$_2$ complex. Since thermolyses of (η^5-C_5Me_5)W(NO)(CH_2CMe_3)$_2$ in neat methylcyclohexane or ethylcyclohexane result in multiple C-H activations of the substrates and formation of the (η^5-C_5Me_5)W(NO)(H)(η^3-C_7H_{11}) and (η^5-C_5Me_5)W(NO)(H)(η^3-C_8H_{13}) hydride complexes, respectively, is it possible to extend these reactions to linear *n*-alkanes?[27] Would a new allyl-hydride complex, obtained from the multiple C-H activations of alkanes, be prone to effect subsequent multiple C-H activation of substrate (releasing the original allyl ligand as an olefin)? Is there a possibility of obtaining an acceptorless dehydrogenation catalyst?

Chapter 2 presents an improved synthetic methodology for obtaining (η^5-$C_5H_4{}^iPr$)W(NO)(CH_2CMe_3)(η^3-CH_2CHCMe_2), and exceptional effects of the η^5-$C_5H_4{}^iPr$ ligand on the reactivity of its precursors. Unprecedented reactivity of the (η^5-$C_5H_4{}^iPr$)W(NO)(CO)$_2$ with PCl_5 is outlined. Interesting features of complexes both in solution and in the solid state are also discussed.

Chapter 3 discusses synthesis of the novel (η^5-$C_5H_4{}^iPr$)W(NO)(H)(η^3-CH_2CHCMe_2) complex and considers its thermal reactivity in comparison to its η^5-C_5Me_5 analogue. Insights into thermally-generated intermediates are provided via trapping reactions of the unsaturated reactive intermediates with PMe_3. In addition, the synthesis and thermal chemistry of *trans*-(η^5-$C_5H_4{}^iPr$)W(NO)(H)(κ^2-$PPh_2C_6H_4$) are presented and compared to the corresponding η^5-C_5Me_5 analogue.

Chapter 4 presents results of multiple C-H activations of linear alkanes by (η^5-C_5Me_5)W(NO)(CH_2CMe_3)$_2$. Investigation of alkene formation in this reaction is discussed. Detailed analysis and characterization of the organometallic products obtained in the reaction are summarized. Studies of multiple C-H activations are also extended to encompass the (η^5-$C_5H_4{}^i$Pr)W(NO)(CH_2CMe_3)$_2$ analogue.

Chapter 5 presents the preliminary investigation of the chemistry of allyl-hydride complexes with aldehydes and phenylacetylene in hopes of synthesizing C-C coupled organic products.

Chapter 6 presents the overall summary and conclusion of the research results discussed in this thesis along with suggestions for potential future research directions.

Chapter 2: Unique Effects of the η^5-$C_5H_4{}^{i}Pr$ Ligand[†]

[†] A version of this chapter has been published. Fabulyak, D.; Baillie, R. A.; Patrick, B. O.; Legzdins, P.; Rosenfeld, D. C. *Inorg. Chem.* **2016**, *55*, 1883-1893. Reprinted with permission from Inorganic Chemistry. Copyright (2016) American Chemical Society.

2.1 Introduction

The η^5-$C_5H_4{}^iPr$ ligand imparts distinctive physical and chemical properties to (η^5-$C_5H_4{}^iPr$)W(NO)(CH_2CMe_3)(η^3-CH_2CHCMe_2) and its precursors. The C-H activations of aromatic substrates initiated by (η^5-$C_5H_4{}^iPr$)W(NO)(CH_2CMe_3)(η^3-CH_2CHCMe_2) occur at a markedly faster rate than those initiated by the analogous systems having a cyclopentadienyl ligand with different substituents.[25] Based on the beneficial kinetic effects on the C-H activations imparted by the η^5-$C_5H_4{}^iPr$ ligand, a more efficient methodology for synthesis of (η^5-$C_5H_4{}^iPr$)W(NO)(CH_2CMe_3)(η^3-CH_2CHCMe_2) has been developed.

2.2 Results and Discussion

2.2.1 Synthesis of (η^5-$C_5H_4{}^iPr$)W(NO)$(CO)_2$ (2.1)

(η^5-$C_5H_4{}^iPr$)W(NO)$(CO)_2$ (**2.1**) can be synthesized on a large scale and in good yields by starting with the reaction of $W(CO)_6$ with Na[$C_5H_4{}^iPr$]. Thermolysis of this mixture in THF affords Na[(η^5-$C_5H_4{}^iPr$)W$(CO)_3$] which is then nitrosylated at ambient temperatures using an equimolar amount of *N*-methyl-*N*-nitroso-*p*-toluenesulfonamide in THF for one day (Scheme 2.1). The analogous nitrosylation of Na[(η^5-C_5H_5)W$(CO)_3$] is complete within 30 minutes under identical experimental conditions.[28] Attempts to isolate **2.1** by recrystallization or sublimation have to date been unsuccessful. Ultimately, column chromatography on a silica column support has been utilized to isolate this complex as an analytically pure orange oil in 61% yield.

Scheme 2.1. Synthesis of 2.1

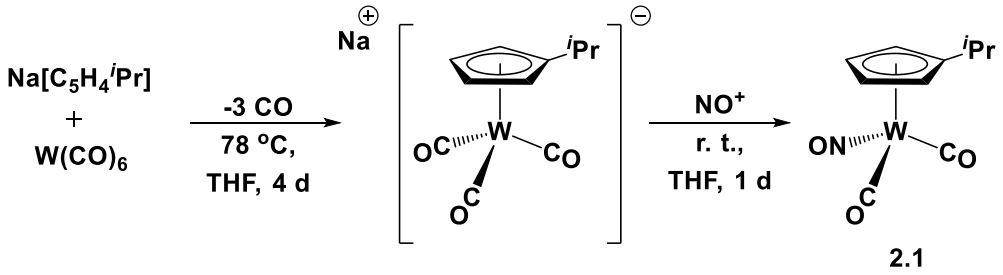

The fact that **2.1** is a liquid at ambient temperatures is the most surprising physical property of the complex. However, there is no obvious steric effect to explain why it is a liquid at room temperature. The analogous complex with the sterically smaller η^5-C_5H_5 ligand, and complexes with the more sterically demanding cyclopentadienyl ligands (η^5-C_5Me_4H, η^5-C_5Me_5, η^5-$C_5Me_4{}^n$Pr) are all solids under ambient conditions. In other words, **2.1** with its η^5-$C_5H_4{}^i$Pr ligand is unique in this family of compounds.

2.2.2 Synthesis of (η^5-$C_5H_4{}^i$Pr)W(NO)I_2 (2.2)

(η^5-$C_5H_4{}^i$Pr)W(NO)I_2 (**2.2**) can be prepared by treatment of **2.1** in toluene with an equimolar amount of I_2 (Scheme 2.2). The final product is recrystallized from a 1:1 mixture of toluene and pentane at -30 °C overnight to obtain a dark brown solid. The final product is purified via pentane washes, and **2.2** is isolated in excellent yield.

Scheme 2.2. Synthesis of 2.2

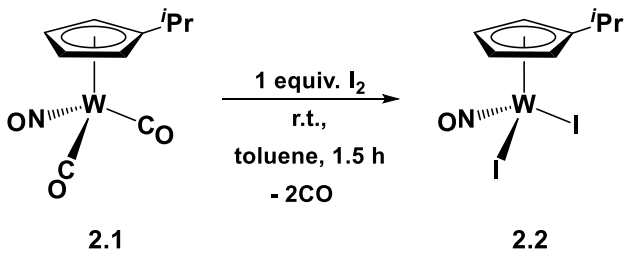

2.1 2.2

The solution IR spectrum of **2.2** in CH_2Cl_2 exhibits a strong absorption band at 1650 cm^{-1}, which is higher than the corresponding NO-stretching frequency of the analogous $(\eta^5\text{-}C_5Me_5)W(NO)I_2$ complex (1630 cm^{-1}).[29] Interestingly, the IR spectrum of solid **2.2** as a Nujol mull exhibits two strong absorptions at 1610 cm^{-1} and 1637 cm^{-1} that can be assigned to symmetric and asymmetric NO-stretching frequencies of the iodo-bridged dimeric form of the complex. The solid-state molecular structure of the similar $[(\eta^5\text{-}C_5Me_5)Mo(NO)Cl_2]_2$ dimer has been previously reported.[30]

2.2.3 Synthesis of $(\eta^5\text{-}C_5H_4{}^i\text{Pr})W(NO)(CH_2CMe_3)(\eta^3\text{-}CH_2CHCMe_2)$ (2.3)

The synthesis of $(\eta^5\text{-}C_5H_4{}^i\text{Pr})W(NO)(CH_2CMe_3)(\eta^3\text{-}CH_2CHCMe_2)$ (**2.3**) from **2.2** can be effected reliably by the sequential addition of stoichiometric amounts of $Mg(CH_2CMe_3)_2$ and $Mg(CH_2CH{=}CMe_2)_2$ (Scheme 2.3). Thermally sensitive **2.3** is isolable as an analytically pure yellow liquid (again a unique property for a member of this family of compounds) from the final reaction mixture by column chromatography on basic alumina using Et_2O as the eluant. Its infrared nitrosyl-stretching frequency is 1599 cm^{-1}, which is considerably higher in energy than the 1546 cm^{-1} exhibited by the analogous $(\eta^5\text{-}C_5Me_5)W(NO)(CH_2CMe_3)(\eta^3\text{-}CH_2CHCMe_2)$.[21]

This feature is again a manifestation of the presence of the less electron-donating η^5-$C_5H_4{}^iPr$ ligand in **2.3**. ^{1}H NMR spectroscopy indicates that **2.3** exists as a single isomer in solution, the *meso H* signal of the allyl ligand having a relatively upfield chemical shift of 3.93 ppm which is characteristic of the allyl ligand being in an *exo* orientation.[31]

Scheme 2.3. Synthesis of 2.3

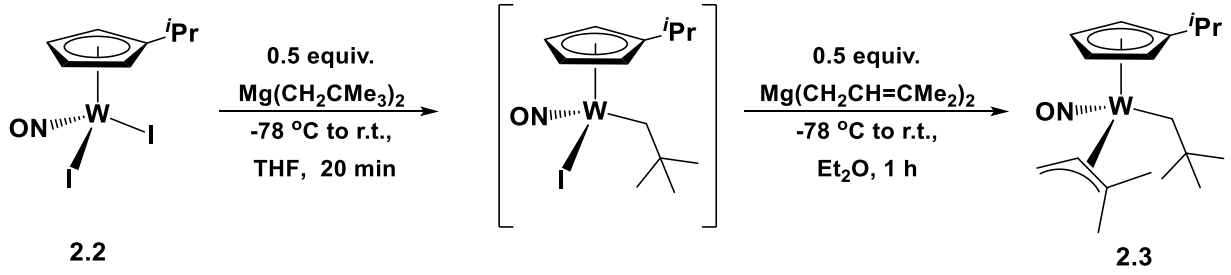

2.2 **2.3**

During the undergraduate thesis project, kinetic analyses of the C-H activations effected by various alkyl-allyl systems have established that the presence of the η^5-$C_5H_4{}^iPr$ ligand significantly increases the rate of the reaction ($k = 1.21(5) \times 10^{-3}$) s^{-1}.[25] In comparison, the analogous systems with more electron-donating ligands η^5-C_5Me_4H, η^5-C_5Me_5, and η^5-$C_5Me_4{}^nPr$ have reaction rate constants of $1.876(8) \times 10^{-4}$ s^{-1}, $2.2(1) \times 10^{-4}$ s^{-1}, and $1.864(6) \times 10^{-4}$ s^{-1} respectively.[21,25] Such outcomes can be attributed to a combination of steric and electronic factors.

Complex **2.3** can also be prepared from **2.1** via an initial reaction with PCl_5 followed by sequential salt metatheses reactions with $Mg(CH_2CMe_3)_2$ and $Mg(CH_2CH{=}CMe_2)_2$ following a similar procedure used in the synthesis of the analogous η^5-C_5Me_5 complex.[32] However, for this methodology to be even slightly successful, the first and final reactions must be effected in Et_2O and the second step must be performed in THF, with the solvent being removed in vacuo after

each step. Nevertheless, this synthetic route has proven to be very inconsistent and affords the desired alkyl-allyl product only in very low yields. As outlined in the next section, the problem appears to be that the initial reaction with PCl_5 with **2.1** does not produce the expected (η^5-$C_5H_4{}^iPr$)W(NO)Cl_2 but rather its PCl_3 adduct.

2.2.4 Unprecedented Formation of the PCl_3 Adduct of the (η^5-$C_5H_4{}^iPr$)W(NO)Cl_2

Treatment of Cp'W(NO)$(CO)_2$ [Cp' = η^5-C_5Me_5 or η^5-C_5H_5] compounds with PCl_5 in Et_2O is generally a convenient way to prepare Cp'W(NO)Cl_2 complexes since the desired organometallic products precipitate from the final reaction mixtures.[30] However, the reaction of **2.1** with an equimolar amount of PCl_5 affords a teal solution in Et_2O from which no tractable solid product can be isolated.

(η^5-C_5Me_5)W(NO)(CH_2CMe_3)(η^3-CH_2CHCMe_2) can be prepared from (η^5-C_5Me_5)W(NO)Cl_2 via sequential salt metatheses reactions with 0.5 equivalents of $Mg(CH_2CMe_3)_2$ and $Mg(CH_2CH{=}CMe_2)_2$ binary reagents. This synthetic route generates an unstable 16e intermediate (η^5-C_5Me_5)W(NO)(CH_2CMe_3)Cl, which is typically not isolated before proceeding with the second metathesis reaction. Due to difficulties encountered during synthesis of the analogous (η^5-$C_5H_4{}^iPr$) complex, 0.5 equivalents of $Mg(CH_2CH{=}CMe_2)_2$ have been added directly to the reaction mixture obtained after the reaction of **2.1** with PCl_5 in order to generate a more stable 18e intermediate, namely (η^5-$C_5H_4{}^iPr$)W(NO)(η^3-CH_2CHCMe_2)Cl.

Surprisingly, addition of the $Mg(CH_2CH{=}CMe_2)_2$ binary reagent results in the formation of (η^5-$C_5H_4{}^iPr$)W(NO)$(PCl_2CMe_2CH{=}CH_2)Cl_2$ (**2.4**), an observation that suggests that the initial product formed in the reaction of **2.1** and PCl_5 is (η^5-$C_5H_4{}^iPr$)W(NO)$(PCl_3)Cl_2$ (Scheme 2.4).

Scheme 2.4. Synthesis of 2.4

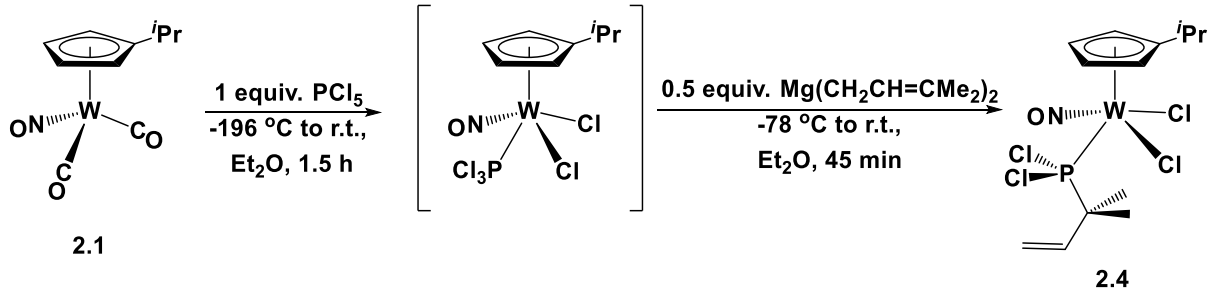

Complex **2.4** has been characterized both in solution and in the solid state. Recrystallization of **2.4** from 1:1 THF:pentane at -33 °C for one week affords yellow crystals suitable for a single-crystal X-ray diffraction analysis. In the solid state **2.4** exists as the two positional isomers, **2.4a** and **2.4b**, whose molecular structures are shown in Figures 2.1 and 2.2, respectively. Both isomers are four-legged piano-stool molecules capped by η^5-$C_5H_4{}^iPr$ ligands in which the two chloro ligands are situated *cis* to each other, as are the nitrosyl and phosphine ligands. The nitrosyl ligands are linear and the W-P bond lengths are similar to those extant in analogous four-legged piano-stool molecules.[26,31] As expected, the W-Cl bonds in **2.4a** and **2.4b** *trans* to the σ-donating $PCl_2CMe_2CH{=}CH_2$ ligands are longer than the W-Cl linkages *trans* to the nitrosyl ligands. This observation is the manifestation of the π-accepting nature of the nitrosyl ligand, which results in a stronger W-Cl bond. Both positional isomers have an alkyl substituent on the phosphorus atom positioned away from the η^5-$C_5H_4{}^iPr$ ligand, minimizing steric interactions between the bulky ligands. In addition, the isopropyl substituent on the cyclopentadienyl ligand is pointing away from the $PCl_2CMe_2CH{=}CH_2$ ligand creating a more sterically favoured conformation of the complex.

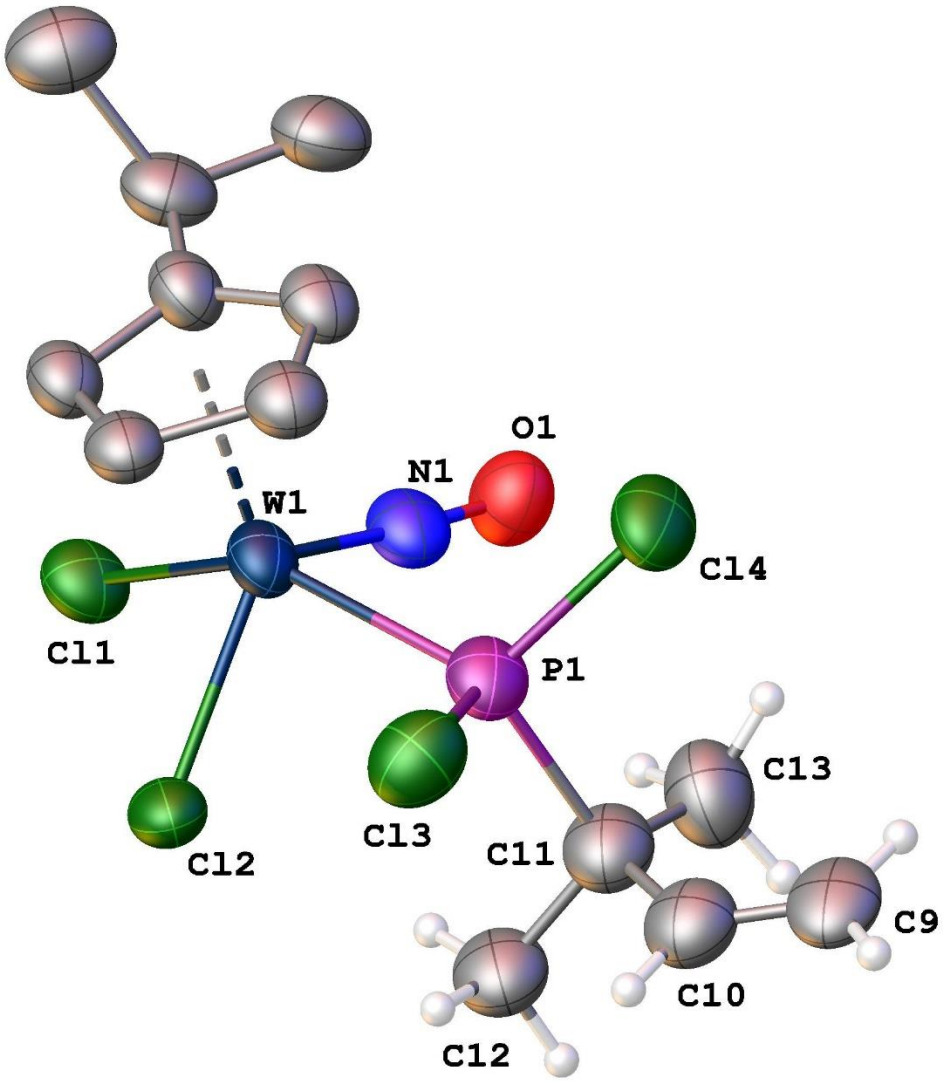

Figure 2.1. Solid-state molecular structure of **2.4a** with 50% probability thermal ellipsoids. Some hydrogen atoms have been omitted for clarity. Selected bond lengths (Å) and angles (deg): W(1)-Cl(1) = 2.437(5), W(1)-Cl(2) = 2.356(14), W(1)-P(1) = 2.498(6), P(1)-Cl(3) = 2.039(8), P(1)-Cl(4) = 2.003(8), P(1)-C(11) = 1.90(2), C(11)-C(12) = 1.47(3), C(11)-C(13) = 1.52(3), C(10)-C(11) = 1.57(4), C(9)-C(10) = 1.28(4), W(1)-N(1) = 1.81(4), N(1)-O(1) = 1.26(6), W(1)-N(1)-O(1) = 176(3), N(1)-W(1)-P(1) = 83.9(19), Cl(2)-W(1)-P(1) = 77.9(3), Cl(1)-W(1)-Cl(2) = 82.7(3), Cl(1)-W(1)-N(1) = 82.7(12).

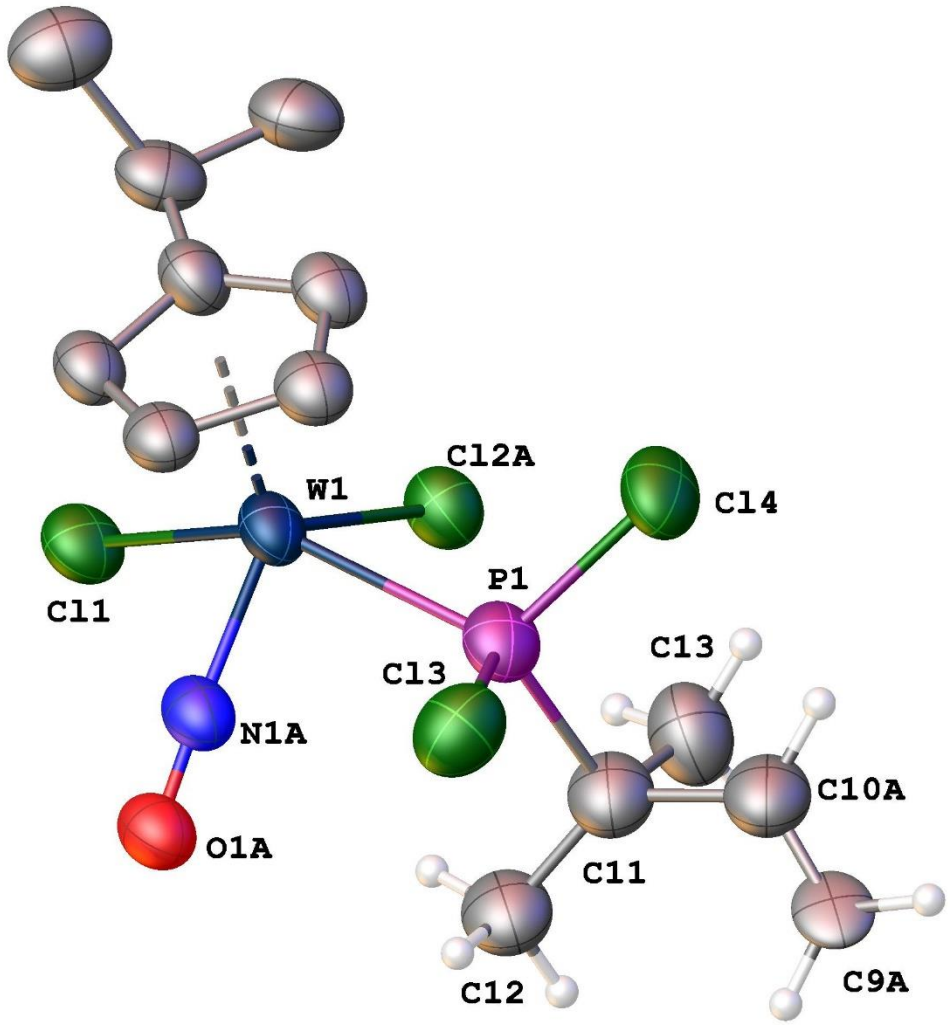

Figure 2.2. Solid-state molecular structure of **2.4b** with 50% probability thermal ellipsoids. Some hydrogen atoms have been omitted for clarity. Selected bond lengths (Å) and angles (deg): W(1)-N(1A) = 1.88(5), W(1)-Cl(2A) = 2.340(15), C(11)-C(10A) = 1.57(4), C(9A)-C(10A) = 1.28(4), N(1A)-O(1A) = 1.17(7),W(1)-N(1A)-O(1A) = 177(4), N(1A)-W(1)-P(1) = 79.4(16), Cl(2A)-W(1)-P(1) = 77.3(4), Cl(1)-W(1)-Cl(2A) = 86.0(3), Cl(1)-W(1)-N(1A) = 85.2(16).

In solution complex **2.4** exists as a single isomer. Interestingly, its ^{1}H NMR spectrum in C_6D_6 exhibits unusual long-range coupling of the alkene protons to phosphorus. Thus, the signals due to the $PCl_2CMe_2CH=C\mathit{H}_2$ protons are doublets of doublets at 5.26 ppm and 5.35 ppm

with $^4J_{HP}$ being 4.2 Hz and 4.3 Hz, respectively (Figure 2.3b). Also, the ^{1}H NMR signal assigned to $PCl_2CMe_2CH{=}CH_2$ is a doublet of doublets of doublets at 5.91 ppm with a $^3J_{HP}$ of 4.5 Hz (Figure 2.3b). The solid-state molecular structures of **2.4a** and **2.4b** reveal that the orientations of the $CMe_2CH{=}CH_2$ fragments with respect to the P(1)-C(11) bonds are such that there could possibly be hyperconjugation from $\sigma_{P(1)\text{-}C(11)}$ to $\pi^*_{C(9)=C(10)}$, an interaction that could explain the long-range coupling to phosphorus detected in the ^{1}H and ^{13}C NMR spectra of **2.4**. Non-bonded coupling can occur via "through-space" interactions resulting in the orbital overlap between two elements[33] even with the long distance between P(1) and C(19) of 3.629 Å.

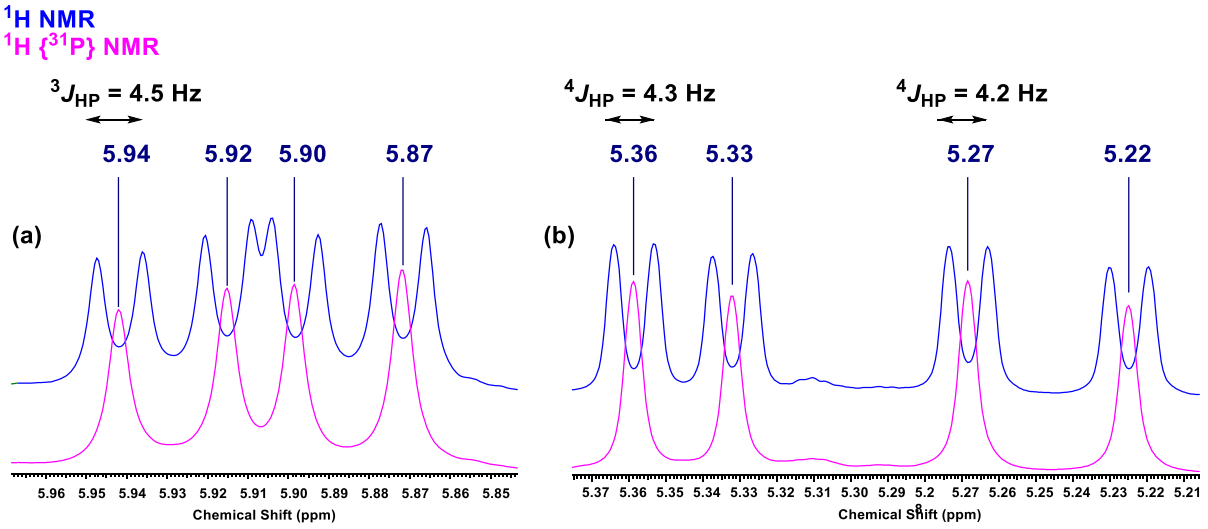

Figure 2.3. (a) Expansion of the overlaid ^{1}H (blue) and ^{1}H{^{31}P} (pink) NMR spectra (δ 5.85 to 5.97 ppm) of **2.4** in C_6D_6 (400 MHz). (b) Expansion of the overlaid ^{1}H (blue) and ^{1}H{^{31}P} (pink) NMR spectra (δ 5.21 to 5.38 ppm) of **2.4** in C_6D_6 (400 MHz).

As shown in Scheme 2.4, the unexpected formation of **2.4** can be explained by invoking the intermediate adduct, $(\eta^5\text{-}C_5H_4{}^i\text{Pr})W(NO)(PCl_3)Cl_2$, with the subsequent metathesis reaction occurring between the binary magnesium reagent and a P-Cl bond of the adduct. This mode of

reactivity evidently has not been observed previously with analogous systems. Evidence consistent with the presence of (η^5-$C_5H_4{}^iPr$)W(NO)(PCl_3)Cl_2 has been obtained by carrying out the reaction of **2.1** with PCl_5 in THF-d_8 and analyzing the mixture in situ by NMR spectroscopy. The ^{1}H NMR spectrum of the mixture contains only signals attributable to the η^5-$C_5H_4{}^iPr$ ligand, and the $^{31}P\{^1H\}$ NMR spectrum contains only a single broad resonance at 218.8 ppm. A dark brown residue can be obtained by removing the solvent in vacuo, an operation that presumably removes some of the PCl_3 and allows for the formation of some of the [(η^5-$C_5H_4{}^iPr$)W(NO)Cl_2]$_2$ dimer. In ethers this dimer would exist as a solvated monomer that can be converted into **2.3** via sequential metatheses reactions with appropriate binary magnesium reagents. Consistent with this point of view is the fact that the analogous (η^5-C_5Me_5)W(NO)Cl_2 is a brown solid as a dimer and a green solvated monomer in coordinating solvents.[30]

In an attempt to displace the $PCl_2CMe_2CH{=}CH_2$ ligand with PMe_3 in **2.4**, a small scale reaction of the organometallic complex with excess PMe_3 in THF-d_8 has been carried out (Scheme 2.5.). Upon addition of the Lewis base to the solution of **2.4** in THF-d_8, the colour of the reaction mixture changes from green to yellow instantaneously. After 3 days at room temperature, red and green crystals have deposited in the J. Young NMR tube, with the red ones being suitable for a single-crystal X-ray diffraction analysis (Figure 2.4). Based on the analysis of the solid-state molecular structure of the green crystals, the product appears to be a phosphite complex whose identity remains uncertain due to a poor quality of the sample.

The solid-state molecular structure of the W(NO)(PMe_3)$_3Cl_3$ (**2.5**) has a capped trigonal antiprismatic coordination geometry with the chloro and PMe_3 ligands in a staggered conformation with respect to each other, and a linear NO ligand at the crown of the structure (W(1)-N(1)-O(1) = 179.5(5)). The bond lengths between the tungsten metal centre and the three

phosphorus atoms are the same. Similarly, the tungsten-chlorine linkages are also identical. The W(1)-P(1) bond (2.5139(18) Å) and W(1)-Cl(1) bond (2.5259(16) Å) appear to be identical, even though PMe_3 is a good σ donor ligand and chlorine is a σ and π donor. The angle between P(1)-W(1)-P(2) is 111.25(6), which is significantly larger than the angle between the chloro ligands (Cl(1)-W(1)-Cl(2) = 92.07(5)) (Figure 2.4). The PMe_3 ligands are more spread out in the metal's coordination sphere possibly due to the bulkiness introduced by the methyl groups on the phosphine ligand.

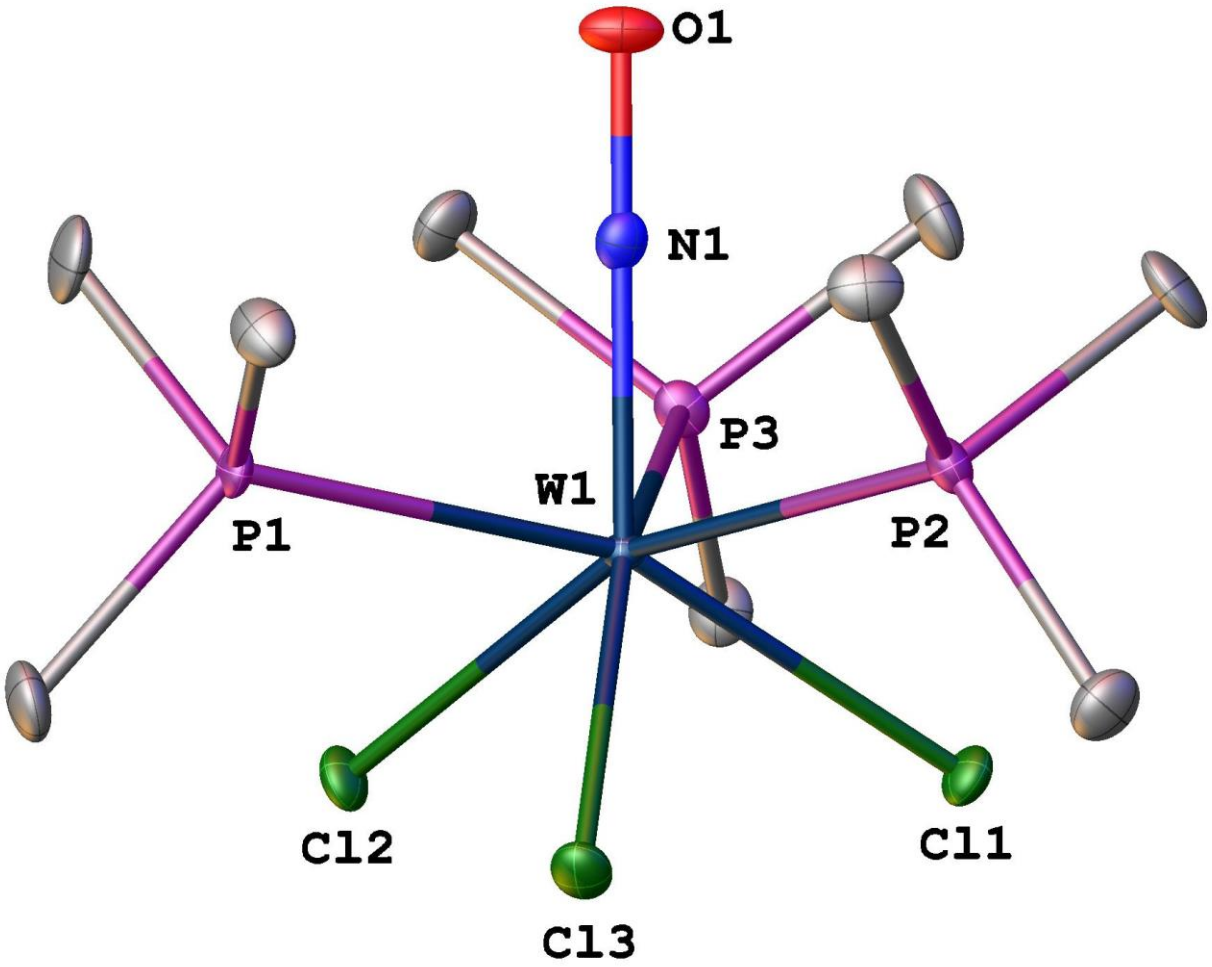

Figure 2.4. Solid-state molecular structure of **2.5** with 50% probability thermal ellipsoids. Some hydrogen atoms have been omitted for clarity. Selected bond lengths (Å) and angles (deg): W(1)-N(1) = 1.789(6), W(1)-P(1) = 2.5139(18), W(1)-P(2) = 2.5138(18), W(1)-P(3) = 2.5099(17), W(1)-Cl(1) = 2.5259(16), W(1)-Cl(2) = 2.5083(16), W(1)-Cl(3) = 2.4837(16), N(1)-O(1) = 1.213(8), W(1)-N(1)-O(1) = 179.5(5), P(1)-W(1)-N(1) = 77.23(19), P(2)-W(1)-N(1) = 76.37(19), P(3)-W(1)-N(1) = 75.05(19), Cl(1)-W(1)-Cl(2) = 92.07(5), Cl(2)-W(1)-Cl(3) = 85.92(6), Cl(1)-W(1)-Cl(3) = 86.42(6), P(1)-W(1)-P(2) = 111.25(6), P(2)-W(1)-P(3) = 115.68(6), P(1)-W(1)-P(3) = 116.53(6).

Scheme 2.5. Reaction of 2.4 with PMe_3

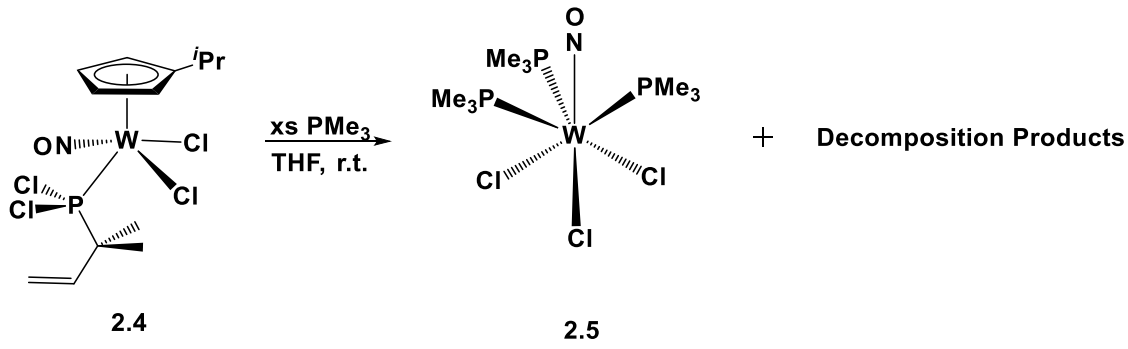

2.4 **2.5**

The solid-state molecular structure of the product has revealed an unexpected mode of reactivity of **2.4** with PMe_3. Upon addition of the Lewis base, complex **2.4** loses the cyclopentadienyl ligand along with $PCl_2CMe_2CH{=}CH_2$. Since **2.5** contains three chloro ligands, it is possible that the loss of the isopropyl cyclopentadienyl and $PCl_2CMe_2CH{=}CH_2$ ligands is accompanied by a dimerization following asymmetric disproportionation and coordination of new phosphine ligands. Unfortunately, other products of this reaction could not be identified to obtain a better understanding of the reaction mechanism.

2.3 Summary

The η^5-$C_5H_4{}^i$Pr ligand imparts distinctive physical and chemical properties to **2.3** and its precursors. Reaction of **2.1** with PCl_5 results in the formation of an unprecedented PCl_3 adduct of the (η^5-$C_5H_4{}^i$Pr)W(NO)Cl_2 complex. Moreover, the subsequent metathesis reaction occurs between the binary magnesium reagent and a P-Cl bond of the adduct forming **2.4**. Therefore, synthesis of **2.3** is best effected via a different di-halogen complex, namely **2.2**, which can be obtained by the reaction of **2.1** with iodine.

2.4 Experimental Section

2.4.1 General Experimental Procedures

All reactions and subsequent manipulations involving organometallic reagents were performed under anhydrous and anaerobic conditions except where noted. All inert gases were purified by passing them through a column containing MnO and then through a column of activated 4 Å molecular sieves. Vacuum and inert atmosphere techniques were performed either using double-manifold Schlenk lines or in Innovative Technologies LabMaster 100 and MS-130 BG glove boxes equipped with freezers maintained at −30 °C. THF and Et_2O were dried over sodium/benzophenone ketyl and freshly distilled prior to use; pentane was dried over calcium hydride and freshly distilled prior to use; solvents such as hexanes, and EtOAc were not dried prior to use; all other solvents were dried according to standard procedures.[34] All binary magnesium reagents used were prepared from the corresponding Grignard reagents.[35] (η^5-C_5Me_5)W(NO)Cl_2, and (η^5-C_5Me_5)W(NO)(CH_2CMe_3)$_2$ were prepared according to the published procedures.[30,36] Pentamethylcyclopentadiene was obtained from the Boulder Scientific Company. All other chemicals and reagents were ordered from commercial suppliers and used as received.

Unless otherwise specified, all IR samples were prepared as Nujol mulls sandwiched between NaCl plates, and their spectra were recorded on a Thermo Nicolet Model 4700 FT-IR spectrometer. Except where noted, all NMR spectra were recorded at room temperature on Bruker AV-400 (direct and indirect probes), and all chemical shifts are reported in ppm and coupling constants are reported in Hz. ^{1}H NMR spectra were referenced to the residual protio

isotopomer present in C_6D_6 (7.16 ppm), C_6D_{12} (1.38 ppm), THF-d_8 (1.73 and 3.58 ppm), or $CDCl_3$ (7.27 ppm). ^{13}C NMR spectra were referenced to C_6D_6 (128.39 ppm), C_6D_{12} (26.43 ppm), THF-d_8 (25.37 and 67.57 ppm), or $CDCl_3$ (77.0). ^{31}P NMR spectra were externally referenced to 85% H_3PO_4. For the characterization of most complexes 2-dimensional NMR experiments, {^1H–^1H} COSY, {^1H–^{13}C} HSQC, and {^1H–^{13}C} HMBC, were performed to correlate and assign ^1H and ^{13}C NMR signals and establish atom connectivity. GC analyses (FID detection) were performed on an Agilent 7890A GC equipped with a HP-5ms (30m x 0.25mm x 0.25 μm) capillary column. Low- and high-resolution mass spectra (EI, 70 eV) and MALDI-TOF spectra were recorded by Mr. Marshall Lapawa of the UBC mass spectrometry facility using a Kratos MS-50 spectrometer, and elemental analyses were performed by Mr. Derek Smith of the UBC microanalytical facility. X-ray crystallographic data collection, solution, and refinement were performed at the UBC X-ray crystallography facility by Dr. Brian Patrick.

2.4.2 Synthesis of (η^5-$C_5H_4{}^i$Pr)W(NO)(CO)$_2$ (2.1)

In a glove box, a 1-L round-bottom flask was charged with Na($C_5H_4{}^i$Pr) (14.720 g, 0.113 mol) and a magnetic stir bar. On a Schlenk line, THF (ca. 300 mL) was cannulated into the reaction flask to obtain a clear yellow solution. Under a flow of N_2 gas, $W(CO)_6$ (39.700 g, 0.113 mol) was added to the solution in the reaction flask. The mixture was then heated to 78 °C while being stirred. After five days, a dark brown solution of Na[(η^5-$C_5H_4{}^i$Pr)$W(CO)_3$] had been produced, and the reaction mixture was cooled to room temperature. A second 0.5-L round-bottom flask was charged with *N*-methyl-*N*-nitroso-*p*-toluenesulfonamide (24.000 g, 0.112 mol) that was then dissolved in THF (ca. 250 mL) affording a light yellow solution. The solution in

the 0.5-L round-bottom flask was added to the 1-L reaction flask dropwise by cannula. Upon addition, CO gas was evolved, and the reaction mixture changed colour from dark brown to dark orange. After the addition had been completed, the reaction mixture was stirred at room temperature for one day, and then the THF was removed in vacuo. The resulting residue was dissolved in CH_2Cl_2 (ca. 300 mL) and washed with H_2O (6 x 100 mL). The organic layer was dried over anhydrous $MgSO_4$, and the solvent was removed in vacuo to obtain a concentrated solution of the final products as a dark orange oil. This oil was then extracted with hexanes (ca. 400 mL). Solvent was removed from the extracts under reduced pressure to obtain impure **2.1** as an orange liquid (31.428 g). Purification of **2.1** was performed by column chromatography using a flash silica support. An orange band was eluted from the column with hexanes, and solvent removal in vacuo from the eluate afforded **2.1** as an analytically pure, bright orange oil (25.608 g, 0.068 mol, 61% yield).

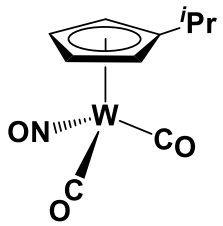

Characterization data for **2.1**. IR (cm^{-1}): 1666 (s, ν_{NO}), 2005 (s, ν_{CO}), 1926 (s, ν_{CO}). MS (LREI, *m/z*, probe temperature 150 °C): 377 [M^+, ^{184}W], 349 [M^+ – CO, ^{184}W], 319 [M^+ – CO, NO, ^{184}W]. ^1H NMR (400 MHz, C_6D_6): δ 0.81 (d, $^3J_{HH}$ = 6.85, 6H, ^{i}Pr CH_3), 2.21 (sept, $^3J_{HH}$ = 6.85, 1H, ^{i}Pr C*H*), 4.62 (t, $^3J_{HH}$ = 2.35, 2H, $C_5H_4{}^i$Pr), 4.85 (t, $^3J_{HH}$ = 2.35, 2H, $C_5H_4{}^i$Pr). ^{13}C APT NMR (100 MHz, C_6D_6): δ 24.2 (^{i}Pr *C*H_3), 27.8 (^{i}Pr *C*H), 90.2 ($C_5H_4{}^i$Pr), 90.6 ($C_5H_4{}^i$Pr), 125.2 (*ipso*-$C_5H_4{}^i$Pr), 219.6 (*C*O). ^1H NMR (400 MHz, THF-d_8): δ 1.18 (d, $^3J_{HH}$ = 6.85, 6H, ^{i}Pr CH_3), 2.75 (sept, $^3J_{HH}$ = 6.85, 1H, ^{i}Pr C*H*), 5.62 (t, $^3J_{HH}$ = 2.35, 2H, $C_5H_4{}^i$Pr), 5.83 (t, $^3J_{HH}$ = 2.35, 2H,

$C_5H_4{}^iPr$). Anal. Calcd. for $C_{10}H_{11}NO_3W$: C, 31.86; H, 2.94; N, 3.71. Found: C, 32.16; H, 3.00; N, 3.77.

For synthetic manipulations involving **2.1**, a standard solution of this complex in Et_2O was prepared under anaerobic conditions. The concentration of **2.1** in this solution was established by adding a known amount of ferrocene to a measured aliquot of the solution in C_6D_6 and recording its ^1H NMR spectrum. The ratio of the Cp_2Fe singlet at 4.00 ppm to the signals due to the ring protons on the $C_5H_4{}^iPr$ ligand at 4.62 and 4.85 ppm then permitted the calculation of the amount of **2.1** in the ^1H NMR sample and thus its concentration in the standard solution.

2.4.3 Reaction of 2.1 with PCl_5

In a glove box, a vial was charged with **2.1** (0.1905 mmol) and THF-d_8 (ca. 2 mL). In another vial, an equimolar amount of PCl_5 (40 mg, 0.1905 mmol) was dissolved in THF-d_8 (ca. 1 mL). The solution of PCl_5 was then added dropwise to the vial containing **2.1** with vigorous stirring. Upon addition, the reaction mixture changed colour from orange to green. The final reaction mixture was analyzed by ^1H NMR and IR spectroscopies.

Characterization data for the product. IR (cm^{-1}): 1640 (m, ν_{NO}). MS (LREI, *m/z*, probe temperature 150 °C): 391 [$M^+ - PCl_3$, ^{184}W], 361 [$M^+ - NO, PCl_3$, ^{184}W]. ^1H NMR (400 MHz, THF-d_8): δ 1.23 (d, $^3J_{HH}$ = 6.9, 6H, ^{i}Pr CH_3), 3.00 (sept, $^3J_{HH}$ = 6.9, 1H, ^{i}Pr C*H*), 6.03 (t, $^3J_{HH}$ = 2.3, 2H, $C_5H_4{}^iPr$), 6.26 (t, $^3J_{HH}$ = 2.3, 2H, $C_5H_4{}^iPr$). $^{31}P\{^1H\}$ NMR (162 MHz, THF-d_8): δ 218.8 (s).

2.4.4 Synthesis of (η^5-$C_5H_4{}^iPr$)W(NO)I_2 (2.2)

While connected to a double manifold, a large Schlenk reaction flask was charged with **2.1** (3.50 mL, 19.0 mmol), a magnetic stir bar, and toluene (ca. 100 mL) to produce a bright orange solution. A second Schlenk flask was similarly charged with I_2 (4.800 g, 18.9 mmol), a magnetic stir bar, and toluene (ca. 100 mL) to produce a dark red-purple solution. The toluene solution of **2.1** was slowly cannulated into the reaction flask containing the I_2 solution while it was being stirred whereupon the reaction mixture turned dark green. After the addition had been completed, the stirred mixture was heated at 40 ºC for 3 h. The volume of the final reaction mixture was reduced in vacuo to ca. 50 mL. An equal volume of pentane was added, and the mixture was maintained at -33 ºC for 2 d to induce the deposition of **2.2** as a dark brown solid that was collected by filtration (10.260 g, 17.9 mmol, 94% yield).

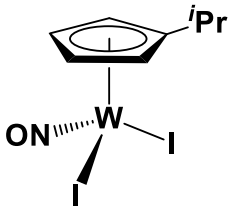

Characterization data for **2.2**. IR (cm^{-1}): 1610, 1637 (s, ν_{NO}), IR (CH_2Cl_2, cm^{-1}) 1649 (s, ν_{NO}). MS (LREI, *m/z*, probe temperature 150 °C): 575 [M^+, ^{184}W]. ^1H NMR (400 MHz, C_6D_6): δ 0.79 (d, $^3J_{HH}$ = 6.9, 6H, ^{i}Pr CH_3), 2.45 (sept, $^3J_{HH}$ = 6.9, 1H, ^{i}Pr C*H*), 5.11 (t, $^3J_{HH}$ = 2.4, 2H, $C_5H_4{}^iPr$), 5.17 (t, $^3J_{HH}$ = 2.4, 2H, $C_5H_4{}^iPr$). ^{13}C APT NMR (100 MHz, C_6D_6): δ 23.2 (^{i}Pr *C*H_3), 28.5 (^{i}Pr *C*H), 103.7 ($C_5H_4{}^iPr$), 104.7 ($C_5H_4{}^iPr$), 129.6 (*ipso*-$C_5H_4{}^iPr$). Anal. Calcd. for $C_9H_{14}I_2NOW$: C, 16.72; H, 1.93; N, 2.44. Found: C, 17.49; H, 2.74; N, 2.39.

2.4.5 Synthesis of (η^5-$C_5H_4{}^iPr$)W(NO)(CH_2CMe_3)(η^3-CH_2CHCMe_2) (2.3)

Method 1. In the glove box a Schlenk reaction flask was charged with **2.2** (0.640 g, 1.11 mmol) and Et_2O (ca. 100 mL), and it was placed into a dry ice/acetone bath at -78 °C. A second Schlenk flask was charged with $Mg(CH_2CMe_3)_2$ (titre: 156 g/mol, 0.155 g, 0.994 mmol) and Et_2O (ca. 50 mL), and the resulting solution was then slowly cannulated into the Schlenk flask containing **2.2**. After the addition had been completed, the reaction mixture that had changed colour from light brown to dark burgundy was removed from the dry ice/acetone bath and was left to warm to room temperature for 15 min while being stirred. The reaction flask containing this mixture was then placed back into a dry ice/acetone bath. In the glove box, another Schlenk flask was charged with $Mg(CH_2CH{=}CMe_2)_2$ (titre: 144 g/mol, 0.841 g, 5.84 mmol) and Et_2O (ca. 30 mL), and the resulting solution was then slowly cannulated into the original reaction flask. After this addition had been completed, the Schlenk flask containing the reaction mixture was removed from the dry ice/acetone bath and was left to warm to room temperature for 30 min while its contents were stirred. The volume of the final reaction mixture, a dark brown solution, was reduced in vacuo and was transferred to the top of a basic alumina column (4 x 2 cm). Elution of the column with Et_2O developed a yellow band that was collected. Removal of solvent from the eluate under reduced pressure afforded **2.3** as a yellow liquid (0.123 g, 0.267 mmol, 27% yield). The thermal instability of **2.3** markedly affects its isolated yields.

Method 2. A Schlenk reaction flask charged with **2.1** (4.66 mmol), PCl_5 (0.970 g, 4.66 mmol) and THF (ca. 100 mL) was placed into a dry ice/acetone bath at -78 °C. Its contents were

then left to warm up to room temperature and react for 1 h. Afterwards, the product mixture was first reacted with $Mg(CH_2CMe_3)_2$ (titre: 124 g/mol, 0.587 g, 4.73 mmol,) in THF (ca. 50 mL) and then with $Mg(CH_2CH{=}CMe_2)_2$ (titre: 159 g/mol, 0.749 g, 4.71 mmol) in Et_2O (ca. 30 mL) in a manner described in the preceding paragraph. Similar work-up of the final mixture by chromatography on basic alumina with Et_2O as eluant again afforded **2.3** as a yellow liquid (0.316 g, 0.685 mmol, 15% yield).

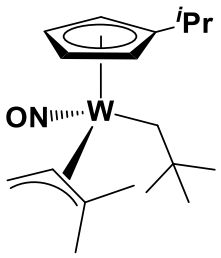

Characterization data for **2.3**. IR (cm^{-1}): 1599 (s, ν_{NO}). MS (LREI, *m/z*, probe temperature 150 °C): 461 [M^+, ^{184}W]. ^1H NMR (400 MHz, C_6D_6): δ 1.09 (d, $^3J_{HH}$ = 6.9, 6H, ^{i}Pr CH_3), 1.13 (s, 3H, CH_2CHCMe_2), 1.14 (s, 3H, CH_2CHCMe_2), 1.37 (s, 9H, CH_2CMe_3), 1.43 (s, 1H, CH_2CMe_3), 1.50 (s, 1H, CH_2CMe_3), 2.22 (dd, $^3J_{HH}$ = 9.5, $^2J_{HH}$ = 4.6, 1H, CH_2CHCMe_2), 2.46 (dd, $^3J_{HH}$ = 9.8, $^2J_{HH}$ = 4.6, 1H, CH_2CHCMe_2), 2.69 (sept, $^3J_{HH}$ = 6.9, 1H, ^{i}Pr CH), 3.94 (dd, $^3J_{HH}$ = 9.8, 1H, CH_2CHCMe_2), 4.42 (dd, $^3J_{HH}$ = 4.9, $^3J_{HH}$ = 2.9, 1H, $C_5H_4{}^i$Pr), 4.96 (m, 1H, $C_5H_4{}^i$Pr), 5.08 (m, 1H, $C_5H_4{}^i$Pr), 5.14 (m, 1H, $C_5H_4{}^i$Pr). ^{13}C APT NMR (100 MHz, C_6D_6): δ 21.4 (CH_2CHCMe_2), 24.1 (^{i}Pr CH$_3$), 27.8 (^{i}Pr CH), 29.2 (CH$_2$CHCMe$_2$), 29.6 (CH_2CHCMe_2), 30.8 (CH$_2$CMe$_3$), 35.5 (CH_2CMe_3), 38.8 (CH_2CMe_3), 93.0 ($C_5H_4{}^i$Pr), 97.2 (CH_2CHCMe_2), 98.5 ($C_5H_4{}^i$Pr), 99.7 ($C_5H_4{}^i$Pr), 104.3 ($C_5H_4{}^i$Pr), 121.9 (*ipso*-$C_5H_4{}^i$Pr). Anal. Calcd. for $C_{18}H_{31}NOW$: C, 46.87; H, 6.77; N, 3.04. Found: C, 46.52; H, 6.85; N, 2.81.

2.4.6 Synthesis of (η^5-$C_5H_4{}^iPr$)W(NO)($Cl)_2$($PCl_2CH_2CH{=}CMe_2$) (2.4)

A Schlenk reaction flask charged with **2.1** (6.86 mmol), PCl_5 (1.429 g, 6.86 mmol) and Et_2O (ca. 100 mL) was placed into a dry ice/acetone bath at -78 °C. A second Schlenk flask was charged with $Mg(CH_2CH{=}CMe_2)_2$ (titre: 144 g/mol, 1.000 g, 6.94 mmol) and Et_2O (ca. 50 mL), and the resulting solution was then slowly cannulated into the first Schlenk flask containing the tungsten reactant. Upon addition, the colour of the solution changed from green to dark yellow. After the addition had been completed, the flask containing the reaction mixture was removed from the dry ice/acetone bath and was left to warm to room temperature for 45 min while its contents were being stirred. The final mixture was filtered through a 1.5 by 2.5 cm Celite plug supported on a porous frit, and removal of the solvent from the green filtrate under reduced pressure afforded **2.4** as a brown solid (1.252 g, 2.22 mmol, 32% yield). Recrystallization of **2.4** from 1:1 THF:pentane at -33 °C for one week produced yellow crystals suitable for a single-crystal X-ray diffraction analysis.

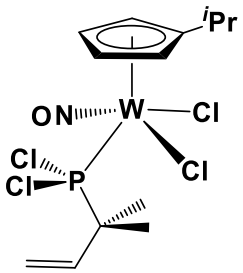

Characterization data for **2.4**. IR (CH_2Cl_2, cm^{-1}): 1645 (s, ν_{NO}). MS (LREI, *m/z*, probe temperature 150 °C): 461 [M^+, ^{184}W]. ^1H NMR (400 MHz, C_6D_6): δ 1.24 (d, $^3J_{HH}$ = 7.0, 6H, ^{i}Pr CH_3), 1.36 (d, $^3J_{PH}$ = 14.9, 6H, $PCl_2CMe_2CHCH_2$), 3.01 (sept, $^3J_{HH}$ = 7.0, 1H, ^{i}Pr C*H*), 5.26 (dd, $^3J_{HH}$ = 17.4, $^4J_{HP}$ = 4.2, 1H, $PCl_2CMe_2CHCH_2$), 5.35 (dd, $^3J_{HH}$ = 10.8, $^4J_{HP}$ = 4.3, 1H,

$PCl_2CMe_2CHCH_2$), 5.91 (ddd, $^3J_{HH}$ = 17.4, $^3J_{HH}$ = 10.8, $^3J_{HP}$ = 4.5, 1H, $PCl_2CMe_2CHCH_2$), 6.04 (s, 2H, $C_5H_4{}^i$Pr), 6.25 (2H, $C_5H_4{}^i$Pr). ^{13}C APT NMR (100 MHz, C_6D_6): δ 14.9 ($PCl_2CMe_2CHCH_2$), 23.2 (^{i}Pr CH_3), 28.6 (^{i}Pr CH), 46.0 ($PCl_2CMe_2CHCH_2$), 106.3 ($C_5H_4{}^i$Pr), 108.6 ($C_5H_4{}^i$Pr), 118.6 (d, $^3J_{CP}$ = 10.1, $PCl_2CMe_2CHCH_2$), 133.5 (*ipso*-$C_5H_4{}^i$Pr), 139.9 (d, $^2J_{CP}$ = 12). $^{31}P\{^1H\}$ NMR (162 MHz, C_6D_6): δ 188.9 (s, $PCl_2CMe_2CHCH_2$).

2.4.7 Preparation of $W(NO)(Cl)_3(PMe_3)_3$ (2.5)

A J. Young NMR tube was loaded with **2.4** (30 mg, 0.051 mmol), THF-d_8 (1 mL) and 5 drops of PMe_3. Upon addition of the Lewis base to the solution of **2.4** in THF-d_8, the colour of the reaction mixture changed from green to yellow instantaneously. Red and green crystals deposited in the J. Young NMR tube after 3 days at room temperature. The red ones were suitable for a single-crystal X-ray diffraction analysis.

2.4.8 X-ray Crystallography

Data collection was carried out at –173.0 ± 2 °C on a Bruker X8 APEX II diffractometer with graphite-monochromated Mo Kα radiation or at –183.0 ± 1 °C on a Bruker APEX DUO diffractometer with cross-coupled multilayer optics using Cu-Kα radiation.

Data for **2.4** were collected to a maximum 2θ value of 115.9° in 0.5° oscillations using 45.0-second exposures. The crystal-to-detector distance was 49.84 mm. The structure was solved by direct methods[37] and expanded using Fourier techniques. The material crystallized as a four-component 'split-crystal'. Integrations were carried out on only the first three components,

including both overlapped and non-overlapped reflections, since the fourth component was too weak to integrate properly. The nitrosyl and one chloro ligand were positionally disordered. Also, the C=C was disordered and was modeled in two different orientations (C(9)-C(10) and C(9A)-C(10A)). All non-hydrogen atoms were refined anisotropically. All hydrogen atoms were included in calculated positions. The final cycle of full-matrix least-squares analysis was based on 2358 observed reflections and 241 variable parameters.

Data for **2.5** were collected to a maximum 2θ value of 55.02° in 0.5° oscillations. The structure was solved by direct methods[38] and expanded using Fourier techniques. All non-hydrogen atoms were refined anisotropically, and all other hydrogen atoms were placed in calculated positions. The final cycle of full-matrix least-squares refinement was based on 18857 observed reflections and 4371 variable parameters.

Neutral atom scattering factors were taken from Cromer and Waber.[39] Anomalous dispersion effects were included in Fcalc[40]; the values for Δf' and Δf'' were those of Creagh and McAuley.[41] The values for the mass attenuation coefficients are those of Creagh and Hubbell.[42] All refinements were performed using the SHELXL-2014[43] via the OLEX2[44] interface.

Table 2.1. X-ray Crystallographic Data for Complexes **2.4** and **2.5**.

Compound	**2.4**	**2.5**
Empirical formula	$C_{13}H_{20}Cl_4NOPW$	$C_9H_{27}Cl_3NOP_3W$
Crystal Habit, color	yellow, irregular	orange, irregular
Crystal size (mm)	0.01 x 0.05 x 0.14	0.18 × 0.12 × 0.11
Crystal system	triclinic	monoclinic
Space group	*P*-1	$P2_1/c$
Volume ($Å^3$)	906.54(12)	1913.8(4)
a (Å)	7.4339(5)	14.6014(18)
b (Å)	9.7509(8)	11.4698(14)
c (Å)	13.2354(10)	11.4362(14)
α (°)	104.013(6)	90
β (°)	93.085(5)	92.239(2)
γ (°)	101.594(6)	90
Z	2	4
Density, ρ (calculated) (g/cm^3)	2.062	1.9033
Absorption coefficient, μ (mm^{-1})	18.046	6.696
F_{000}	540	1065
Measured Reflections: Total	19048	18857
Measured Reflections: Unique	2358	4371
Final R Indices[a]	R_1 = 0.0794, wR_2 = 0.1924	R_1 = 0.0356, wR_2 = 0.0945
Goodness-of-fit on F^2 [b]	1.050	0.986
Largest diff. peak/hole ($e^- Å^{-3}$)	1.70/-1.86	4.82/-1.66

[a] R1 on $F = \Sigma \mid (|F_o| - |F_c|) \mid / \Sigma |F_o|$; $wR2 = [(\Sigma (F_o^2 - F_c^2)^2) / \Sigma w(F_o^2)^2]^{1/2}$; $w = [\sigma^2 F_o^2]^{-1}$;

[b] $GOF = [\Sigma (w (|F_o| - |F_c|)^2) / \textit{degrees of freedom}]^{1/2}$

Chapter 3: Investigation of the Effects of the η^5-$C_5H_4{}^iPr$ Ligand on Different Tungsten-Nitrosyl Systems

† A version of this chapter has been published. Fabulyak, D.; Handford, R. C.; Holmes, A. S.; Levesque, T. M.; Wakeham, R. J.; Patrick, B. O.; Legzdins, P.; Rosenfeld, D. C. *Inorg. Chem.* **2017**, *56*, 573-582.

3.1 Introduction

Recent investigations of the chemistry of the family of (η^5-C_5Me_5)W(NO)(H)(η^3-allyl) complexes, where η^3-allyl = η^3-$CH_2CHCHMe$, η^3-CH_2CHCMe_2, and η^3-$CH_2CHCHPh$, have shown the rich and varied chemistry of this class of compounds.[45] Upon thermolysis, a reactive η^2-alkene intermediate is formed which then initiates the C-H activation of *n*-alkanes (Scheme 3.1).[46] Functionalization of the activated substrate can be achieved via carbonylation reactions with the organometallic products of the C-H activation.[45] In light of these results, an investigation of the effects of the η^5-$C_5H_4{}^i$Pr ligand on the C-H activation chemistry of the allyl-hydride systems has been conducted.

Scheme 3.1. Proposed mechanism for the C-H activation of *n*-pentane effected by (η^5-C_5Me_5)W(NO)(H)(η^3-CH_2CHCMe_2)

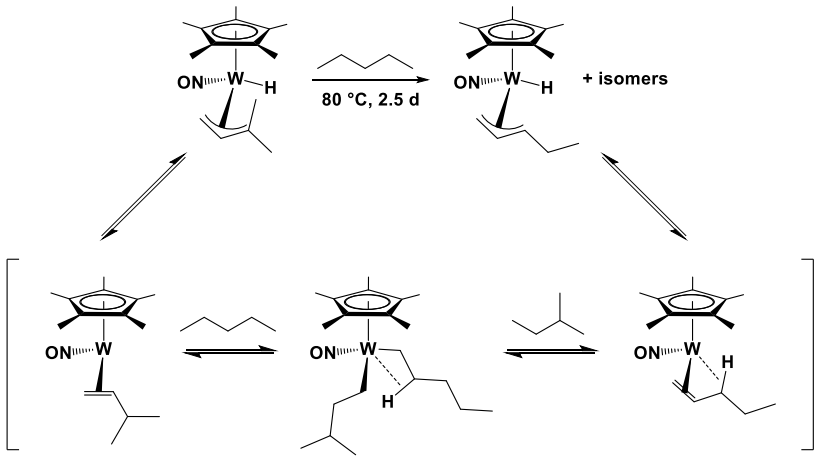

Treatment of (η^5-C_5Me_5)W(NO)(CH_2CMe_3)$_2$ in *n*-pentane with H_2 (ca. 1 atm) in presence of a Lewis base (L) results in formation of (η^5-C_5Me_5)W(NO)(CH_2CMe_3)(H)(L). The thermal behaviour of these complexes is highly dependent on the nature of L. Thus some can be isolated

at ambient temperatures (L = $P(OMe)_3$; $P(OPh)_3$; or $P(OCH_2)_3CMe$), while others undergo reductive elimination of neopentane and form a (η^5-C_5Me_5)W(NO)(L) reactive intermediate which then can effect intermolecular C-H activation of C_6H_6 (L = $P(OMe)_3$; $P(OPh)_3$; and PPh_3), or intramolecular C-H activation of L in benzene (L = PPh_3). *Cis*-(η^5-C_5Me_5)W(NO)(H)(κ^2-$PPh_2C_6H_4$) is the product of the intramolecular activation of the PPh_3 ligand. The designation of this geometrical isomer as *cis* indicates the relative positions of the W-C bond of the intramolecularly activated phenyl group of the PPh_3 and the hydrido ligands in the base of a four-legged piano-stool molecular structure. While thermolysis of *cis*-(η^5-C_5Me_5)W(NO)(H)(κ^2-$PPh_2C_6H_4$) in benzene at 50 °C for 24 h affords the hydrido phenyl complex *cis*-(η^5-C_5Me_5)W(NO)(H)(Ph)(PPh_3)[47]; thermolysis in *n*-pentane at 80 °C for 18 h affords *trans*-(η^5-C_5Me_5)W(NO)(H)(κ^2-$PPh_2C_6H_4$), which probably occurs via the (η^5-C_5Me_5)W(NO)(H)(*o*-$C_6H_5(PPh_2)$) intermediate (Scheme 3.2).[48]

Scheme 3.2. Thermolysis of *cis*-(η^5-C_5Me_5)W(NO)(H)(κ^2-$PPh_2C_6H_4$) in benzene and *n*-pentane

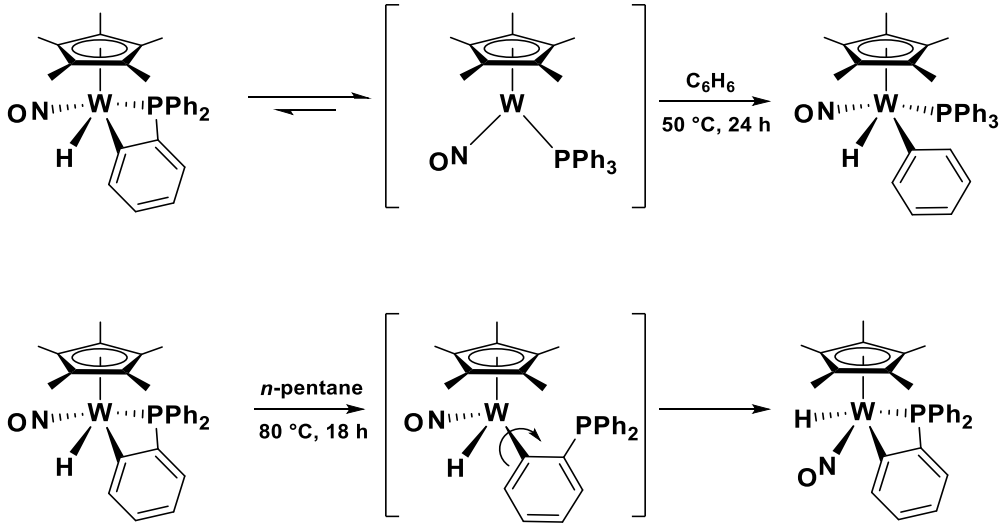

The beneficial kinetic effects on the C-H activation chemistry of the alkyl-allyl system imparted by η^5-$C_5H_4{}^i$Pr ligand have inspired further investigation of the effects of this ligand on the reactivity of this system. Results of these investigations are summarized in this chapter.

3.2 Results and Discussion

3.2.1 Synthesis and Thermal Chemistry of (η^5-$C_5H_4{}^i$Pr)W(NO)(H)(η^3-CH_2CHCMe_2)

3.2.1.1 Synthesis of (η^5-$C_5H_4{}^i$Pr)W(NO)(H)(η^3-CH_2CHCMe_2) (3.1)

(η^5-$C_5H_4{}^i$Pr)W(NO)(H)(η^3-CH_2CHCMe_2) (**3.1**) is obtained via sequential salt metathesis reactions of **2.2** with 0.5 equivalents of $Mg(CH_2CH{=}CMe_2)_2$ followed by a reaction with two equivalents of lithium borohydride (Scheme 3.3). This synthesis is completed within two hours, and the final product is isolated as an air- and moisture-stable yellow oil in good yield after purification via column chromatography on a silica column support. Synthesis of this complex cannot be effected in a manner similar to the (η^5-C_5Me_5) analogue[31] due to the unexpected mode of reactivity described in the previous section.

Scheme 3.3. Synthesis of 3.1

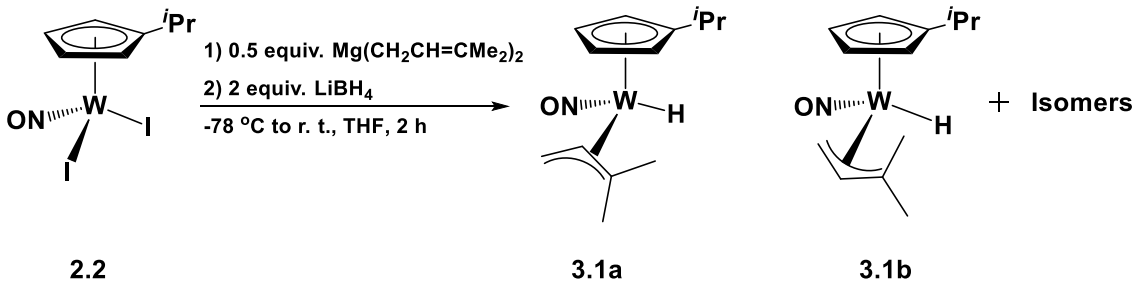

2.2 3.1a 3.1b

Complex **3.1** exists as four coordination isomers in C_6D_6 that differ in the orientation of the allyl ligand. The ratio of isomers has been determined using hydride signals in the ^{1}H NMR spectrum (Figure 3.1a). The major isomer **3.1a** (73.4%) has the 1,1-dimethylallyl ligand in the *exo* orientation with methyl groups proximal to the hydride ligand. The *meso* signal is a doublet of doublets at 3.08 ppm in the ^{1}H NMR spectrum with $^3J_{HH}$ coupling constants of 7.8 and 13.1 Hz (Figure 3.1b). The larger coupling constant is due to coupling to the proton *trans* to the *meso H*, a trend that is consistent with other systems.[31,46]

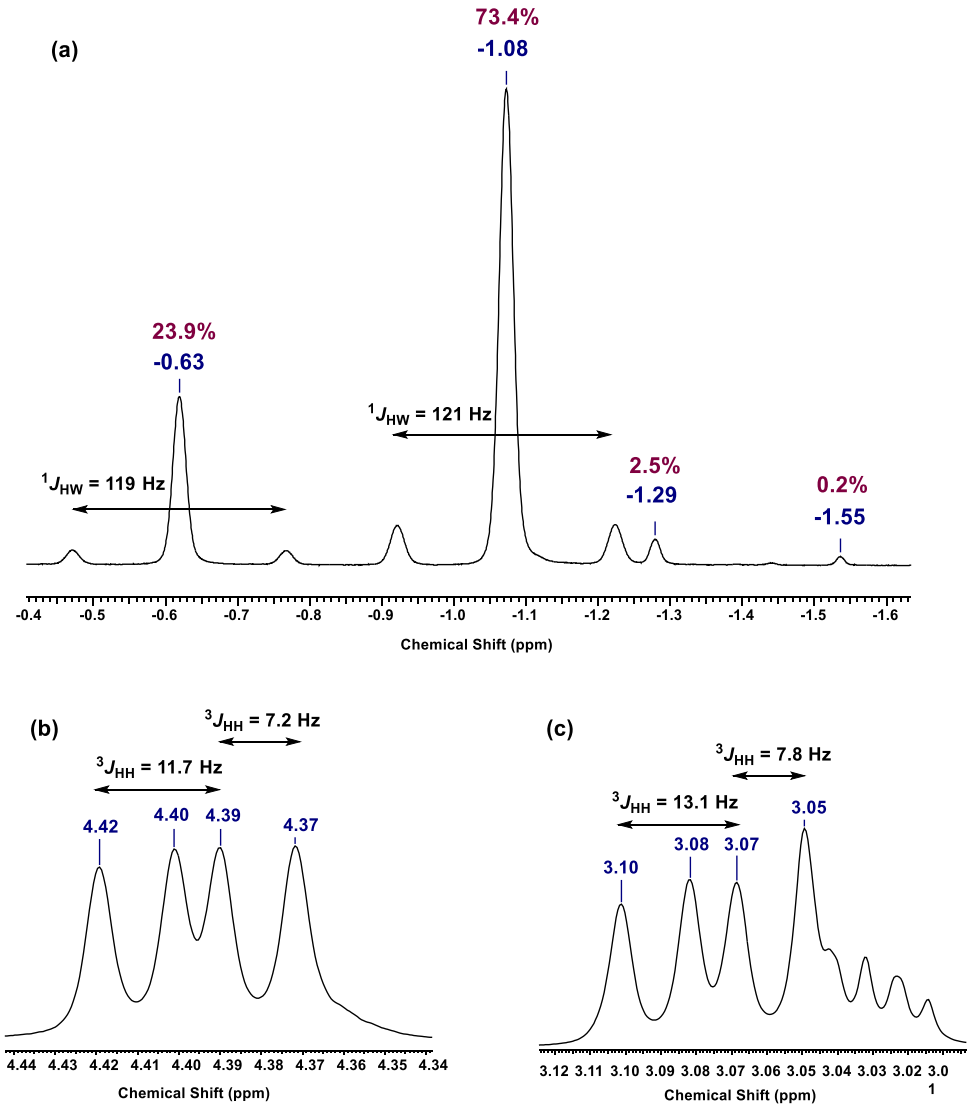

Figure 3.1. (a) Expansion of the ^{1}H NMR spectrum (δ -1.63 to -0.40 ppm) of **3.1** in C_6D_6 displaying the W-H signal of four isomer of **3.1** (400 MHz). (b) Expansion of the ^{1}H NMR spectrum (δ 4.34 to 4.44 ppm) of **3.1** in C_6D_6 displaying the *meso H* signal of the *endo* isomer (400 MHz). (c) Expansion of the ^{1}H NMR spectrum (δ 3.01 to 3.12 ppm) of **3.1** in C_6D_6 displaying the *meso H* signal of the *exo* isomer (400 MHz).

The orientation of the allyl ligand is deduced from the chemical shift of the *meso* signal in the ^{1}H NMR spectrum. Previously the molecular structures in solution of the analogous (η^5-

C_5Me_5)W(NO)(H)(η^3-CH_2CHCMe_2) complex have been determined using Sel NOE and NOESY NMR spectroscopy.[31] There is a correlation between the *meso H* signal in the ^{1}H NMR spectra and the *endo/exo* orientation of the allyl ligand such that *endo* isomers have a more downfield signal compared to the *exo* isomer: 4.71 ppm vs 2.68 ppm respectively.[31] The same trend is also observed in similar complexes with different allyl ligands. 23.9 % of the final product mixture of **3.1** in C_6D_6 is the *endo* isomer **3.1b** with the *meso H* signal having a more downfield chemical shift, as expected, at δ 4.40 ppm in the ^{1}H NMR spectrum (Figure 3.1b). The other two isomers with the 1,1-dimethylallyl ligand proximal to the nitrosyl ligand comprise the rest of the final product mixture. This trend in the isomer distribution in solution is consistent with the analogous (η^5-C_5Me_5) system, and it is attributable primarily to steric factors.[31]

The IR-stretching frequency of the nitrosyl ligand of **3.1** as a Nujol mull is 1614 cm^{-1}, which is higher than the 1601 cm^{-1} exhibited by its η^5-C_5Me_5 analogue. This feature is again due to a less inductively donating η^5-$C_5H_4{}^i$Pr ligand, and as a result a smaller degree of tungsten-nitrosyl back-bonding.

Recrystallization of **3.1** from Et_2O at -33 °C for one week affords yellow crystals suitable for a single-crystal X-ray diffraction analysis. The solid-state molecular structure of this complex has a three-legged piano stool geometry capped with the cyclopentadienyl ligand (Figure 3.2). Only one coordination isomer is observed in the solid state, namely **3.1a**. It has the 1,1-dimethyl allyl ligand in the *exo* orientation with methyl groups proximal to the hydride ligand. This coordination isomer is the major product in solution based on the NMR spectroscopic analysis. The σ-π distortion of the allyl ligand is evident with C(9)-C(10) and C(10)-C(11) bond lengths of 1.460(10) and 1.388(10) Å accordingly. The shorter bond is *trans* to the π-acceptor nitrosyl ligand. This arrangement results in a strong backbonding interaction

leaving less electron density at the metal centre for back-donation to the allyl C(10)-C(11) bond. This phenomenon is also evident in the ^{13}C APT NMR spectrum with the C(9) signal having a significantly more upfield shift at 33.0 ppm compared to C(10) and C(11) signals at 100.5 and 98.1 ppm accordingly.

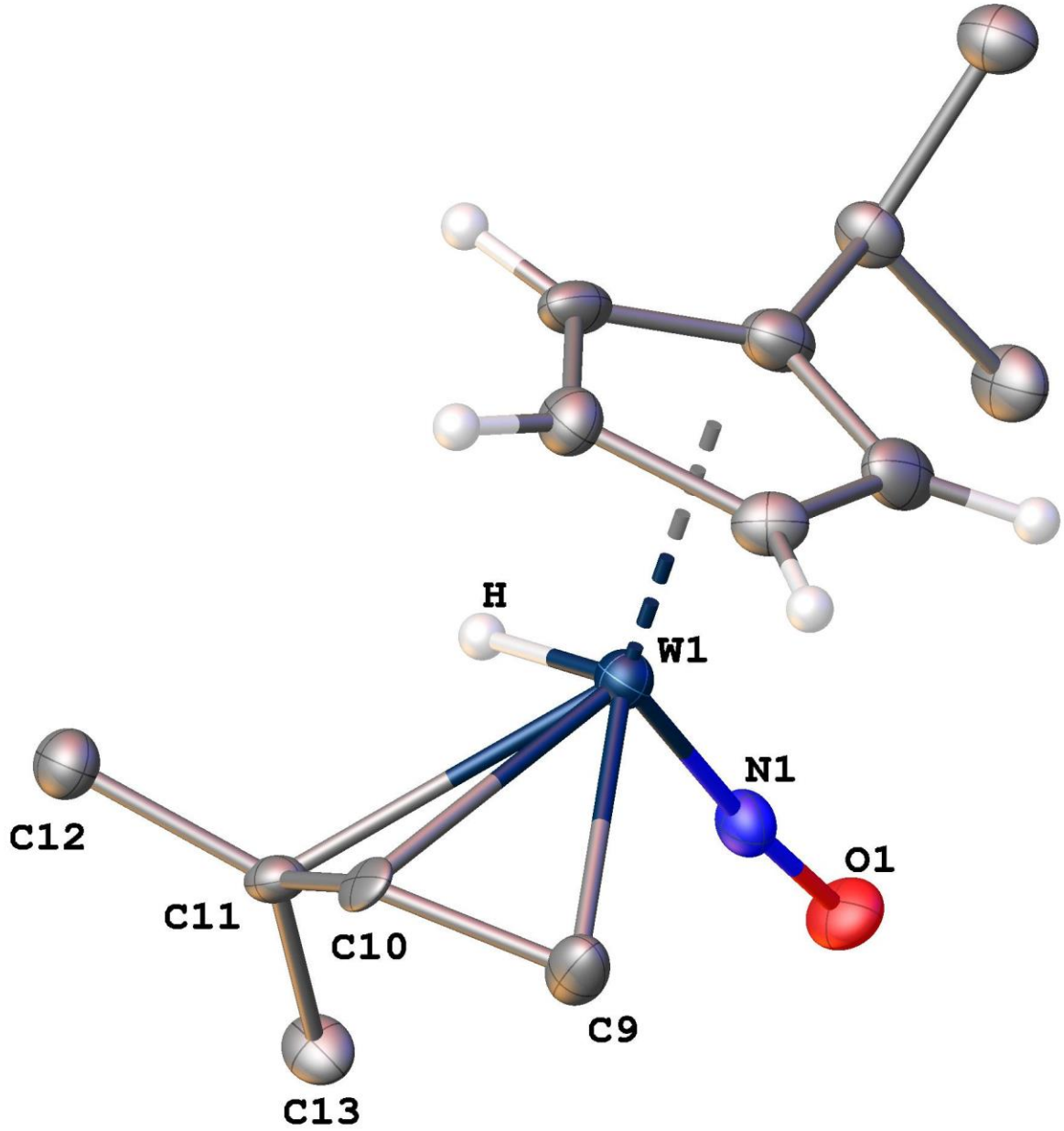

Figure 3.2. Solid-state molecular structure of **3.1** with 50% probability thermal ellipsoids. Some hydrogen atoms have been omitted for clarity. Selected bond lengths (Å) and angles (deg): W(1)-N(1) = 1.723(7), N(1)-O(1) = 1.205(9), C(9)-C(10) = 1.460(10), C(10)-C(11) = 1.388(10), C(11)-C(12) = 1.509(10), C(11)-C(13) = 1.519(7), W(1)-C(9) = 2.286(7), W(1)-C(10) = 2.338(7), W(1)-C(11) = 2.531(7), W(1)-N(1)-O(1) = 174.8(6), C(9)-C(10)-C(11) = 123.1(6), C(12)-C(11)-C(13) = 114.3(6).

3.2.1.2 Trapping Reactions with a Lewis Base

Previous investigations of the family of (η^5-C_5Me_5)W(NO)(H)(η^3-allyl) complexes [η^3-allyl = η^3-CH_2CHCMe_2; η^3-$CH_2CHCHMe$; η^3-$CH_2CHCHPh$] have shown that upon thermolysis the lowest-energy thermal-decomposition pathway involves the formation of the (η^5-C_5Me_5)W(NO)(η^2-alkene) intermediate which then effects intermolecular C-H activations of substrates.[31,46] In order to investigate the thermal behaviour of **3.1**, it has been thermalized in the presence of PMe_3 to trap any coordinatively unsaturated intermediates generated. Thermolysis of the reaction mixture of **3.1** in PMe_3 at 60 ºC for 16 h results in a complete conversion of the starting material to (η^5-$C_5H_4{}^iPr$)W(NO)(H)(η^1-$CH_2CH{=}CMe_2$)(PMe_3) (**3.2**) (Scheme 3.4). This complex exists as a single coordination isomer in solution. The IR nitrosyl-stretching frequency of **3.2** is 1552 cm^{-1}, which is significantly lower than in **3.1** with a υ_{NO} = 1614 cm^{-1}. This observation is indicative of a weaker NO bond in **3.2** resulting from a greater degree of tungsten-nitrosyl backbonding. In comparison to the starting material, the PMe_3 adduct of the η^1-intermediate has more electron density at the metal centre due to the presence of the Lewis basic phosphine ligand in the metal's coordination sphere.

Scheme 3.4. Thermolysis of 3.1 in PMe_3 at 60 ºC

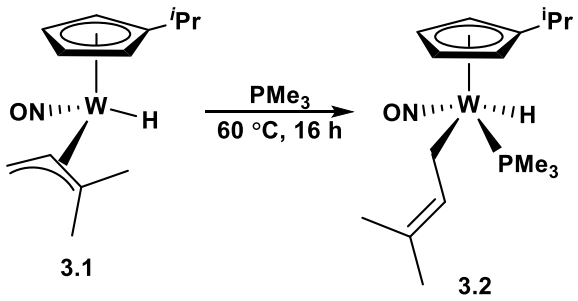

3.1 3.2

Interestingly, there is no evidence for the formation of the η^2-alkene intermediate even after three days at this temperature. The reaction conditions employed in the trapping reaction of the η^2-alkene unsaturated intermediate in the $(\eta^5\text{-}C_5Me_5)W(NO)(H)(\eta^3\text{-}CH_2CHCMe_2)$ system have been replicated in the thermolysis of **3.1** in PMe_3.[31] Nevertheless, the desired PMe_3 adducts of the η^2-alkene intermediates have not been detected even after maintaining the reaction mixture at 80 ºC for 18 h. Only after three days does the thermolysis reaction at 80 ºC yield the desired adducts (Scheme 3.5).

Scheme 3.5. Thermolysis of 3.1 in PMe_3 at 80 ºC for 3 days

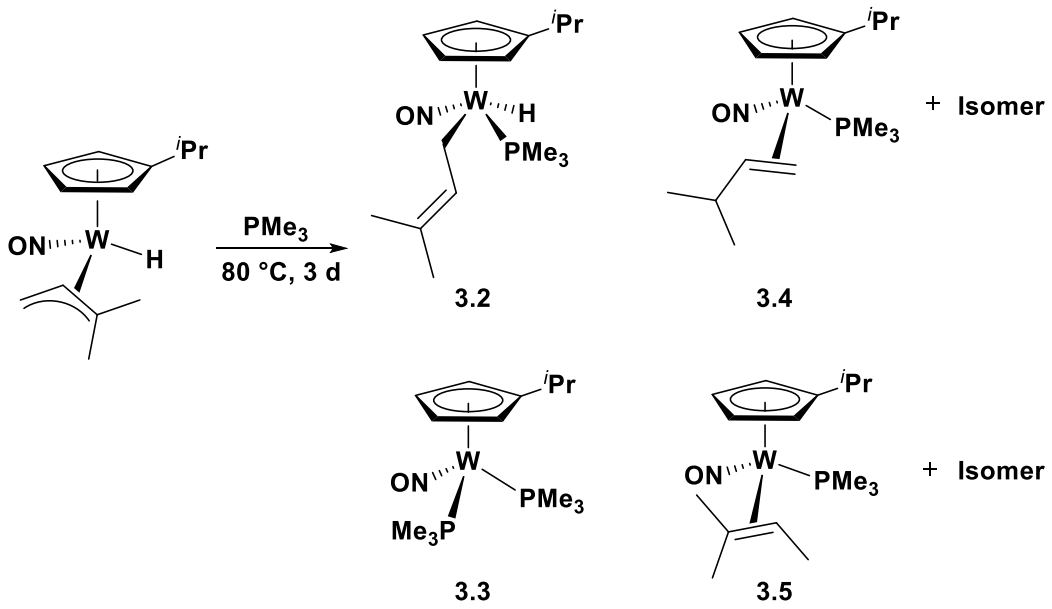

In the case of the $\eta^5\text{-}C_5Me_5$ system, three isomers of the PMe_3 adduct of the η^2-alkene intermediate comprise 37% of the final reaction mixture by ^1H NMR spectroscopy, while the rest is $(\eta^5\text{-}C_5Me_5)W(NO)(PMe_3)_2$ (63%).[31] In contrast, in the case of **3.1**, even after three days the PMe_3 adduct of the η^1-intermediate persists in the reaction mixture. Six products can be identified in the final reaction mixture via ^1H and $^{31}P\{^1H\}$ NMR spectroscopies (Figure 3.3),

including **3.2**, (η^5-$C_5H_4{}^i$Pr)W(NO)(PMe_3)$_2$ (**3.3**), two coordination isomers of (η^5-$C_5H_4{}^i$Pr)W(NO)(η^2-CH_2=CHCHMe_2)(PMe_3) (**3.4**), and two coordination isomers of (η^5-$C_5H_4{}^i$Pr)W(NO)(η^2-MeCH=CMe_2)(PMe_3) (**3.5**). The orientation of the η^2-ligand in **3.4** and **3.5** is proposed to be such that the steric interactions between the ligand and the methyl groups of the PMe_3 are minimized. These complexes can be differentiated by their ^{1}H NMR spectra. Thus, the ^{1}H NMR spectrum of **3.5** has three singlets due to the three methyl groups of the η^2-MeCH=CMe_2 ligand at 1.47, 1.81 and 2.33 ppm; while the ^{1}H NMR spectrum of **3.4** has only two singlets due to the two methyl groups of the η^2-CH_2=CHCHMe_2 ligand at 1.50 and 1.57 ppm. All products have been partially separated by column chromatography prior to their characterization by NMR spectroscopy.

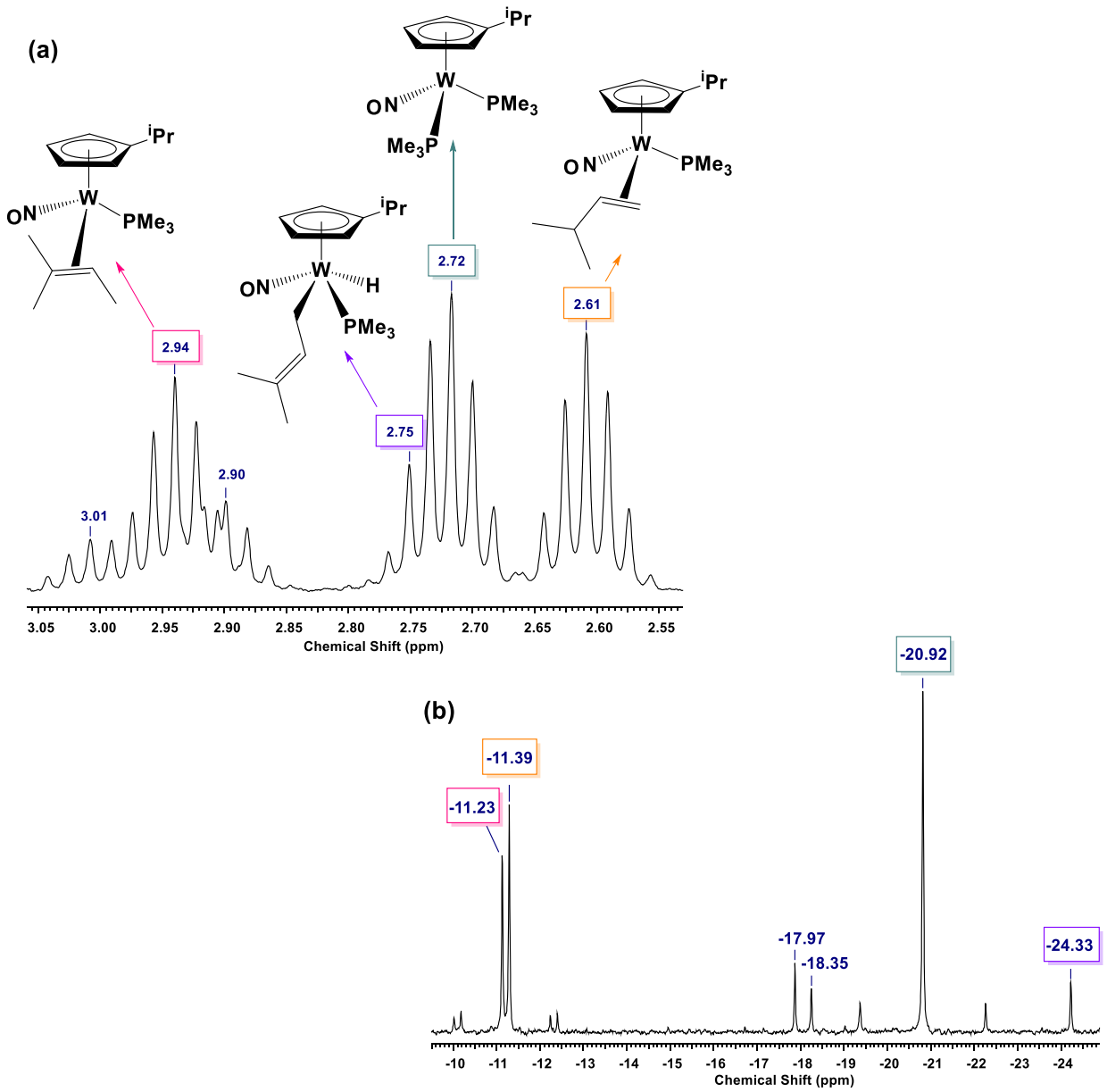

Figure 3.3. (a) Expansion of the ^{1}H NMR spectrum (δ 2.55 to 3.05 ppm) of the product mixture resulting from the thermolysis reaction of **3.1** in PMe_3 at 80 °C for 3 days displaying the signals due to η^5-$C_5H_4CHMe_2$ protons (C_6D_6, 400 MHz). (b) Expansion of the $^{31}P\{^{1}H\}$ NMR spectrum (δ -25 to -10 ppm) of the final product mixture resulting from the thermolysis reaction of **3.1** in PMe_3 at 80 °C for 3 days displaying phosphorus resonances (C_6D_6, 162 MHz).

The $^{31}P\{^{1}H\}$ NMR spectrum of the final reaction mixture (Figure 3.3) displays six resonances due to W-*P*Me_3 phosphorus nuclei. The singlet at -20.9 ppm with tungsten-183 satellites having $^{1}J_{PW}$ = 217 Hz is due to the phosphorus atom of **3.3**. The resonances due to phosphorus nuclei in the trapped η^2-alkene intermediates have more downfield shifts (-18.35 to -11.23 ppm) with much larger coupling constants ($^{1}J_{PW}$ = 358 Hz), which are in the range typical for (η^5-C_5Me_5)W(NO)(η^2-alkene)(PMe_3) complexes.[31]

Two signals at -17.97 and -18.35 ppm in the $^{31}P\{^{1}H\}$ NMR spectrum of the product mixture are proposed to be due to PMe_3 ligands of the minor coordination isomers of **3.4** and **3.5**. The large number of products prevented further analysis via NOESY NMR spectroscopy to determine the exact coordination of the η^2-ligands in **3.4**, **3.5**, and their coordination isomers in solution.

3.2.1.3 Thermolysis of 3.1 in Hydrocarbons

Thermolyses of **3.1** in *n*-pentane at 60 ºC and at 80 ºC for various durations do not yield any tractable organometallic products, namely the expected (η^5-$C_5H_4{}^{i}Pr$)W(NO)(H)(η^3-$CH_2CHCHEt$), (η^5-$C_5H_4{}^{i}Pr$)W(NO)(H)(η^3-MeCHCHCHMe) and their coordination isomers. Upon thermolysis the reaction mixture changes colour from yellow to dark brown with a brown residue forming at the bottom of the reaction flask. The starting material appears to decompose at higher temperatures in the absence of a Lewis base to capture any coordinatively unsaturated complexes that form along the way. In contrast, the analogous (η^5-C_5Me_5) system when thermolized in the presence of a *n*-alkane undergoes intramolecular isomerization to the η^2-

alkene intermediate followed by the multiple C-H activation of the substrate accompanied by the loss of the original allyl ligand and formation of the new allyl-hydride complex.[46]

Trapping experiments involving (η^5-$C_5H_4{}^iPr$)W(NO)(H)(η^3-CH_2CHCMe_2) have demonstrated that it is resistant to the formation of the η^2-alkene intermediate under typical reaction conditions. Increasing the temperature helps the intramolecular rearrangement of **3.1** to the desired intermediate, but unfortunately C-H activation cannot be carried out at very high temperatures due to the thermal instability of the starting material and the possible product.

3.2.2 Synthesis and Thermal Chemistry of (η^5-$C_5H_4{}^iPr$)W(NO)(H)[κ^2-(C_6H_4)PPh_2]

3.2.2.1 Synthesis of *trans*-(η^5-C_5Me_5)W(NO)(H)[κ^2-(C_6H_4)PPh_2] (3.6)

The overnight reaction at ambient temperatures of (η^5-C_5Me_5)W(NO)(CH_2CMe_3)$_2$ in *n*-pentane with PPh_3 under 1 atm of H_2 results in a complete conversion of the starting material to *cis*-(η^5-C_5Me_5)W(NO)(H)(κ^2-$PPh_2C_6H_4$).[49] This complex is formed from the (η^5-C_5Me_5)W(NO)(PPh_3) intermediate via intramolecular C-H activation of the phenyl substituent on the PPh_3 ligand at the *ortho* position. Thermolysis of *cis*-(η^5-C_5Me_5)W(NO)(H)(κ^2-$PPh_2C_6H_4$) in benzene at 50 °C for 24 h results in the C-H activation of the substrate yielding the *cis*-(η^5-C_5Me_5)W(NO)(H)(Ph)(PPh_3) complex.[47] In contrast, thermolysis of the *cis*-(η^5-C_5Me_5)W(NO)(H)(κ^2-$PPh_2C_6H_4$) in *n*-pentane at 80 °C results in it isomerizing to *trans*-(η^5-C_5Me_5)W(NO)(H)(κ^2-$PPh_2C_6H_4$) (**3.6**).[48] Unfortunately, the isolation of the product of the intramolecular isomerization obtained via this route has not been successful.

Scheme 3.6. Reaction of (η^5-C_5Me_5)W(NO)(η^3-CH_2CHCMe_2)(Ph) with PPh_3

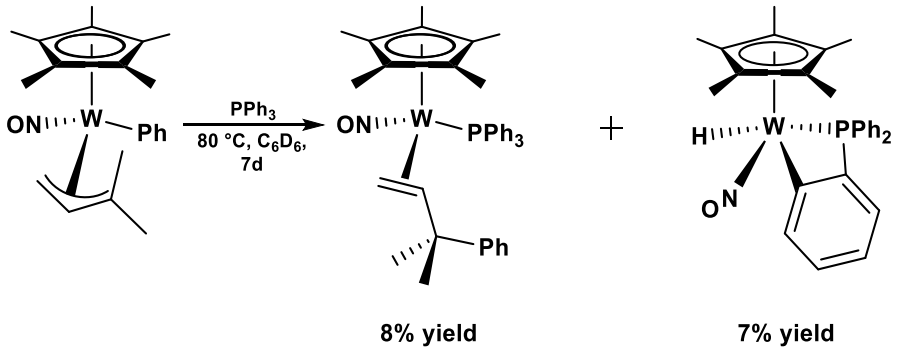

The alternative way of preparation of **3.6** involves the reaction of (η^5-C_5Me_5)W(NO)(η^3-CH_2CHCMe_2)(Ph) with excess PPh_3 in benzene-d_6, in an attempt to isolate the coupled product, namely (η^5-C_5Me_5)W(NO)(η^2-H_2C=$CHCMe_2Ph$)(PPh_3) (Scheme 3.6).[26] After maintaining the reaction mixture at 70 °C for 8 days, **3.6** can be extracted with pentane from the crude reaction mixture. Then it can be recrystallized from pentane, affording a light yellow solid in 7% yield. Formation of this complex results from the displacement of the coupled allyl-phenyl product and subsequent intramolecular C-H activation of the PPh_3 ligand followed by the intramolecular isomerization from the *cis* to the *trans* isomer.

3.2.2.2 Synthesis of (η^5-$C_5H_4{}^i$Pr)W(NO)(CH_2CMe_3)$_2$ (3.7) and its Reactivity with Oxygen

(η^5-$C_5H_4{}^i$Pr)W(NO)(CH_2CMe_3)$_2$ (**3.7**) can be synthesized from **2.2** via a metathesis reaction with one equivalent of Mg(CH_2CMe_3)$_2$ binary reagent affording a burgundy red solid. Similar to **2.3**, this complex effects C-H activations of aryl substituents at a much faster rate than its η^5-C_5Me_5 analogue ($k = 1.2(1) \times 10^{-4}$ s^{-1} vs $k = 4.6(1) \times 10^{-5}$ s^{-1}).[27,50] This trend is also attributable to the less electron-donating nature of the η^5-$C_5H_4{}^i$Pr ligand and the resulting

electron-poor metal centre reflected by the nitrosyl stretching-frequency of 1594 cm^{-1} comparing to 1557 cm^{-1} in the η^5-C_5Me_5 analogue.[36]

The family of 16e complexes Cp'M(NO)$(R)_2$ [M = Mo, W, R = CH_2SiMe_3, CH_2CMe_3, CH_2CMe_2Ph, or CH_2Ph) when treated with molecular oxygen under ambient conditions produce dioxo alkyl complexes Cp'M$(O)_2$(R).[51] Similarly, when exposed to oxygen **3.7** converts to (η^5-$C_5H_4{}^iPr$)W$(O)_2(CH_2CMe_3)$ (**3.8**). The ^{1}H NMR spectrum of this complex displays a resonance at 2.17 ppm with tungsten-183 satellites having $^1J_{HW}$ = 11.2 Hz assigned to CH_2CMe$_3$ (Figure 3.4). The two protons appear anisotropically equivalent unlike the methylene protons of the neopentyl ligands in the starting material, which have a large chemical shift difference in the ^{1}H NMR spectrum. In the spectrum of **3.7** one resonance appears at -1.43 ppm indicating a strong α-agostic interaction, while the second chemically inequivalent methylene proton signal occurs at 3.58 ppm and is assigned to the hydrogens on the neopentyl ligand that are not involved in an agostic interaction with the tungsten metal centre.

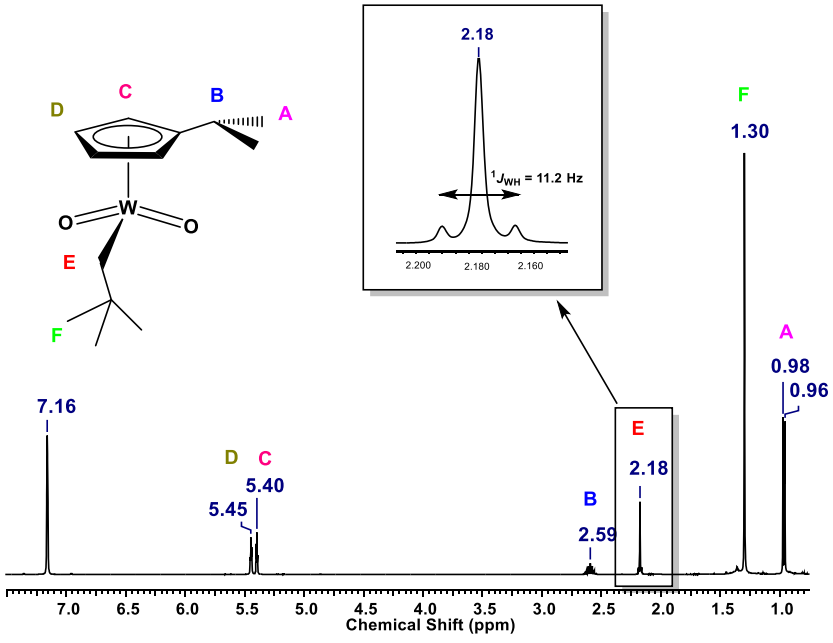

Figure 3.4. Expansion of the ^{1}H NMR spectrum (δ 0.80 to 7.50 ppm) of **3.8** (C_6D_6, 400 MHz).

3.2.2.3 Synthesis of *trans*-(η^5-$C_5H_4{}^iPr$)W(NO)(H)(κ^2-$PPh_2C_6H_4$) (3.9)

The overnight reaction of **3.7** with PPh_3 in *n*-pentane under 1 atm H_2 results in a complete conversion of the starting material to *trans*-(η^5-$C_5H_4{}^iPr$)W(NO)(H)(κ^2-$PPh_2C_6H_4$) (**3.9**). (Scheme 3.7) This complex has been fully characterized in solution and in the solid state. The signal due to the hydride ligand in the ^1H NMR spectrum of this complex has an almost identical chemical shift and coupling constants to the analogous signal exhibited by **3.6** (Figure 3.5).

Scheme 3.7. Synthesis of 3.9

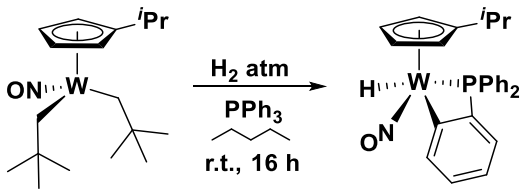

While the isomerization from the *cis* to *trans* isomer in the η^5-C_5Me_5 system occurs upon thermolysis, in the η^5-$C_5H_4{}^iPr$ complex this transformation occurs instantaneously and there is no evidence for the *cis* isomer being present in the reaction mixture. In other words, replacement of η^5-C_5Me_5 with the η^5-$C_5H_4{}^iPr$ ligand in this system enhances the rate of *cis* to *trans* isomerization rather than simply facilitating intramolecular C-H activation and formation of the reactive *cis* isomer.

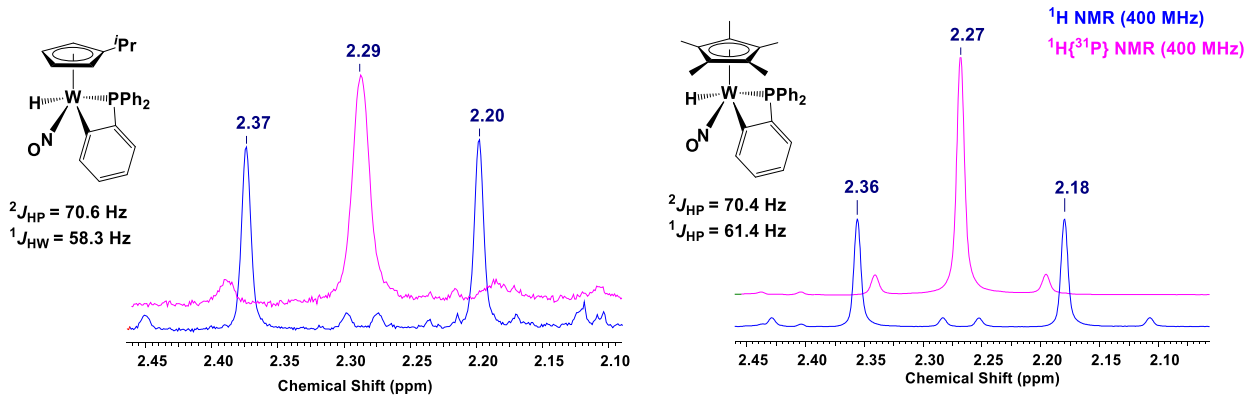

Figure 3.5. (a) Expansion of the overlaid ^{1}H (blue) and $^{1}H\{^{31}P\}$ (pink) NMR spectra (δ 2.10 to 2.45 ppm) of **3.9** in C_6D_6 (400 MHz). (b) Expansion of the overlaid ^{1}H (blue) and $^{1}H\{^{31}P\}$ (pink) NMR spectra (δ 2.05 to 2.45 ppm) of *trans*-(η^5-C_5Me_5)W(NO)(H)(κ^2-$PPh_2C_6H_4$) in C_6D_6 (400 MHz).

The infrared nitrosyl stretching-frequency of **3.9** is 1579 cm^{-1}, which is significantly higher than that of the analogous **3.6** (1552 cm^{-1}). This fact is again typical when comparing complexes with such substituents on the cyclopentadienyl ligand.

Recrystallization of **3.9** from CH_2Cl_2/hexanes at -33 °C affords yellow crystals suitable for a single-crystal X-ray diffraction analysis (Figure 3.6). This complex is a four-legged piano-stool molecule capped by a η^5-$C_5H_4{}^{i}Pr$ ligand with the hydride ligand situated *cis* to the phosphorus atom. The nitrosyl ligand is linear and the W(1)-P(1) bond length is similar to those found in previously investigated four-legged piano stool molecules.[25,26,31]

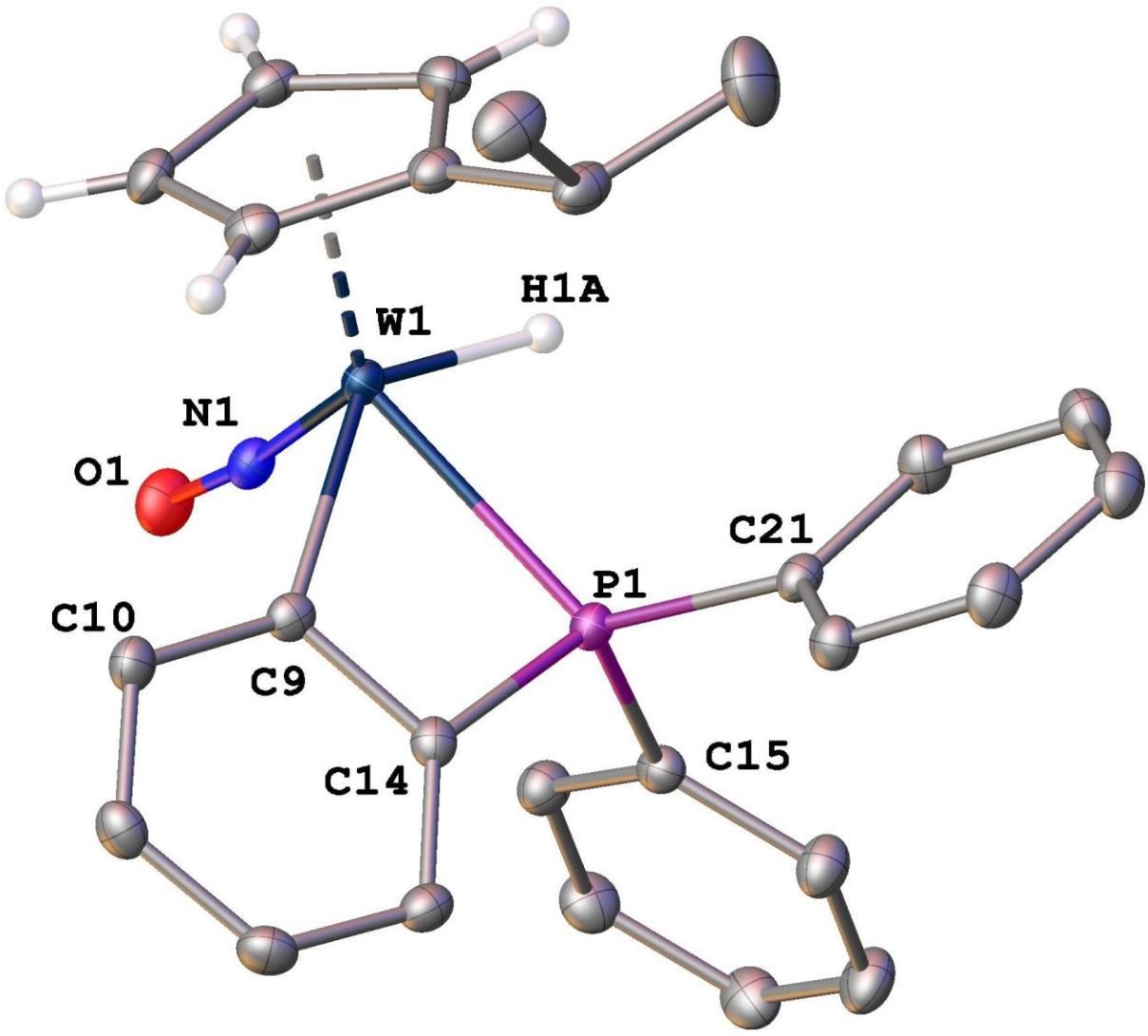

Figure 3.6. Solid-state molecular structure of **3.9** with 50% probability thermal ellipsoids. Some hydrogen atoms have been omitted for clarity. Selected bond lengths (Å) and angles (deg): W(1)-H(1A) = 1.64(2), W(1)-P(1) = 2.4892(5), W(1)-C(9) = 2.2134(18), P(1)-C(14) = 1.7870(19), P(1)-C(15) = 1.823(2), P(1)-C(21) = 1.8124(19), W(1)-N(1) = 1.7837(17), N(1)-O(1) = 1.226(2), C(9)-C(14) = 1.406(3), W(1)-N(1)-O(1) = 173.21(14), C(9)-W(1)-P(1) = 62.34(5), W(1)-C(9)-C(14) = 110.52(13), P(1)-C(14)-C(9) = 99.27(13), W(1)-P(1)-C(14) = 87.87(6).

3.2.2.4 Thermolysis of 3.9 in Hydrocarbons

Complex **3.9** is an air- and moisture-stable solid that is also quite thermally stable. For instance, heating of a C_6D_6 solution of this complex at 80 ºC for several days results in only minimal decomposition of the organometallic complex and no activation of the solvent as determined by NMR spectroscopy. Thermolysis at higher temperatures has also been attempted yielding similar results.

The proposed mechanism of the intermolecular C-H activation of benzene by *cis*-(η^5-C_5Me_5)W(NO)(H)(κ^2-$PPh_2C_6H_4$) is based on the formation of the (η^5-C_5Me_5)W(NO)(PPh_3) intermediate, which then effects the desired transformation (Scheme 3.2).[47] Nevertheless, the *trans* isomer of this complex also appears to be inert. This observation can be explained by the possible difficulty of intramolecular reductive elimination of the phenyl group of the PPh_3 ligand and formation of the reactive 16e intermediate. This kind of transformation is only possible when the hydride ligand is located *cis* to the phenyl end of the κ^2-$PPh_2C_6H_4$ ligand.

Again the η^5-$C_5H_4{}^i$Pr ligand has imparted distinctive chemical properties to another tungsten-nitrosyl system. In this case, increasing the rate of isomerization from the *cis* to *trans* isomer hinders the C-H activation chemistry of the complex.

3.3 Summary

Complex **3.1** shows preferential isomerization to the η^1 intermediate (η^5-$C_5H_4{}^i$Pr)W(NO)(H)(η^1-$CH_2CH{=}CMe_2$), isolable as its PMe_3 adduct **3.2**, rather than the formation of the reactive η^2 intermediates (η^5-$C_5H_4{}^i$Pr)W(NO)(H)(η^2-$CH_2{=}CHCHMe_2$) and (η^5-

$C_5H_4{}^iPr)W(NO)(H)(\eta^2$-MeCH=$CMe_2$), isolable as their PMe_3 adducts **3.4** and **3.5**, under typical thermal conditions. Increasing the temperature helps the intramolecular rearrangement to the desired intermediate, but unfortunately C-H activation cannot be carried out at very high temperatures due to the thermal instability of the starting material or of any products formed. In the absence of a Lewis base to trap the coordinatively unsaturated species formed upon isomerization of the hydride, decomposition of the starting material occurs.

Alternatively, replacement of η^5-C_5Me_5 with the η^5-$C_5H_4{}^iPr$ ligand in the reaction of **3.7** with hydrogen gas and PPh_3 enhances the rate of *cis* to *trans* isomerization of the ortho-metallated complex to form **3.9**, rather than simply facilitating the intramolecular C-H activation and formation of the reactive *cis* isomer. In this case, the complex is very reactive thereby hindering the C-H activation mode of reactivity.

3.4 Experimental Section

Reactions described in this section were performed following the general experimental procedures outline in section 2.4.1.

3.4.1 Synthesis of (η^5-$C_5H_4{}^iPr$)W(NO)(H)(η^3-CH_2CHCMe_2) (3.1)

In a glove box, a Schlenk flask was charged with **2.2** (2.209 g, 3.843 mmol) and a stir bar. A second reaction flask was charged with $Mg(CH_2CH=CMe_2)_2$ (titre:144 g/mol, 0.579 g, 4.021 mmol) and a magnetic stir bar. Once connected to the double manifold, THF was cannulated into each flask (ca. 100 mL each), and the reaction flasks were placed into a dry

ice/acetone bath. Afterwards, the contents of the second flask were slowly cannulated into the Schlenk flask containing the organometallic reagent dissolved in THF. Following the addition, the reaction mixture was allowed to warm to room temperature and was then stirred for 1 h to obtain a brown mixture. The Schlenk flask was then placed into a dry ice/acetone bath, and 2 equivalents of $LiBH_4$ (3.8 mL, 7.6 mmol, 2.0 M in THF) were slowly added via syringe. Then the reaction flask was removed from the dry ice/ acetone bath, and its contents were warmed to room temperature and stirred for two hours affording a dark brown reaction mixture. The solvent was then removed in vacuo, and the resulting residue was dissolved in Et_2O (ca. 150 mL). Liquid-liquid extractions with distilled water (3 x 50 mL) were carried out, and the organic layer was dried over anhydrous $MgSO_4$. After removing the solvents in vacuo from the organic layer, a dark brown residue has been obtained and purified by flash chromatography on silica. A yellow band was eluted with a gradient of 0-20% EtOAc in hexanes affording a yellow eluate. Solvent was removed from the eluate in vacuo to obtain **3.1** as a dark yellow oil (0.365 g, 0.993 mmol, 24% yield). Recrystallization of **3.1** from Et_2O at -33 °C for one week afforded yellow crystals suitable for a single-crystal X-ray diffraction analysis.

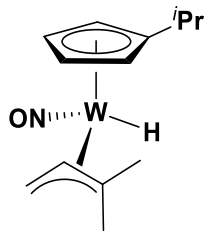

Characterization data for **3.1a** (73.4%). IR (cm^{-1}): 1614 (s, υ_{NO}). MS (LREI, *m/z*, probe temperature 150 °C): 391 [M^+, ^{184}W]. ^1H NMR (400 MHz, C_6D_6): δ -1.08 (s, $^1J_{HW}$ = 121.0, 1H, W-*H*), 1.07 (d, $^3J_{HH}$ = 6.9, 3H, *i*-Pr C*H*$_3$), 1.07 (d, $^3J_{HH}$ = 6.9, 3H, *i*-Pr C*H*$_3$), 1.85 (s, 3H, CH_2CHCMe_2), 2.10 (dd, $^3J_{HH}$ = 13.1, $^3J_{HH}$ = 3.0, 1H, C*H*$_2$CHCMe$_2$), 2.35 (s, 3H, CH_2CHCMe_2) ,

2.58 (sept, $^3J_{HH}$ = 6.9, 1H, *i*-Pr C*H*), 2.75 (dd, $^3J_{HH}$ = 7.8, $^3J_{HH}$ = 3.0, 1H, C*H*$_2$CHCMe$_2$), 3.08 (dd, $^3J_{HH}$ = 13.1, $^3J_{HH}$ = 7.8, 1H, CH$_2$C*H*CMe$_2$), 4.59 (m, 1H, C$_5$*H*$_4$(*i*-Pr)), 4.71 (m, 1H, C$_5$*H*$_4$(*i*-Pr)), 4.85 (m, 1H, C$_5$*H*$_4$(*i*-Pr)), 5.09 (m, 1H, C$_5$*H*$_4$(*i*-Pr)). ^{13}C APT NMR (100 MHz, C$_6$D$_6$): δ 24.0 (1C, CH$_2$CHC*Me*$_2$), 24.0 (*i*-Pr *C*H$_3$), 28.4 (*i*-Pr *C*H), 30.2 (1C, *C*H$_2$CHCMe$_2$), 32.0 (1C, CH$_2$CHC*Me*$_2$), 88.5 (CH$_2$*C*HCMe$_2$), 90.2 (*C*$_5$H$_4$(*i*-Pr)), 90.6 (*C*$_5$H$_4$(*i*-Pr)), 92.5 (*C*$_5$H$_4$(*i*-Pr)), 93.5 (*C*$_5$H$_4$(*i*-Pr)), 101.9 (CH$_2$CH*C*Me$_2$), 122.4 (*ipso*-*C*$_5$H$_4$(*i*-Pr)). Anal. Calcd. for C$_{13}$H$_{21}$NOW: C, 39.92; H, 5.41; N, 3.58. Found: C, 40.15; H, 5.58; N, 3.53.

Characterization data for **3.1b** (23.9%). ^{1}H NMR (400 MHz, C$_6$D$_6$): δ -0.63 (s, $^1J_{HW}$ = 119.0, 1H, W-*H*), 0.82 (s, 3H, CH$_2$CHC*Me*$_2$), 1.14 (d, $^3J_{HH}$ = 6.9, 3H, *i*-Pr C*H*$_3$), 1.15 (d, $^3J_{HH}$ = 6.9, 3H, *i*-Pr C*H*$_3$), 1.30 (dd, $^3J_{HH}$ = 11.7, $^3J_{HH}$ = 3.6, 1H, C*H*$_2$CHCMe$_2$), 2.45 (s, 3H, CH$_2$CHC*Me*$_2$) , 2.71 (sept, $^3J_{HH}$ = 6.9, 1H, *i*-Pr C*H*), 3.08 (dd, $^3J_{HH}$ = 7.2, $^3J_{HH}$ = 3.6, 1H, C*H*$_2$CHCMe$_2$), 4.40 (dd, $^3J_{HH}$ = 11.7, $^3J_{HH}$ = 7.2, 1H, CH$_2$C*H*CMe$_2$), 4.59 (m, 1H, C$_5$*H*$_4$(*i*-Pr)), 4.77 (m, 1H, C$_5$*H*$_4$(*i*-Pr)), 5.16 (m, 1H, C$_5$*H*$_4$(*i*-Pr)), 5.20 (m, 1H, C$_5$*H*$_4$(*i*-Pr)). ^{13}C APT NMR (100 MHz, C$_6$D$_6$): δ 23.9 (1C, CH$_2$CHC*Me*$_2$), 24.1 (*i*-Pr *C*H$_3$), 28.2 (*i*-Pr *C*H), 31.4 (1C, CH$_2$CHC*Me*$_2$), 33.0 (1C, *C*H$_2$CHCMe$_2$), 92.0 (*C*$_5$H$_4$(*i*-Pr)), 92.6 (*C*$_5$H$_4$(*i*-Pr)), 96.5 (*C*$_5$H$_4$(*i*-Pr)), 96.97 (*C*$_5$H$_4$(*i*-Pr)), 98.1 (CH$_2$CH*C*Me$_2$), 100.5 (CH$_2$*C*HCMe$_2$), 122.4 (*ipso*-*C*$_5$H$_4$(*i*-Pr)).

Characterization data for the remaining coordination isomers. (2.5%): δ -1.29 (s, $^1J_{HW}$ = 126.8, 1H, W-*H*). (0.2%): δ -1.55 (s, $^1J_{HW}$ = 116.0, 1H, W-*H*).

3.4.2 Preparation of (η^5-$C_5H_4{}^iPr$)W(NO)(H)(η^1-$CH_2CH{=}CMe_2$)(PMe_3) (3.2)

In a glove box, a small reaction flask was charged with **3.1** (0.067 g, 0.171 mmol) and excess PMe_3 (ca. 3 mL). The reaction mixture was placed in an ethylene-glycol bath maintained at 60 ºC for 16 h. After thermolysis, the colour of the solution changed from light yellow to a darker shade of yellow. Removal of the solvent in vacuo afforded the product as a yellow solid (0.076 g, 0.163 mmol, 95% yield). The same product was obtained when the reaction was carried out under an inert atmosphere at room temperature.

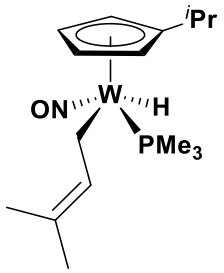

Characterization data for **3.2**. IR (cm^{-1}): 1552 (s, υ_{NO}). MS (LREI, *m/z*, probe temperature 150 °C): 467 [M^+, ^{184}W]. ^1H NMR (400 MHz, C_6D_6): δ -1.44 (d, $^2J_{HP}$ = 83.5, $^1J_{HW}$=58.6, 1H, W-*H*), 1.04 (d, $^2J_{HP}$ = 8.6, 9H, P*Me*$_3$), 1.17 (d, $^3J_{HH}$ = 6.9, 3H, *i*-Pr C*H*$_3$), 1.17 (d, $^3J_{HH}$ = 6.9, 3H, *i*-Pr C*H*$_3$), 1.86 (dd, $^3J_{HP}$ = 18.8, $^3J_{HH}$ = 10.2, 1H, C*H*$_2$CH=CMe$_2$), 1.98 (s, 3H, CH$_2$CH=C*Me*$_2$), 1.99 (s, 3H, CH$_2$CH=C*Me*$_2$), 2.30 (m, 1H, C*H*$_2$CH=CMe$_2$), 2.74 (sept, $^3J_{HH}$ = 6.9, 1H, *i*-Pr C*H*), 4.74 (dd, $^3J_{HH}$ = 4.9, $^3J_{HH}$ = 2.8, 1H, C$_5$*H*$_4$(*i*-Pr)), 5.05 (dd, $^3J_{HH}$ = 4.9, $^3J_{HH}$ = 2.8, 1H, C$_5$*H*$_4$(*i*-Pr)), 5.23 (m, 1H, C$_5$*H*$_4$(*i*-Pr)), 5.33 (m, 1H, C$_5$*H*$_4$(*i*-Pr)), 6.03 (m, 1H, CH$_2$C*H*=CMe$_2$). ^{13}C APT NMR (100 MHz, C_6D_6): δ 9.6 (d, $^2J_{CP}$ = 12.8, *C*H$_2$CH=CMe$_2$), 18.5 (1C, CH$_2$CH=C*Me*$_2$), 19.1 (d, $^1J_{PC}$ = 31.5, P*Me*$_3$), 23.8 (*i*-Pr *C*H$_3$), 24.6 (*i*-Pr *C*H$_3$), 26.4 (1C, CH$_2$CH=C*Me*$_2$), 28.4 (*i*-Pr *C*H), 90.4 (*C*$_5$H$_4$(*i*-Pr)), 93.5 (*C*$_5$H$_4$(*i*-Pr)), 93.5 (*C*$_5$H$_4$(*i*-Pr)), 99.4

(C_5H_4(*i*-Pr)), 121.1 (CH_2CHCMe_2), 122.0 (*ipso*-C_5H_4(*i*-Pr)), 136.1 (d, $^3J_{PC}$ = 11.8, 1C, $CH_2CH{=}CMe_2$). $^{31}P\{^1H\}$ NMR (162 MHz, C_6D_6) δ -24.3 ($^1J_{PW}$ = 217.0 Hz, PMe_3).

3.4.3 Trapping Reaction of 3.1 with PMe_3 at 80°C

In a glove box, a small reaction flask was charged with **3.1** (0.042 g, 0.107 mmol) and excess PMe_3 (3 mL). The reaction mixture was placed in an ethylene-glycol bath maintained at 80 ºC for 3 d. After thermolysis, the colour of the solution had changed from light yellow to a dark yellow. Removal of the solvent *in vacuo*, afforded the mixture of products as a yellow solid (39 mg).

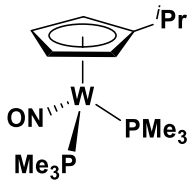

Characterization data for **3.3** (40%). ^1H NMR (400 MHz, C_6D_6): δ 1.23 (d, $^3J_{HH}$ = 6.9, 6H, *i*-Pr CH_3), 1.32 (d, $^2J_{HP}$=7.82, 18H, P*Me*$_3$), 2.72 (sept, $^3J_{HH}$ = 6.9, 1H, *i*-Pr C*H*), 4.26 (m, 2H, C_5H_4(*i*-Pr)), 5.14 (m, 2H, C_5H_4(*i*-Pr)). ^{13}C APT NMR (100 MHz, C_6D_6): δ 23.8 (*i*-Pr *C*H_3), 24.6 (*i*-Pr *C*H_3), 29.0 (*i*-Pr *C*H), 90.4 (C_5H_4(*i*-Pr)), 93.5 (C_5H_4(*i*-Pr)), 115.1 (*ipso*-C_5H_4(*i*-Pr)). $^{31}P\{^1H\}$ NMR (162 MHz, C_6D_6): δ -20.9 ($^1J_{PW}$ = 217, PMe_3).

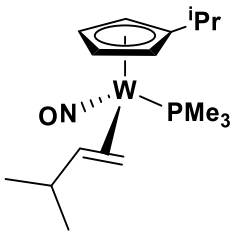

Characterization data for **3.4** (24%). ^{1}H NMR (400 MHz, C_6D_6): δ 0.67 (ddd, $^{3}J_{HH}$ = 9.8, $^{3}J_{HH}$ = 7.4, $^{2}J_{HH}$ = 5.3,1H, C*H*$_2$=CHCHMe$_2$), 0.87 (d, $^{2}J_{HP}$ = 12.7, 9H, P*Me*$_3$), 0.90 (d, $^{3}J_{HH}$ = 6.9, 3H, *i*-Pr C*H*$_3$), 1.21 (d, $^{3}J_{HH}$ = 6.9, 3H, *i*-Pr C*H*$_3$), 1.26 (obscured m, 1H, C*H*$_2$=CHCHMe$_2$), 1.50 (d, $^{3}J_{HH}$ = 6.3, 3H, CH$_2$=CHCH*Me*$_2$), 1.57 (d, $^{3}J_{HH}$ = 6.3, 3H, CH$_2$=CHCH*Me*$_2$), 1.85 (m, $^{3}J_{HH}$ = 6.3, 1H, CH$_2$=CHC*H*Me$_2$), 1.90 (m, 1H, CH$_2$=C*H*CHMe$_2$), 2.61 (sept, $^{3}J_{HH}$ = 6.9, 1H, *i*-Pr C*H*), 4.11 (dd, $^{3}J_{HH}$ = 2.6, 1H, C$_5$*H*$_4$(*i*-Pr)), 4.67 (m, 1H, C$_5$*H*$_4$(*i*-Pr)), 5.10 (s, 1H, C$_5$*H*$_4$(*i*-Pr)), 5.41 (s, 1H, C$_5$*H*$_4$(*i*-Pr)). ^{13}C APT NMR (100 MHz, C_6D_6): δ 17.9 (d, $^{1}J_{CP}$ = 32.5, P*Me*$_3$), 22.8 (*C*H$_2$=CHCHMe$_2$), 24.0 (*i*-Pr *C*H$_3$), 24.1 (*i*-Pr *C*H$_3$), 25.6 (CH$_2$=CHCH*Me*$_2$), 28.4 (*i*-Pr *C*H), 30.6 (CH$_2$=CHCH*Me*$_2$), 39.0 (CH$_2$=CH*C*HMe$_2$), 44.9 (CH$_2$=*C*HCHMe$_2$), 86.9 (*C*$_5$H$_4$(*i*-Pr)), 92.5 (*C*$_5$H$_4$(*i*-Pr)),94.5 (*C*$_5$H$_4$(*i*-Pr)), 95.1 (*C*$_5$H$_4$(*i*-Pr)), 123.6 (*ipso*-*C*$_5$H$_4$(*i*-Pr)). ^{31}P{^{1}H} NMR (162 MHz, C_6D_6): δ -11.4 ($^{1}J_{PW}$ = 358.0, *P*Me$_3$).

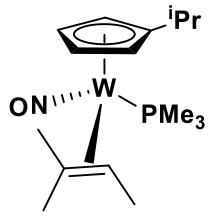

Characterization data for **3.5** (19%). ^{1}H NMR (400 MHz, C_6D_6): δ 0.87 (d, $^{2}J_{HP}$ =12.7, 9H, P*Me*$_3$), 1.31 (obscured, 6H, *i*-Pr C*H*$_3$), 1.47 (m, 3H, *Me*CH=CMe$_2$), 1.81 (s, 3H, MeCH=C*Me*$_2$), 1.94 (m, 1H, MeC*H*=CMe$_2$), 2.33 (s, 3H, MeCH=C*Me*$_2$), 2.94 (sept, $^{3}J_{HH}$ = 6.9, 1H, *i*-Pr C*H*), 3.93 (dd, $^{3}J_{HH}$ = 2.6, 1H, C$_5$*H*$_4$(*i*-Pr)), 4.69 (m, 1H, C$_5$*H*$_4$(*i*-Pr)), 4.88 (m, 1H, C$_5$*H*$_4$(*i*-Pr)), 5.54 (m, 1H, C$_5$*H*$_4$(*i*-Pr)). ^{13}C APT NMR (100 MHz, C_6D_6): δ 18.7 (P*Me*$_3$), 21.4 (*Me*CH=CMe$_2$), 23.1 (*i*-Pr *C*H$_3$), 28.3 (*i*-Pr *C*H), 29.3 (d, $^{3}J_{CP}$ = 1.5, MeCH=C*Me*$_2$), 37.5 (d, $^{3}J_{CP}$ = 1.5, MeCH=C*Me*$_2$), 41.6 (d, $^{3}J_{CP}$ = 10.8, Me*C*H=CMe$_2$), 84.3 (*C*$_5$H$_4$(*i*-Pr)), 95.5 (*C*$_5$H$_4$(*i*-Pr)), 97.0 (*C*$_5$H$_4$(*i*-Pr)), 97.9 (*C*$_5$H$_4$(*i*-Pr)), 125.7 (*ipso*-*C*$_5$H$_4$(*i*-Pr)). ^{31}P{^{1}H} NMR (162 MHz, C_6D_6): δ -11.2 ($^{1}J_{PW}$ = 358.0 Hz, *P*Me$_3$).

Partial characterization data for another coordination isomer (7%). ^{1}H NMR (400 MHz, C_6D_6): δ 1.17 (d, $^{2}J_{HP}$ = 7.4, 9H, P*Me*$_3$), 1.28 (obscured, 6H, *i*-Pr C*H*$_3$), 2.90 (sept, $^{3}J_{HH}$ = 6.9, 1H, *i*-Pr C*H*), 3.97 (m, 2H, C_5H_4(*i*-Pr)), 4.84 (m, 1H, C_5H_4(*i*-Pr)), 5.49 (m, 1H, C_5H_4(*i*-Pr)). ^{13}C APT NMR (100 MHz, C_6D_6): δ 19.3 (d, $^{1}J_{CP}$ = 29.5, P*Me*$_3$), 28.3 (*i*-Pr *C*H), 82.6 (*C*$_5$H$_4$(*i*-Pr)), 92.5 (*C*$_5$H$_4$(*i*-Pr)), 95.9 (*C*$_5$H$_4$(*i*-Pr)), 96.6 (*C*$_5$H$_4$(*i*-Pr)), 124.6 (*ipso*-*C*$_5$H$_4$(*i*-Pr)). ^{31}P{^{1}H} NMR (162 MHz, C_6D_6): δ -18.0 (*P*Me$_3$).

Partial characterization of coordination isomer (4%). ^{1}H NMR (400 MHz, C_6D_6): δ 3.01 (sept, $^{3}J_{HH}$ = 6.9, 1H, *i*-Pr C*H*). ^{31}P{^{1}H} NMR (162 MHz, C_6D_6): δ -18.0 (*P*Me$_3$).

3.4.4 Preparation of *trans*-(η^5-C$_5$Me$_5$)W(NO)(H)(κ^2-PPh$_2$C$_6$H$_4$) (3.6)

In a glove box a thick-walled flask equipped with a Kontes stopcock was loaded with (η^5-C$_5$Me$_5$)W(NO)(η^3-CH$_2$CHCMe$_2$)(Ph) (0.095 g, 0.192 mmol), benzene-*d*$_6$ (ca. 5 mL), and an excess of PPh$_3$ (0.059g, 0.225 mmol) to obtain a yellow mixture. The reaction flask was sealed, and its contents were heated for 8 d in an ethylene-glycol bath at 70 ˚C during which time the colour of the solution changed to dark brown. Removal of the solvent in vacuo produced a dark brown oil that was dissolved in a 1:1 mixture of Et$_2$O and *n*-pentane, and the solution was maintained at -30 ˚C for 14 h to induce the deposition of a light orange precipitate (0.046 g). The precipitate was removed by filtration, and the brown filtrate was left at room temperature for 10 min whereupon a light yellow precipitate deposited. This product was identified as **3.6** (0.008 g, 0.013 mmol, 7% yield).

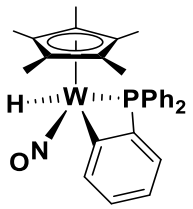

Characterization data for **3.7**. IR (cm^{-1}): 1552 (s, υ_{NO}). MS (LREI, *m/z*, probe temperature 150 ˚C): 611 [M^+, ^{184}W]. HR-MALDI-TOF (LDI) *m/z*: [M^+, ^{184}W] Calcd for $C_{28}H_{30}NOP^{184}W$ 611.15746. Found 611.15796. ^1H NMR (400 MHz, C_6D_6): δ 1.75 (s, 15H, $C_5\mathit{Me}_5$), 2.29 (d, $^2J_{HP}$ = 70.4, $^1J_{HW}$ =61.1, 1H, W*H*), 6.88 (m, 1H, aryl *H*), 6.93 (m, 1H, *m*-aryl *H*), 6.98-7.04 (m, 5H, aryl *H*), 7.01 (m, 1H, *m*-aryl *H*), 7.31 (t, 1H, $^3J_{HH}$ = 7.4, *p*-aryl *H*), 7.39 (m, 2H, aryl *H*), 7.79 (dd, 1H, $^3J_{HH}$ = 7.8, $^3J_{HP}$ = 3.1, *o*-aryl *H*), 7.94 (m, 2H, aryl *H*). ^{13}C NMR(100 MHz, C_6D_6): δ 11.1 (s, $C_5\mathit{Me}_5$), 106.1 (s, C_5Me_5), 125.4 (d, J_{CP} = 8.3, aryl *C*), 129.9 (d, J_{CP} = 9.2, aryl *C*), 129.2 (aryl *C*), 130.0 (d, $^3J_{CP}$ = 1.8, *m*-aryl *C*), 131.2 (d, $^3J_{CP}$ = 2.8, *m*-aryl *C*), 132.2 (d, $^4J_{CP}$ = 4.6, *p*-aryl *C*), 132.7 (d, J_{CP} = 10.1, aryl *C*), 134.2 (d, $^1J_{CP}$ = 41.4, *ipso*-aryl *C*), 135.2 (d, J_{CP} = 11.9, aryl *C*), 139.1 (d, $^2J_{CP}$ = 27.6, *o*-aryl C), 151.5 (s, *ipso*-aryl *C*), 167.8 (d, $^1J_{CP}$ = 14.7, *ipso*-aryl *C*). ^{31}P NMR (162 MHz, C_6D_6): δ -39.5 ($^1J_{PW}$ = 148.5, $C_6H_4\mathit{P}Ph_2$).

3.4.5 Synthesis of (η^5-$C_5H_4{}^i$Pr)W(NO)(CH_2CMe_3)$_2$ (3.7).

In a glove box two Schlenk flasks were charged with **2.2** (5.062 g, 8.806 mmol) and $Mg(CH_2CMe_3)_2$ (titer: 179 g/mol, 3.158 g, 17.64 mmol), respectively. Et_2O (150 mL) was cannulated into both flasks which were then placed into a dry ice/acetone bath at -78 ˚C. The contents of the second Schlenk flask containing the binary magnesium reagent were slowly cannulated into the Schlenk flask containing **2.2**. Upon addition the reaction mixture changed colour from dark green to light red. The reaction flask was removed from the dry ice/acetone

bath and left to warm to room temperature for 20 min while its contents were being stirred. The volume of the reaction mixture was then reduced in vacuo and transferred to the top of a basic alumina column (4 x 2 cm). Elution of the column with Et_2O as eluant developed a bright red band that was collected. Removal of solvent from the eluate in vacuo afforded **3.7** as a red solid (0.985 g, 2.127 mmol, 24% yield).

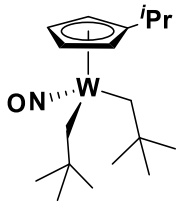

Characterization data for **3.7**. IR (cm^{-1}): 1594 (s, υ_{NO}). MS (LREI, *m/z*, probe temperature 150 ˚C): 463 [M^+, ^{184}W]. HRMS-EI *m/z*: [M^+, ^{182}W] Calcd for $C_{18}H_{33}NO^{182}W$ 461.20444 Found 461.20414. ^1H NMR (400 MHz, C_6D_6): δ -1.43 (d, $^2J_{HH}$ = 11.9, 2H, C*H*$_2$CMe$_3$), 0.97 (d, $^3J_{HH}$ = 6.9, 6H, ^{i}Pr C*H*$_3$), 1.34 (s, 18H, CH$_2$C*Me*$_3$), 2.49 (sept, $^3J_{HH}$ = 6.9, 1H, ^{i}Pr C*H*), 3.80 (d, $^2J_{HH}$ = 11.9, 2H, C*H*$_2$CMe$_3$), 5.08 (s, 4H, C$_5$*H*$_4$(^{i}Pr)). ^{13}C APT NMR (100 MHz, C_6D_6): δ 23.7 (^{i}Pr *C*H$_3$), 27.6 (^{i}Pr *C*H), 34.7 (CH$_2$C*Me*$_3$), 39.8 (CH$_2$*C*Me$_3$), 92.8 (*C*H$_2$C*Me*$_3$), 100.5 (*C*$_5$H$_4$(^{i}Pr)), 102.3 (*C*$_5$H$_4$(^{i}Pr)), 122.9 (*ipso*-*C*$_5$H$_4$(^{i}Pr)).

3.4.6 Preparation of (η^5-C$_5$H$_4$^{i}Pr)W(O)$_2$(CH$_2$CMe$_3$) (3.8).

A small amount of **3.7** was exposed to oxygen for 30 min resulting in a colour change from a burgundy red solid to a golden yellow solid.

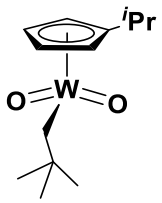

Characterization data for **3.8**. IR (cm^{-1}): 912, 954 (s, $\nu_{W=O}$). MS (LREI, *m/z*, probe temperature 150 °C): 394 [M^+, ^{184}W]. ^1H NMR (400 MHz, C_6D_6): δ 0.96 (d, $^3J_{HH}$ = 6.9, 6H, ^{i}Pr C*H*$_3$), 1.29 (s, 9H, CH_2C*Me*$_3$), 2.17 (s, $^1J_{HW}$ = 11.2, W-*H*), 2.59 (sept, $^3J_{HH}$ = 6.9, 1H, ^{i}Pr C*H*), 5.39 (t, $^3J_{HH}$ = 2.5, 2H, $C_5H_4{}^i$Pr), 5.44 (t, $^3J_{HH}$ = 2.5, 2H, $C_5H_4{}^i$Pr). ^{13}C APT NMR (100 MHz, C_6D_6): δ 22.8 (^{i}Pr *C*H$_3$), 28.1 (^{i}Pr *C*H), 33.2 (CH_2C*Me*$_3$), 33.6 (CH_2*C*Me$_3$), 51.1 (*C*H_2CMe$_3$), 106.4 (*C*$_5H_4{}^i$Pr), 110.4 (*C*$_5H_4{}^i$Pr), 134.5 (*ipso*-*C*$_5H_4{}^i$Pr).

3.4.7 Preparation of *trans*-(η^5-$C_5H_4{}^i$Pr)W(NO)(H)(κ^2-$PPh_2C_6H_4$) (3.9)

In a glove box a small reaction flask equipped with a Kontes stopcock was loaded with **3.7** (0.200 g, 0.432 mmol), PPh_3 (0.118 g, 0.450 mmol), and pentane (20 mL) to obtain a burgundy-coloured solution. The reaction vessel was then charged with H_2 (1 atm), and the contents were stirred for 16 h. The colour of the reaction mixture changed to brown, and a light yellow precipitate formed. The solvent was removed from the final mixture in vacuo to obtain a yellow solid. Purification of this solid was performed by column chromatography using a flash silica support. A yellow band was eluted from the column with 20:80 mixture of EtOAc and hexanes, and solvent removal from the eluate in vacuo afforded **3.9** as an analytically pure, bright yellow solid (0.081 g, 0.139 mmol, 32% yield). Recrystallization from a 50:50 mixture of

DCM:hexanes at -33 °C for one week produced yellow crystals suitable for a single-crystal X-ray diffraction analysis.

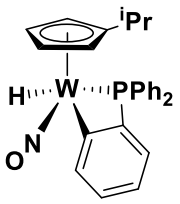

Characterization data for **3.9**. IR (cm^{-1}): 1880 (w, ν_{WH}), 1579 (s, ν_{NO}). MS (LREI, *m/z*, probe temperature 150 °C): 583 [M^+, ^{184}W], 553 [M^+-NO, ^{184}W]. ^1H NMR (400 MHz, C_6D_6): δ 1.07 (d, $^3J_{HH}$ = 6.9, 3H, ^{i}Pr C*H*$_3$), 1.05 (d, $^3J_{HH}$ = 6.9, 3H, ^{i}Pr C*H*$_3$), 2.27 (d, $^2J_{HP}$ = 70.6, $^1J_{HW}$ = 58.3, W*H*), 2.64 (sept, $^3J_{HH}$ = 6.9, 1H, ^{i}Pr C*H*), 4.80 (dd, $^3J_{HH}$ = 2.9, 1H, $C_5H_4{}^i$Pr), 5.06 (dd, $^3J_{HH}$ = 2.9, 1H, $C_5H_4{}^i$Pr), 5.26 (m, 1H, $C_5H_4{}^i$Pr), 5.44 (m, 1H, $C_5H_4{}^i$Pr), 6.94 (m, 1H, aryl *H*), 6.94 (m, 1H, *m*-aryl *H*), 7.01 (m, 5H, aryl *H*), 7.01 (m, 1H, *m*-aryl *H*), 7.27 (t, $^3J_{HH}$ = 7.4, *p*-aryl *H*), 7.52 (m, 2H, aryl *H*), 7.69 (dd, $^3J_{HH}$ = 7.4, $^3J_{HP}$ = 2.7, *o*-aryl *H*), 7.94 (dd, $^3J_{HH}$ = 7.0, $^3J_{HP}$ = 1.37, 2H, aryl *H*). ^{13}C APT NMR (100 MHz, C_6D_6): δ 23.9 (^{i}Pr *C*H$_3$), 24.3 (^{i}Pr *C*H$_3$), 28.2 (^{i}Pr *C*H), 91.3 (*C*$_5$H$_4{}^i$Pr), 91.7 (*C*$_5$H$_4{}^i$Pr), 95.3 (*C*$_5$H$_4{}^i$Pr), 97.9 (*C*$_5$H$_4{}^i$Pr), 123.8 (*ipso*-*C*$_5$H$_4{}^i$Pr), 129.1 (d, J_{CP} = 9.6, aryl *C*), 129.2 (d, J_{CP} = 9.6, aryl *C*), 129.4 (aryl *C*), 130.5 (d, $^3J_{CP}$ = 2.02, *m*-aryl *C*), 131.2 (*m*-aryl *C*), 132.1 (d, $^4J_{CP}$ = 4.6, *p*-aryl *C*), 132.8 (d, J_{CP} = 10.6, aryl *C*), 133.7 (d, $^1J_{CP}$ = 41.9, *ipso*-aryl *C*), 134.4 (d, J_{CP} = 11.6, aryl *C*), 134.7 (d, $^1J_{CP}$ = 39.4, *ipso*-aryl *C*), 140.1 (d, $^2J_{CP}$ = 27.3, *o*-aryl *C*), 152.5 (d, $^1J_{CP}$ = 50.0, *ipso*-aryl *C*), 160.4 (d, $^2J_{CP}$ = 17.7, *ipso*-aryl *C*). $^{31}P\{^1H\}$ NMR (162 MHz, C_6D_6): δ -41.7 ($^1J_{PW}$ = 157.5, *P*Ph$_2$C$_6$H$_4$). ^{31}P NMR (162 MHz, C_6D_6): δ -41.7 (d, $^2J_{PH}$ = 71.9, *P*Ph$_2$C$_6$H$_4$). Anal. Calcd for $C_{26}H_{26}NOPW$: C, 53.54; H, 4.49; N, 2.40. Found: C, 53.66; H, 4.50; N, 2.30. Melting point (reversible): 142.0-144.0 ºC.

3.4.8 X-ray Crystallography

Data collection was carried out at –173.0 ± 2 °C on a Bruker X8 APEX II diffractometer with graphite-monochromated Mo Kα radiation or at –183.0 ± 1 °C on a Bruker APEX DUO diffractometer with cross-coupled multilayer optics using Cu-Kα radiation.

Data for **3.1** were collected to a maximum 2θ value of 60.1° in 0.5° oscillations using 3.0-second exposures. The crystal-to-detector distance was 59.89 mm. The structure was solved by direct methods[43] and expanded using Fourier techniques. All non-hydrogen atoms were refined anisotropically. All other hydrogen atoms were placed in calculated positions. The material crystallizes as a two-component 'split crystal' with components one and two related by a 175.5º rotation about the (0.039 1.00 0.036) real axis. Data were integrated for both components, including both overlapped and non-overlapped reflections. The final cycle of full-matrix least-squares refinement was based on 29911 reflections (14640 from component one only, 14449 from component two only, 822 overlapped).

Data for **3.9** were collected to a maximum 2θ value of 60.2° in 0.5° oscillations using 3.0-second exposures. The crystal-to-detector distance was 39.81 mm. The structure was solved by direct methods[43] and expanded using Fourier techniques. All non-hydrogen atoms were refined anisotropically. H1A was located in a difference map and refined isotropically, and all other hydrogen atoms were placed in calculated positions. The final cycle of full-matrix least-squares refinement was based on 6516 observed reflections and 277 variable parameters.

Neutral atom scattering factors were taken from Cromer and Waber.[39] Anomalous dispersion effects were included in Fcalc[40]; the values for Δf' and Δf'' were those of Creagh and

McAuley.[41] The values for the mass attenuation coefficients are those of Creagh and Hubbell.[42] All refinements were performed using the SHELXL-2014[43] via the OLEX2[44] interface.

Table 3.1. X-ray Crystallographic Data for Complexes **3.1** and **3.9**.

Compound	**3.1**	**3.9**
Empirical formula	$C_{13}H_{21}NOW$	$C_{26}H_{26}NOPW$
Crystal Habit, color	yellow, irregular	yellow, irregular
Crystal size (mm)	0.12 × 0.12 × 0.05	0.4 × 0.14 × 0.11
Crystal system	monoclinic	triclinic
Space group	$P2_1/m$	P-1
Volume (Å^3)	648.4(2)	1110.34(9)
a (Å)	8.9137(16)	10.4607(5)
b (Å)	7.5202(14)	10.9054(5)
c (Å)	10.3328(19)	11.9258(6)
α (°)	90	104.2990(10)
β (°)	110.582(3)	105.5530(10)
γ (°)	90	112.7670(10)
Z	2	2
Density, ρ (calculated) (g/cm^3)	2.003	1.745
Absorption coefficient, μ (mm^{-1})	8.888	5.292
F_{000}	376	572
Measured Reflections: Total	2037	29890
Measured Reflections: Unique	2037	6516
Final R Indices[a]	R_1 = 0.0293, wR_2 = 0.0767	R_1 = 0.0169, wR_2 = 0.0365
Goodness-of-fit on F^2 [b]	1.080	1.036
Largest diff. peak/hole (e$^-$ Å^{-3})	3.76/-2.58	0.84/-1.11

[a] R1 on $F = \Sigma \mid (|F_o| - |F_c|) \mid / \Sigma |F_o|$; $wR2 = [(\Sigma (F_o^2 - F_c^2)^2) / \Sigma w(F_o^2)^2]^{1/2}$; $w = [\sigma^2 F_o^2]^{-1}$;

[b] $GOF = [\Sigma (w (|F_o| - |F_c|)^2) / \textit{degrees of freedom}]^{1/2}$

Chapter 4: Multiple C-H Activations of Linear Alkanes by (η^5-C_5Me_5) and (η^5-$C_5H_4{}^{i}Pr$) Tungsten Nitrosyl Bis-alkyl Complexes

4.1 Introduction

Thermolyses of (η^5-C_5Me_5)W(NO)(CH_2CMe_3)$_2$ (**4.1**) in neat hydrocarbons result in elimination of neopentane and formation of the transient (η^5-C_5Me_5)W(NO)(=$CHCMe_3$) complex, which subsequently effects C-H activations of substrates (Scheme 1.12). Interestingly, thermolysis of (η^5-C_5Me_5)W(NO)(CH_2CMe_3)$_2$ in neat methylcyclohexane or ethylcyclohexane results in multiple C-H activations of the substrates and formation of the (η^5-C_5Me_5)W(NO)(H)(η^3-C_7H_{11}) and (η^5-C_5Me_5)W(NO)(H)(η^3-C_8H_{13}) hydride complexes respectively.[27] In light of these results, the thermal chemistry of the bis-alkyl complex has been extended to encompass *n*-alkanes as substrates.

4.2 Results and Discussion

4.2.1 Reactions of 4.1 with Short-Chain *n*-Alkanes

Thermolysis of **4.1** at 100 ºC in neat *n*-butane at 250 psig results in three successive C-H activations of the alkane substrate and formation of four isomers of (η^5-C_5Me_5)W(NO)(H)(η^3-C_4H_7) which differ in the *exo*/*endo* orientation of the allyl ligands with the methyl groups being either proximal or distal to the nitrosyl ligand. (Scheme 4.1). The ratio of different isomers has been determined via integration of the *meso* signal of the allyl ligands in the ^{1}H NMR spectrum of the final product mixture. The relative abundance of different isomers is a manifestation of steric factors, with the most abundant isomer having the allyl ligand in the *endo* orientation with

the methyl group distal to the nitrosyl ligand. The solid-state molecular structure of this isomer has been previously reported.[31]

Scheme 4.1. Reaction of 4.1 with *n*-butane

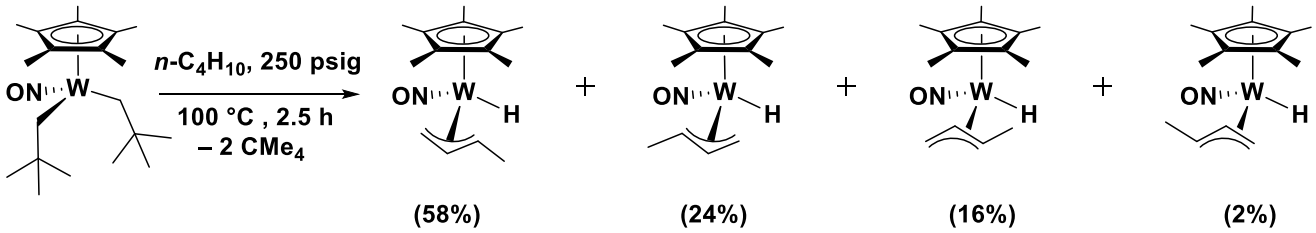

$(\eta^5\text{-}C_5Me_5)W(NO)(H)(\eta^3\text{-}C_4H_7)$ is isolable in 49% yield after purification via column chromatography on silica support under aerobic conditions. The evident moisture- and air-stability of $(\eta^5\text{-}C_5Me_5)W(NO)$ allyl-hydride complexes is due to the lack of a strong negative charge on the hydrido ligand.[31] Albeit in lower yields (19%), all isomers of this tungsten-hydride complex have been previously synthesized in similar ratios via a metathesis route by the sequential treatment of $(\eta^5\text{-}C_5Me_5)W(NO)Cl_2$ with 0.5 equivalents of $Mg(CH_2CH{=}CHMe)_2$ followed by 2 equivalents of $LiBH_4$.[31]

The similar reaction of **4.1** with propane affords two isomers of $(\eta^5\text{-}C_5Me_5)W(NO)(H)(\eta^3\text{-}C_3H_5)$ complex which differ in the *exo* and *endo* orientation of the allyl ligand.[52]

4.2.2 Thermolysis of 4.1 with Longer-Chain Alkanes

The reactions of **4.1** with longer-chain alkanes have all been performed in a similar manner. Deep burgundy red reaction solutions of the organometallic reactant in the neat

degassed *n*-alkanes have been maintained at 80 ºC for 17 h to produce golden-brown final reaction mixtures. The corresponding allyl-hydride products have been separated via column chromatography on silica column supports using a gradient of 0-20% EtOAc in hexanes. This method of purification affords the tungsten-hydride complexes as yellow solids in good yields. They have been characterized by conventional spectroscopic techniques. The isomers of (η^5-C_5Me_5)W(NO)(H)(η^3-C_5H_9) and (η^5-C_5Me_5)W(NO)(H)(η^3-C_7H_{13}) resulting from the reactions with *n*-pentane and *n*-heptane, respectively, have been previously synthesized by thermolysis of (η^5-C_5Me_5)W(NO)(H)(η^3-allyl) [η^3-allyl = η^3-CH_2CHCMe_2, η^3-$CH_2CHCHMe$, or η^3-$CH_2CHCHPh$] in the corresponding *n*-alkanes.[46]

Thermolysis of **4.1** in neat *n*-hexane leads to the formation of (η^5-C_5Me_5)W(NO)(H)(η^3-C_6H_{11}) that is isolable in a 44% yield. The ^{1}H NMR spectrum of this complex in C_6D_6 displays typical hydride signals ranging from -0.77 to -1.67 ppm with ^{183}W satellites ($^1J_{HW}$ = 120 to 123 Hz) (Figure 4.1). In solution six isomers of (η^5-C_5Me_5)W(NO)(H)(η^3-C_6H_{11}) have been identified, but only three of them have been spectroscopically characterized. Two isomers with a monosubstituted allyl ligand constitute 67% of the final product mixture, and they have been fully characterized. Partially characterized 1,3-disubstituted isomers of the product comprise 27% of the mixture, while the remaining isomers make up 6% of the product mixture. The IR spectrum of (η^5-C_5Me_5)W(NO)(H)(η^3-C_6H_{11}) displays a nitrosyl stretching frequency at 1590 cm^{-1} and a W-H stretching frequency at 1908 cm^{-1}, which is typical for such bonds.[46,53]

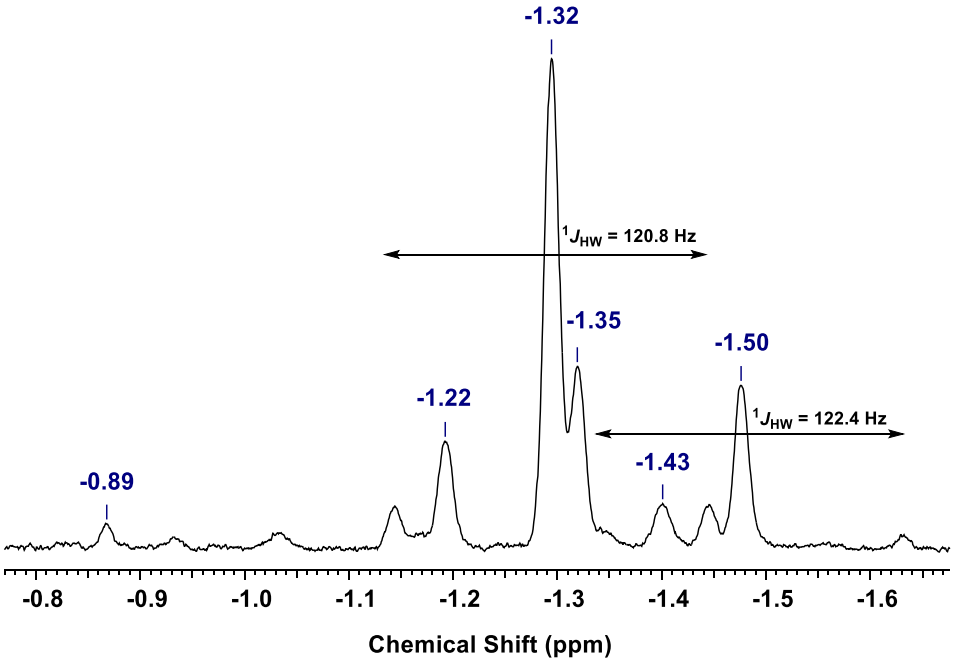

Figure 4.1. Expansion of the ^{1}H NMR spectrum (δ -1.67 to -0.77 ppm) of (η^5-C_5Me_5)W(NO)(H)(η^3-C_6H_{11}) in C_6D_6 (400 MHz) displaying the resonances due to the W-*H* proton in different isomers.

The major isomer of (η^5-C_5Me_5)W(NO)(H)(η^3-C_6H_{11}) exhibits the customary σ-π distortion of the allyl ligand.[31] The C(2)-C(3) bond located *trans* to the nitrosyl ligand has more *sp*^{2}-character than the C(1)-C(2) bond. This feature is apparent in the ^{13}C APT NMR spectrum of the complex (Figure 4.2) in which signals due to C(3) and C(2) are at 85.6 ppm and 102.7 ppm respectively, and the C(1) signal is at 39.3 ppm with ^{183}W satellites ($^1J_{CW}$ = 30.2 Hz). The allyl ligand coordination to the metal centre can be described as the C(2)=C(3) bond coordinating in a π-fashion to the tungsten centre accompanied by a W-C(1) single bond. The coordination of the double bond to the metal centre is stabilized by the electron withdrawing nitrosyl ligand located *trans* to the bond.

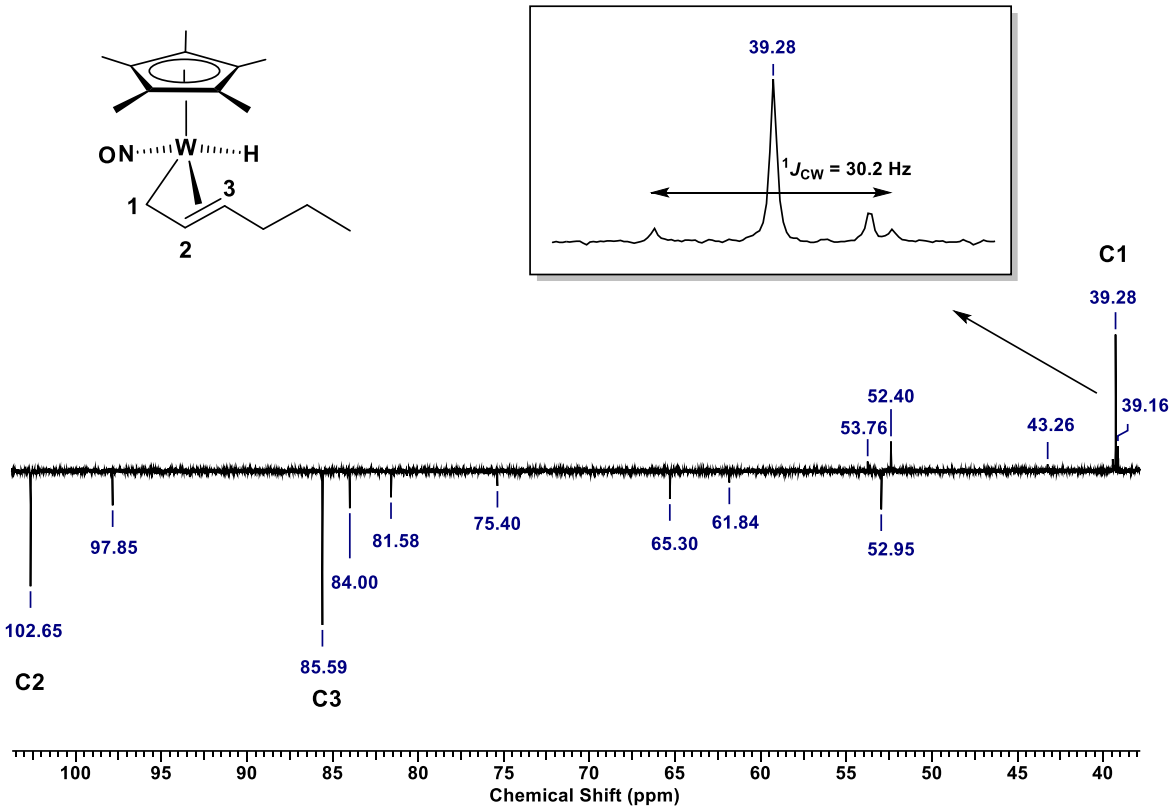

Figure 4.2. Expansion of the ^{13}C APT NMR spectrum (δ 38 to -104 ppm) of (η^5-C_5Me_5)W(NO)(H)(η^3-C_6H_{11}) in C_6D_6 (100 MHz) with the emphasis on the allyl ligand signals of the major product isomer.

Similar to the *n*-hexane example, the neopentylidene intermediate also effects multiple C-H activations of *n*-octane. In this case there are significantly more isomers of the (η^5-C_5Me_5)W(NO)(H)(η^3-C_8H_{15}) complex detectable in the final product mixture, which is not surprising since the longer carbon chain allows for the formation of more isomers having disubstituted allyl ligands. (Figure 4.3). The spectroscopic features of this complex are similar to those of the previously discussed allyl-hydride complexes.

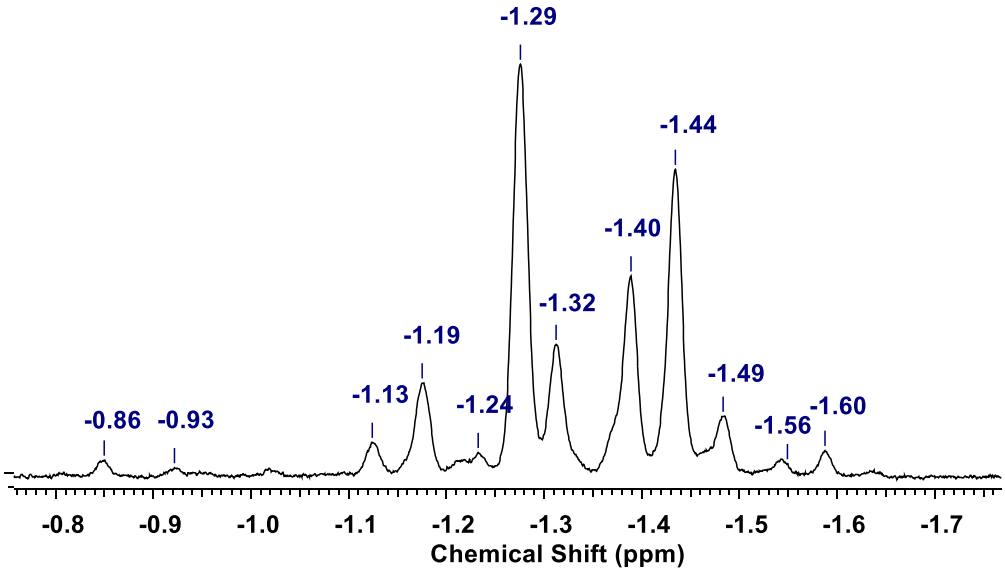

Figure 4.3. Expansion of the ^{1}H NMR spectrum (δ - 1.76 to -0.76 ppm) of (η^5-C_5Me_5)W(NO)(H)(η^3-C_8H_{15}) in C_6D_6 (400 MHz) displaying the resonances due to the W-*H* proton of different isomers.

4.2.3 Isomer Distribution of the Various (η^5-C_5Me_5)W(NO) Allyl-Hydride Products

The relative abundance of (η^5-C_5Me_5)W(NO)(H)(η^3-allyl) isomers with the monosubstituted allyl ligand decreases with increasing length of the *n*-alkane chain (Table 4.1). Thus, thermolysis of **4.1** in *n*-pentane yields predominantly the terminal allyl coordination isomers of (η^5-C_5Me_5)W(NO)(H)(η^3-$CH_2CHCHCH_2Me$) complex, while the analogous reaction with *n*-octane affords approximately equal amounts of (η^5-C_5Me_5)W(NO)(H)(η^3-C_8H_{15}) isomers with mono- and disubstituted allyl ligands.

Table 4.1. Relative abundance of (η^5-C_5Me_5)W(NO)(H)(η^3-allyl) isomers with monosubstituted and disubstituted allyl ligands

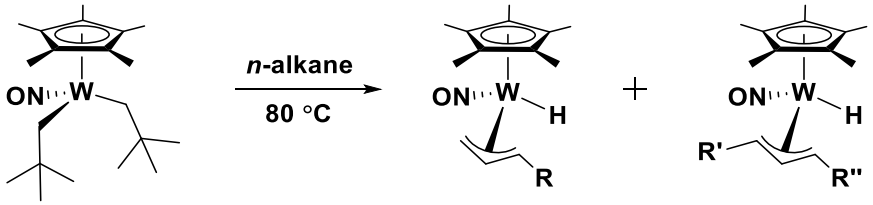

n-alkane	Isomers containing a monosubstituted allyl ligand		Isomers containing a 1,3-disubstituted allyl ligand		Unassigned allyl-hydride isomers
	R =	Relative abundance (%)	R' + R'' =	Relative abundance (%)	Relative abundance (%)
n-pentane	C_2H_5	87	C_2H_6	13	0
n-hexane	C_3H_7	67	C_3H_8	27	6
n-heptane	C_4H_9	56	C_4H_{10}	35	9
n-octane	C_5H_{11}	46	C_5H_{12}	46	8

Due to steric factors the most abundant isomer in all cases has a monosubstituted allyl ligand in the *endo* orientation with the alkyl end distal to the nitrosyl ligand: 58% for (η^5-C_5Me_5)W(NO)(H)(η^3-$CH_2CHCHMe$); 63% for (η^5-C_5Me_5)W(NO)(H)(η^3-$CH_2CHCHCH_2Me$); 52% for (η^5-C_5Me_5)W(NO)(H)(η^3-$CH_2CHCH(CH_2)_2Me$); 41% for (η^5-C_5Me_5)W(NO)(H)(η^3-$CH_2CHCH(CH_2)_3Me$); and 35% for (η^5-C_5Me_5)W(NO)(H)(η^3-$CH_2CHCH(CH_2)_4Me$).

4.2.4 Formation of the Olefin

Interestingly, the ^{1}H NMR spectra of the in-situ reaction mixtures of **4.1** with various *n*-alkanes reveal that alkenes begin to appear in the reaction mixtures after some of the (η^5-C_5Me_5)W(NO)(H)(η^3-allyl) products have been formed. The organic components of the reaction mixture can be separated from the crude mixture via distillation. The ^{1}H NMR spectra in C_6D_6 indicate that the ratio of internal vs terminal alkenes is similar to the isomer distribution of the precursor allyl-hydride complexes summarized in Table 4.1. As illustrated in Figure 4.4, the ^{1}H NMR spectrum of the distilled organic products obtained from the reaction of **4.1** with *n*-octane shows approximately equal amounts of internal and terminal octene isomers. This observation mirrors the equal distribution of mono- and disubstituted isomers of (η^5-C_5Me_5)W(NO)(H)(η^3-C_8H_{15}) in the final product mixture (Table 4.1). The mixture of octenes has also been subjected to GC-FID analysis using an experimental method developed by Joseph M. Clarkson (Figure 4.5).

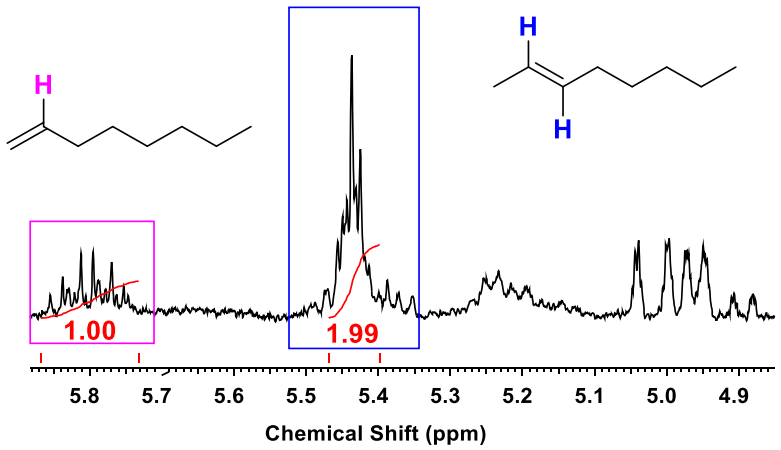

Figure 4.4. Expansion of the ^{1}H NMR spectrum (δ 4.95 to 5.88 ppm) of the distilled organic products obtained after thermolysis of **4.1** in *n*-octane (C_6D_6, 400 MHz).

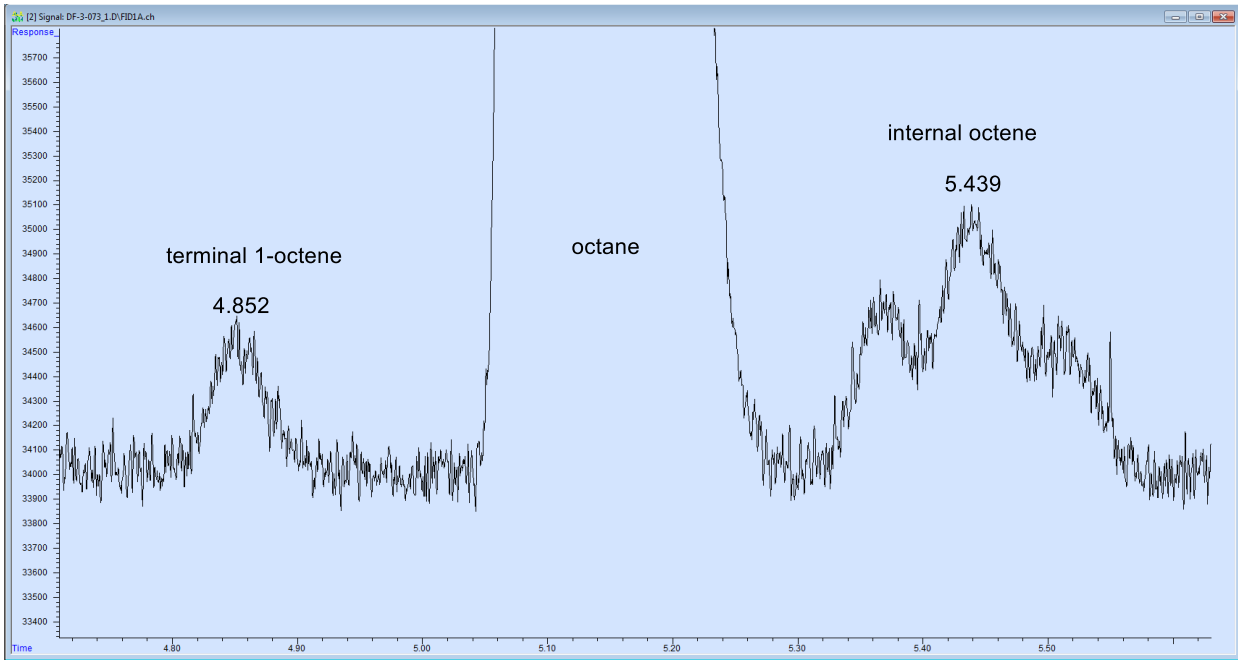

Figure 4.5. Representative GC-FID chromatogram of the distilled organic products.

4.2.5 Mechanistic Investigation of the Reactivity

4.2.5.1 Theoretical Perspective on Reactivity

The theoretical investigation of the reactivity of this system and its molybdenum analogue using *n*-pentane as a representative alkane substrate has been carried out by Dr. Guillaume P. Lefèvre. Complex **4.1** readily evolves neopentane forming a neopentylidene complex which then effects the single terminal C-H activation of *n*-pentane. The emerging bis-alkyl complex is stabilized via agostic interactions. This complex then undergoes β-H elimination leading to the evolution of neopentane and formation of the unsaturated 16e η^2-alkene intermediate.

This unsaturated complex can follow three different pathways (Scheme 4.2). The first pathway involves isomerization to the corresponding 18e allyl-hydride complex. This reaction occurs readily due to its innate exothermic nature; also, under thermal conditions the computed energy barrier of 14.9 kJ mol^{-1} can be easily overcome to form the hydride complex. The second pathway is a symmetric ligand scrambling reaction in which the η^2-alkene intermediate effects single C-H activation of *n*-pentane forming the symmetric bis-pentyl complex stabilized by agostic interactions. The computed energy barrier for this transformation is 58.6 kJ mol^{-1}.

The third pathway leads to a catalytic terminal dehydrogenation process of pentane to 1-pentene. The first step is a terminal C-H activation of *n*-pentane with a computed activation energy barrier of 113.2 kJ mol^{-1} leading to the formation of (η^5-C_5Me_5)W(NO)(H)(η^1-C_5H_{11})(η^2-$H_2C{=}CH(CH_2)_2CH_3$). Then this complex undergoes an exothermic release of 1-pentene (32.9 kJ mol^{-1}) affording (η^5-C_5Me_5)W(NO)(H)(η^1-C_5H_{11}). Afterwards, the alkyl-hydride complex undergoes dehydrogenation of a pentyl ligand (computed barrier 103.5 kJ mol^{-1}) and formation of the σ-H_2 complex. The release of H_2 and regeneration of the 16e η^2-alkene complex is a slightly endothermic reaction (2.7 kJ mol^{-1}).

The large energetic spans required for dehydrogenation and energetically readily available alternative reaction pathways prevent effective catalytic activity. Indeed, analysis of the organic products from the thermolysis of **4.1** in *n*-alkanes showed limited amounts of alkenes.

Scheme 4.2. The three different pathways of reactivity for the (η^5-C_5Me_5)M(NO)(η^2-$H_2C{=}CH(CH_2)_2CH_3$) [M = W, or Mo] transient intermediate

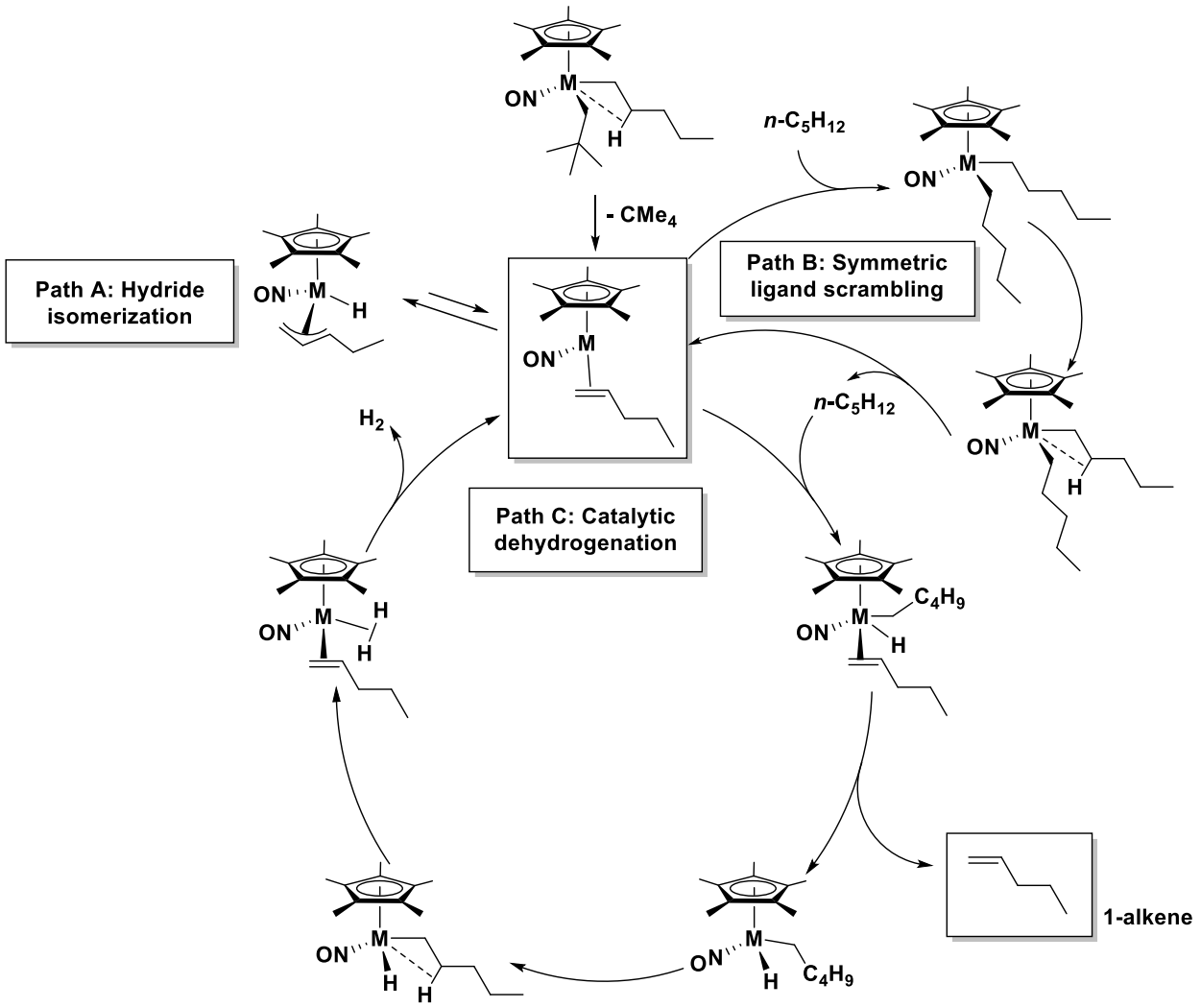

4.2.5.2 Sequential Thermolysis Reactions

Alkene formation can also be initiated by the (η^5-C_5Me_5)W(NO)(H)(η^3-allyl) complexes as illustrated by the sequential thermolyses reactions presented in Scheme 4.3. These conversions can be effected in a reaction flask by removing the organic compounds from each final reaction mixture in vacuo and then introducing a new neat *n*-alkane as the solvent for the

next step. The organic and organometallic products formed after each step have been analyzed, and the final brown reaction mixture has been purified by flash chromatography on silica using a gradient of 0-20% EtOAc in hexanes as eluant to obtain the mixture of isomers of (η^5-C_5Me_5)W(NO)(H)(η^3-C_8H_{15}) as a dark yellow oil in 10% yield.

Scheme 4.3. Sequential thermolyses reactions involving (η^5-C_5Me_5)W(NO)(H)(η^3-allyl) complexes

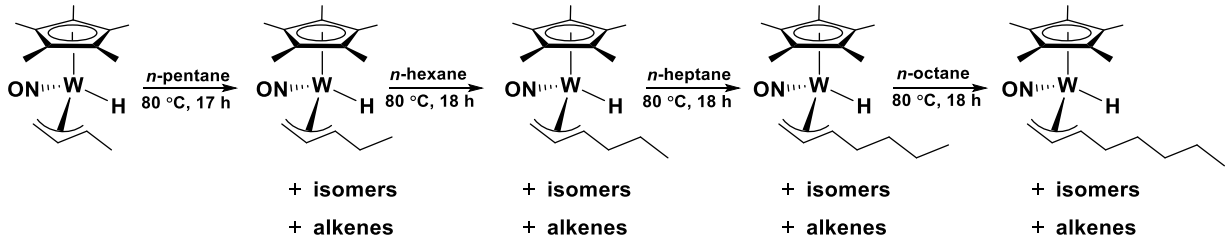

The products obtained after each step have been identified using ^{1}H NMR spectroscopy (Figure 4.6). Additionally, the product mixtures have been analyzed by low-resolution EI mass spectrometry after each step to confirm the formation of the new (η^5-C_5Me_5)W(NO)(H)(η^3-allyl) complexes.

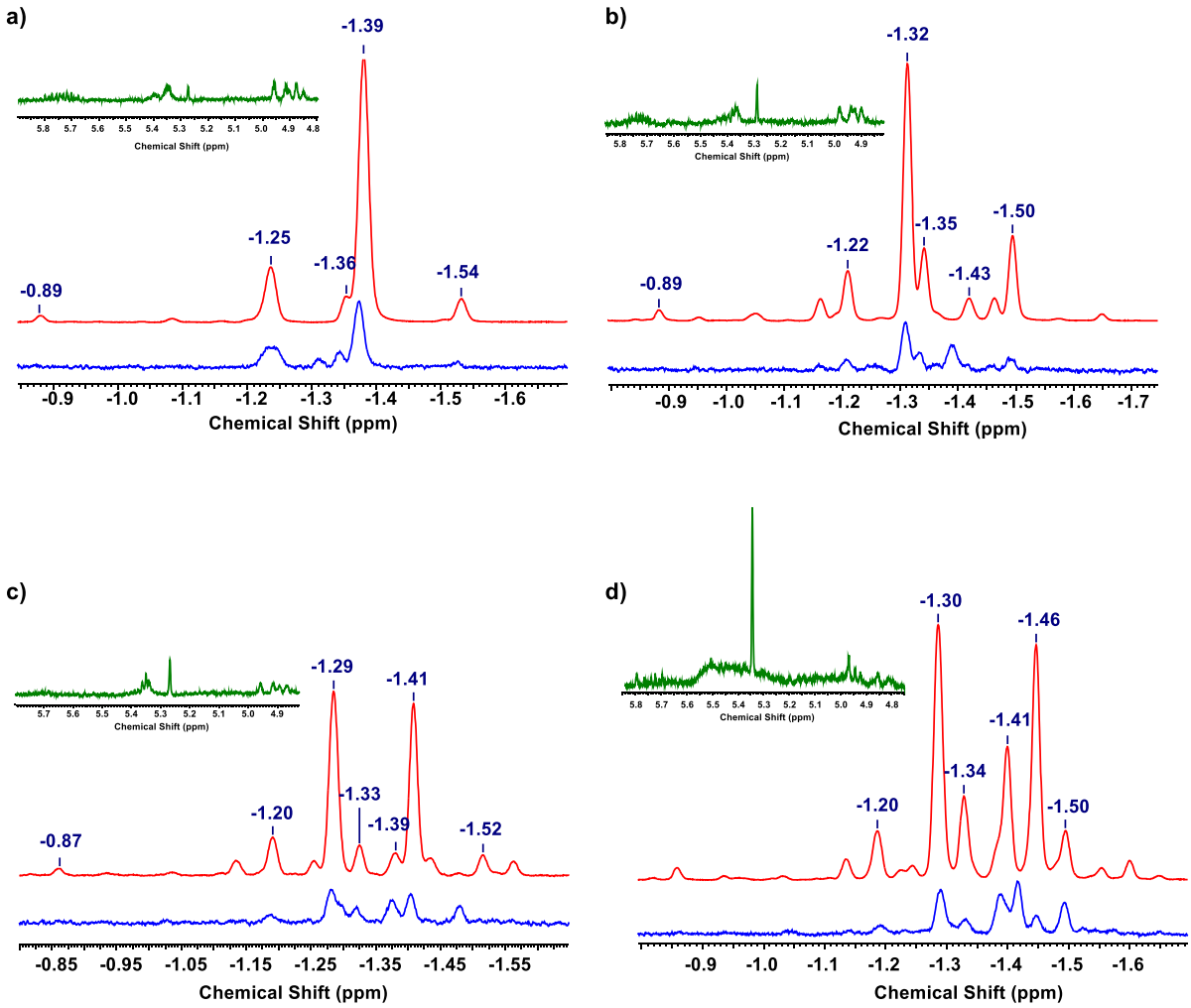

Figure 4.6. Overlaid ^{1}H NMR spectra of the (η^5-C_5Me_5)W(NO)(H)(η^3-allyl) complexes formed in the thermolysis reactions in various *n*-alkanes (red), spectra of the final product mixtures obtained after removing solvents in vacuo (blue), and spectra of the final reaction mixtures (green): (a) Reaction of (η^5-C_5Me_5)W(NO)(H)(η^3-C_4H_7) in *n*-pentane. (b) Reaction of (η^5-C_5Me_5)W(NO)(H)(η^3-C_5H_9) in *n*-hexane. (c) Reaction of (η^5-C_5Me_5)W(NO)(H)(η^3-C_6H_{11}) in *n*-heptane. (d) Reaction of (η^5-C_5Me_5)W(NO)(H)(η^3-C_7H_{13}) in *n*-octane. (C_6D_6, 400 MHz).

In Figure 4.6, the ^{1}H NMR spectrum of the final reaction mixture (blue) is overlaid with the typical hydride signals (red) of the (η^5-C_5Me_5)W(NO) allyl-hydride complexes expected to

be formed upon thermolysis in each step. For example, in the reaction of (η^5-C_5Me_5)W(NO)(H)(η^3-C_4H_7) with *n*-pentane, different isomers of (η^5-C_5Me_5)W(NO)(H)(η^3-C_5H_9) are formed. The hydride signals of the final product mixture and of the actual spectrum of the organometallic complex are comparable and can be used to identify the product. Similar ^{1}H NMR spectra have been obtained for the other products. Figure 4.6 also shows the ^{1}H NMR spectra of the in-situ reaction mixture (green) confirming the presence of alkenes. In these spectra a signal around 5.3 ppm also appears, but attempts to isolate and identify the minor product causing this signal have been unsuccessful. The final (η^5-C_5Me_5)W(NO)(H)(η^3-C_8H_{15}) complex has been isolated in low yield confirming the dehydrogenation reactivity pathway of the η^2-alkene intermediate. After purification of the final product mixture via column chromatography, the mixture of isomers of (η^5-C_5Me_5)W(NO)(H)(η^3-C_8H_{15}) has been isolated in 10% yield. Such a low yield and the presence of intractable organometallic products in the final reaction mixtures also suggest alternative reaction pathways which are competing with the dehydrogenation process.

4.2.6 Factors Influencing the Dehydrogenation Reactivity

4.2.6.1 Isomerization of the η^2-Alkene Reactive Intermediate to the Allyl-Hydride Complex

There are several factors that need to be considered when analyzing the thermal chemistry of the η^2-alkene reactive intermediate. Based on theoretical investigations of this system, elevated temperatures are required to effect the desired transformation of *n*-alkanes to

the corresponding alkenes, but under these conditions there are alternative less energy-demanding reaction pathways available to the intermediate. Specifically, isomerization of the η^2-alkene species to the corresponding allyl-hydride complex is favoured over the dehydrogenation path. Nevertheless, this transformation is reversible.

Previously, the investigations of the thermal properties of the tungsten-hydride complexes have shown that at elevated temperatures they undergo intramolecular isomerization to form a 16e (η^5-C_5Me_5)W(NO)(η^2-alkene) transient intermediate which then effects intermolecular C-H activation of a substrate. Multiple C-H activation of linear alkanes results in formation of a new allyl-hydride complex and the loss of the original allyl ligand.[46] Based on these observations, (η^5-C_5Me_5)W(NO)(H)(η^3-CH_2CHCMe_2) has also been utilized as a starting material for the dehydrogenation studies. This complex can undergo the desired intramolecular isomerization to the active η^2-alkene transient intermediate, which then can follow the third reaction pathway outlined in Scheme 4.2.

4.2.6.2 Effects of H_2

Based on the proposed mechanism of dehydrogenation, the possibility of catalyst inhibition by released H_2 gas has been considered. Thermolyses reactions of (η^5-C_5Me_5)W(NO)(H)(η^3-CH_2CHCMe_2) or **4.1** in neat *n*-alkane in an open system using a reflux set-up (instead of the reaction flask sealed with a Kontes stopcock) have been conducted. No significant changes in the reactivity have been observed. Thermolysis of the organometallic reagent in *n*-alkane under H_2 atmosphere also shows no effect on the reactivity. In order to determine if hydrogen gas can react with the η^2-alkene intermediate, and if the overall reaction is

reversible, a thermolysis reaction of (η^5-C_5Me_5)W(NO)(H)(η^2-C_5H_9) in 1-pentene with D_2 gas (ca. 1 atm) has been performed by Monica V. Shree. There is no evidence of deuterium incorporation into the metal's coordination sphere, thus H_2 gas appears to have no effect on the reactivity of the system.

4.2.6.3 Dilution Effects

The final reaction mixtures, obtained after thermolysis at 80 °C for 17 h of bis-alkyl or allyl-hydride complexes in a *n*-alkane substrate, contain a dark precipitate which appears to be a multi-metallic tungsten cluster complex. The formation of this type of complex could occur when two η^2-alkene complexes react with each other resulting in degradation of the catalyst. Alternatively, two (η^5-C_5Me_5)W(NO)(η^2-alkene)H_2 molecules could form a multi-metallic complex. Changing dilution factors would then be beneficial to reduce the proximity of reactive intermediates to one another. Nevertheless, decreasing the percent loading of (η^5-C_5Me_5)W(NO)(H)(η^3-CH_2CHCMe_2) (0.1% vs 0.4%) has not resulted in a significant improvement of the reactivity. Another probable side reaction contributing to the catalyst degradation could be associated with the symmetric ligand scrambling pathway. Attempts to synthesize and isolate a symmetric bis-pentyl complex to investigate its reactivity have been to date unsuccessful.

4.2.6.4 Temperature Effects

The catalyst's degradation due to thermal decomposition has also been investigated. Thermolyses reactions at 80, 100, 150, and 200 °C show no difference in the formation of the alkene products. The only difference is the rate of reaction, and all final product mixtures still contain a dark precipitate. Decreasing the heating temperature of the reaction to 60 °C has also been investigated using the (η^5-C_5Me_5)W(NO)(H)(η^3-CH_2CHCMe_2) system. The only difference observed is a significantly slower rate of multiple C-H activations (5 days instead of 17 hours).

4.2.6.5 Effects of the Substitution of the Cyclopentadienyl Ligand

Complex **3.7** has been utilized to effect multiple C-H activations of linear alkanes in hopes of eliminate the need for the high temperatures typically required for such transformations due to the previously reported beneficial kinetic effects of the η^5-$C_5H_4{}^i$Pr ligand on the reactivity of the alkyl-allyl systems.[25] Activation of *n*-pentane by **3.7** is most effective at 60 °C for two days (Scheme 4.4). Typical reaction conditions used for this kind of transformation with the η^5-C_5Me_5 analogue result in rapid decomposition of the starting material.

Scheme 4.4. Thermolysis of 3.7 in *n*-pentane

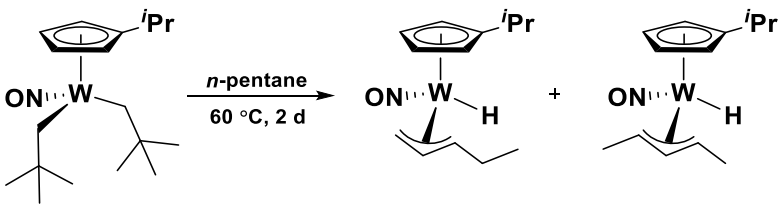

(η^5-$C_5H_4{}^iPr$)W(NO)(H)(η^3-C_5H_9)(**4.2**) is isolable in 17% yield. The ^{1}H NMR spectrum of this complex displays typical hydride signals with ^{183}W satellites ranging from $^1J_{HW}$ = 115 to 121 Hz (Figure 4.7). In solution five isomers of **4.2** have been identified, and three of them have been characterized. Two isomers with monosubstituted allyl ligand comprise 55% of the final product mixture, and one isomer with a 1,3-disubstituted allyl ligand comprises 44% of the mixture, with the remaining 1% due to other isomers in the product mixture. The ratio of complexes with mono- and di-substituted allyl ligand is significantly different than that for the analogous η^5-C_5Me_5 complex (Table 4.1). This could be due to a longer time of thermolysis of **4.2** allowing for isomerization to occur. The IR spectrum of this complex displays a nitrosyl stretching frequency at 1610 cm^{-1}, which is higher than the corresponding signal in the η^5-C_5Me_5 analogue (1596 cm^{-1}), as expected. There is no evidence suggesting that this system is more effective in transforming alkanes to alkenes.

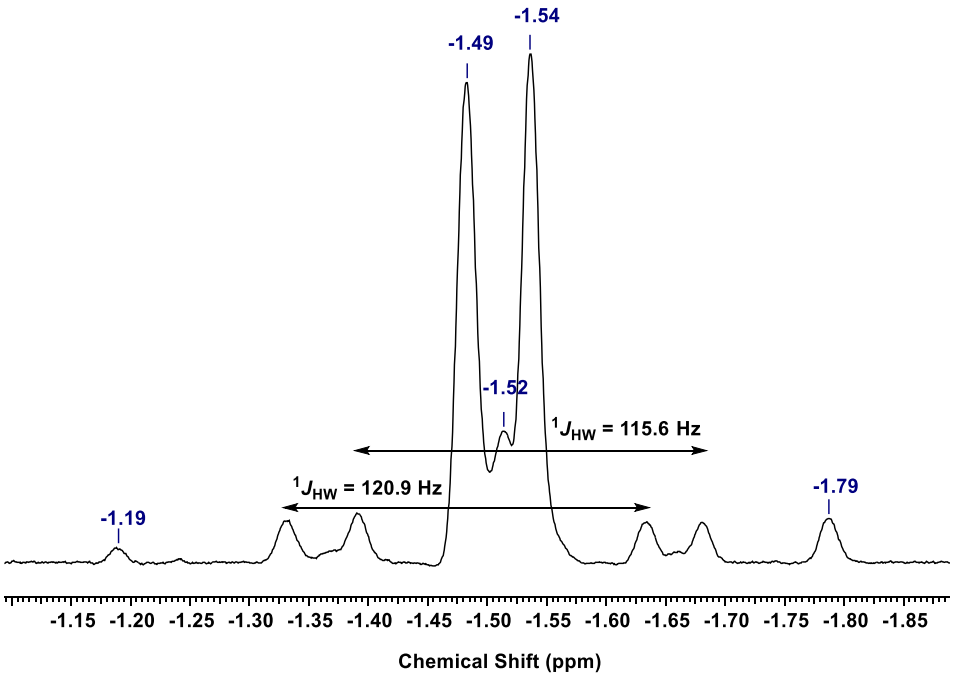

Figure 4.7. Expansion of the ^{1}H NMR spectrum (δ - 1.89 to -1.10 ppm) of **4.2** in C_6D_6 (400 MHz) displaying the resonances due to the W-*H* proton of different isomers.

The synthesis of the $TpW(NO)(CH_2CMe_3)_2$ complex [Tp = $HB(3,5\text{-}Me_2C_3HN_2)_3$] has been attempted in hopes of improving the thermal stability of the system and preventing thermal decomposition. $TpW(NO)(CO)_2$ and $TpW(NO)Br_2$ have been synthesized following synthetic methodology developed by the Harman group.[54] Unfortunately, metathesis reactions of the bis-halide species with the $Mg(CH_2CMe_3)_2$ binary reagent have not yielded the desired $TpW(NO)(CH_2CMe_3)_2$ complex, presumably due to the bulkiness of the Tp ligand.

4.2.6.6 Effects of H_2 Acceptor

The possibility that the η^2-alkene intermediate partakes in the transfer dehydrogenation of *n*-alkanes has also been considered based on extensive mechanistic investigations of the (^{tBu4}PCP)IrH_2 carried out by Goldman (Scheme 1.3).[55] The biggest difference from the previously proposed mechanism is the addition of TBE across a W-H bond of the dihydride complex, affording (η^5-C_5Me_5)W(η^2-alkene)(H)($CH_2CH_2CMe_3$) which then undergoes reductive elimination of TBA thereby regenerating the (η^5-C_5Me_5)W(η^2-alkene) intermediate (Scheme 4.5). To test this hypothesis, various quantities of TBE have been added to the reaction mixtures of bis-alkyl and allyl-hydride complexes in *n*-alkanes. Nevertheless, no significant changes in alkane production result.

Scheme 4.5. Proposed mechanism of transfer dehydrogenation

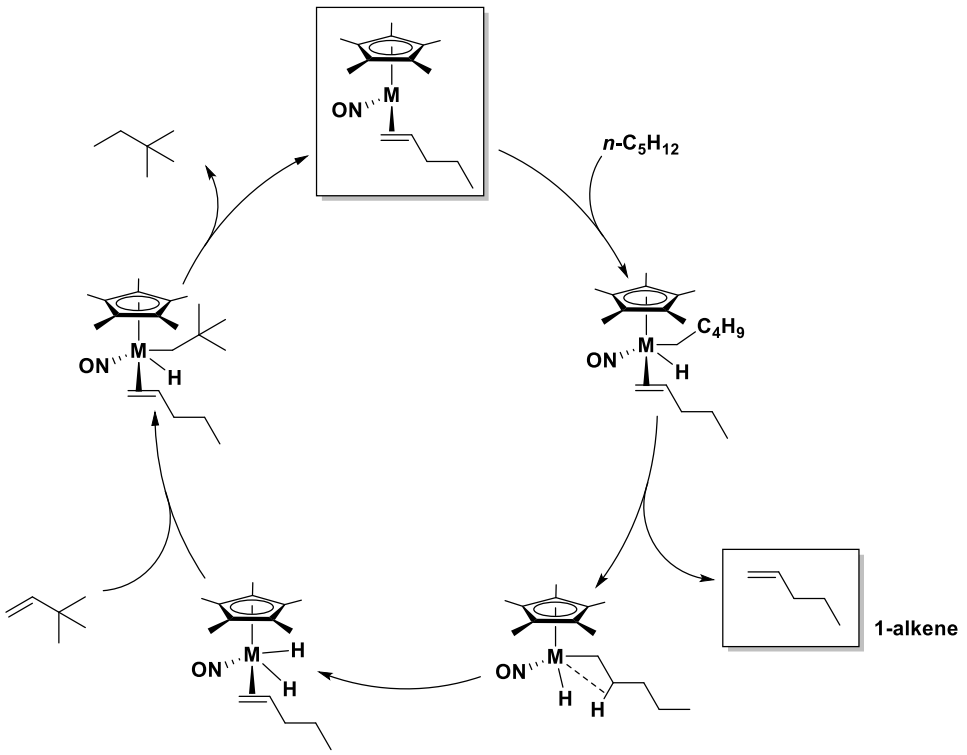

4.3 Summary

Although thermolyses of **4.1** or (η^5-C_5Me_5)W(NO)(H)(η^3-CH_2CHCMe_2) in linear alkane substrates result in multiple C-H activations and the formation of the reactive η^2-alkene intermediate complexes, the fundamental problem appears to be the relatively slow C-H activation of the alkanes and decomposition of the organometallic intermediates under thermal conditions. Attempts to enhance the rate by implementing different experimental variations described above have shown no significant improvements of the reactivity.

4.4 Experimental Section

Reactions described in this section were performed following the general experimental procedures outline in section 2.4.1.

4.4.1 Reaction of 4.1 with *n*-Butane

In a glove box, a Parr 5500 pressure reactor was charged with **4.1** (1.092 g, 2.222 mmol). The reactor was sealed and removed from the glove box and purged six times with *n*-butane. Then the reactor was placed in a dry ice/acetone bath (-78 ºC) and its contents cooled to -1 ºC. Butane gas was condensed into the pressure reactor by opening the reactor to the butane gas cylinder for 1 min. Afterwards the reaction mixture was warmed to room temperature. The contents of the reactor were then stirred and heated to 100 ºC at which temperature the pressure of *n*-butane was 250 psig. After 2.5 h the contents of the pressure reactor were allowed to cool

to room temperature, and the gas was slowly vented. A dark brown solid residue was obtained and purified by flash chromatography on silica. A yellow band was eluted with a gradient of 0-20% EtOAc in hexanes affording a golden yellow eluate. Solvent was removed from the eluate in vacuo to obtain (η^5-C_5Me_5)W(NO)(H)(η^3-C_4H_7) as a dark yellow oil (0.440 g, 1.09 mmol, 49% yield). In solution four isomers of this complex have been identified.[56,57]

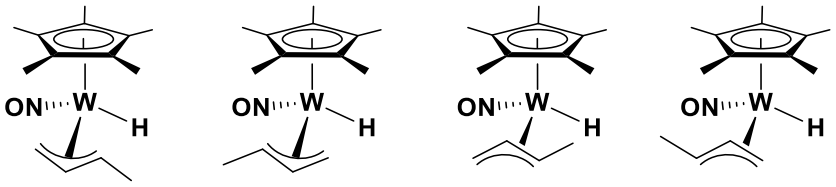

Characterization data for (η^5-C_5Me_5)W(NO)(H)(η^3-C_4H_7). IR (cm^{-1}): 1597 (s, υ_{NO}). MS (LREI, *m/z*, probe temperature 150 ºC): 405 [M^+, ^{184}W]. HRMS-EI *m/z*: [M^+, ^{186}W] Calcd for $C_{14}H_{23}NO^{186}W$ 407.13234. Found 407.13219. Anal. Calcd. for $C_{14}H_{23}NOW$: C, 41.50; H, 5.72; N, 3.46. Found: C, 42.26; H, 5.70; N, 3.24. Complete characterization data for all four isomers have been recently reported.[31]

4.4.2 Reaction of 4.1 with *n*-Pentane

In a glove box a reaction flask was charged with **4.1** (0.172 g, 0.350 mmol) and *n*-pentane (ca. 20 mL) affording a burgundy red reaction mixture. The flask was sealed with a Kontes greaseless stopcock, and then its contents were heated for 17 h at 80 ºC to produce a brown mixture. After removal of the solvent in vacuo, a dark brown solid residue was obtained and purified by flash chromatography on silica. A yellow band was eluted with a gradient of 0-20% EtOAc in hexanes affording golden yellow eluate. Solvent was removed from the eluate in

vacuo to obtain (η^5-C_5Me_5)W(NO)(H)(η^3-C_5H_9) as a dark yellow oil (0.074g, 0.177 mmol, 50% yield). In solution four isomers of this complex have been identified.[58,59]

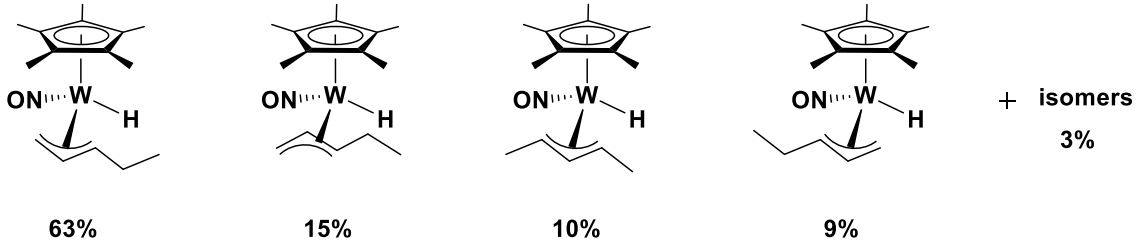

Characterization data for (η^5-C_5Me_5)W(NO)(H)(η^3-C_5H_9). IR (cm^{-1}): 1596 (s, υ_{NO}). MS (LREI, *m/z*, probe temperature 150 ºC): 419 [M^+, ^{184}W]. Anal. Calcd. for $C_{15}H_{25}NOW$: C, 42.98; H, 6.01; N, 3.34. Found: C, 42.94; H, 6.03; N, 2.95. Complete characterization data for all four isomers have been recently reported.[46]

4.4.3 Reaction of 4.1 with *n*-Hexane

This reaction was performed by employing the same procedure as used in the reaction of **4.1** with *n*-pentane. A reaction flask was charged with **4.1** (0.197 g, 0.401 mmol) and *n*-hexane (ca. 20 mL), and then the solution was maintained at 80 ºC for 17 h. Following the same purification method, (η^5-C_5Me_5)W(NO)(H)(η^3-C_6H_{11}) was isolated as a dark yellow oil (0.077 g, 0.178 mmol, 44% yield). In solution five isomers of this complex have been identified, and three of these isomers have been characterized.[60,61]

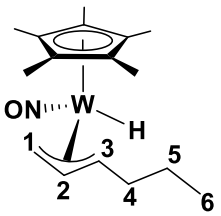

Characterization data for (η^5-C_5Me_5)W(NO)(H)(η^3-C_6H_{11}) containing an *endo* monosubstituted allyl ligand (52%). IR (cm^{-1}): 1590 (s, ν_{NO}), 1908 (w, ν_{WH}). MS (LREI, *m/z*, probe temperature 150 ºC): 433 [M^+, ^{184}W]. HRMS-EI *m/z*: [M^+, ^{186}W] Calcd for $C_{16}H_{27}NO^{186}W$ 435.16364. Found 435.16361. ^{1}H NMR (400 MHz, C_6D_6): δ -1.32 (s, $^1J_{HW}$ = 120.8, 1H, W*H*), 0.19 (d, $^3J_{HH}$ = 10.2, 1H, allyl C1H_2), 0.90 (t, $^3J_{HH}$ = 7.4, 3H, allyl C6H_3), 1.37 – 1.46 (m, 1H, allyl C5H_2), 1.54 – 1.61 (m, 1H, allyl C5H_2), 1.76 (s, 15H, C_5Me_5), 1.84 – 1.90 (m, 1H, allyl C3*H*), 2.39 (m, 2H, allyl C4H_2), 2.80 (dt, $^3J_{HH}$ = 7.0, $^2J_{HH}$ = 2.8, 1H, allyl C1H_2), 4.59 (ddd, $^3J_{HH}$ = 13.1, $^3J_{HH}$ = 10.2, $^3J_{HH}$ = 7.0, 1H, allyl C2*H*). ^{13}C NMR (100 MHz, C_6D_6): δ 11.03 (C_5Me_5), 14.3 (allyl *C*6H_3), 27.1 (allyl *C*5H_2), 37.7 (allyl *C*4H_2), 39.3 ($^1J_{CW}$ = 30.2, allyl *C*1H_2), 85.6 (allyl *C*3H), 102.7 (allyl *C*2H), 104.9 (C_5Me_5). Anal. Calcd for $C_{16}H_{27}NOW$: C, 44.36; H, 6.28; N, 3.23. Found: C, 45.08; H, 6.30; N, 3.25.

Characterization data for (η^5-C_5Me_5)W(NO)(H)(η^3-C_6H_{11}) containing the *endo* 1,3-disubstituted allyl ligand (16%). ^{1}H NMR (400 MHz, C_6D_6): δ -1.50 (s, $^1J_{HW}$ = 122.4, 1H, W*H*), 0.76 – 0.84 (m, 1H, allyl C*H*), 1.12 (t, $^3J_{HH}$ = 7.3, 3H, allyl CH_3), 1.59 – 1.63 (m, 1H, allyl C*H*), 1.75 (s, 15H, C_5Me_5), 2.02 (d, $^3J_{HH}$ = 5.9, 3H, allyl CH_3), 2.37 – 2.45 (m, 1H, allyl CH_2), 2.48 – 2.59 (m, 1H, allyl CH_2), 4.42 (dd, $^3J_{HH}$ = 12.7, $^3J_{HH}$ = 9.4, 1H, allyl C2*H*). ^{13}C NMR (100 MHz, C_6D_6): δ 10.8 (C_5Me_5), 18.0 (allyl *C*H_3), 18.9 (allyl *C*H_3), 28.5 (allyl *C*H_2), 53.0 (allyl *C*H), 84.0 (allyl *C*H), 104.8 (C_5Me_5), 105.3 (allyl *C*H).

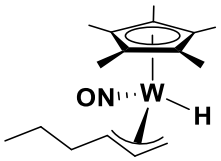

Partial characterization data for (η^5-C_5Me_5)W(NO)(H)(η^3-C_6H_{11}) containing the *endo* monosubstituted allyl ligand (15%). ^{1}H NMR (400 MHz, C_6D_6): δ -1.35 (s, $^1J_{HW}$ = 120.8, 1H,

W*H*), 0.63 (d, $^{3}J_{HH}$ = 13.5, 1H, allyl CH_2), 1.75 (s, 15H, C_5Me_5), 4.11 (d, $^{3}J_{HH}$ = 7.4, 1H, allyl CH_2), 4.32 (ddd, $^{3}J_{HH}$ = 13.5, $^{3}J_{HH}$ = 10.2, $^{3}J_{HH}$ = 7.4, 1H, allyl C*H*). ^{13}C NMR (100 MHz, C_6D_6): δ 52.4 (allyl *C*H_2), 104.2 (allyl *C*H).

4.4.4 Reaction of 4.1 with *n*-Heptane

This reaction was performed by employing the same procedure as used in the reaction of **4.1** with *n*-pentane. A reaction flask was charged with **4.1** (0.142g, 0.289 mmol) and *n*-heptane (ca. 20 mL), and then the solution was maintained at 80 ºC for 17 h. Following the same purification method, (η^5-C_5Me_5)W(NO)(H)(η^3-C_7H_{13}) was isolated as a dark yellow oil (0.075g, 0.168 mmol, 58% yield). In solution six isomers of this complex have been identified.[62,63]

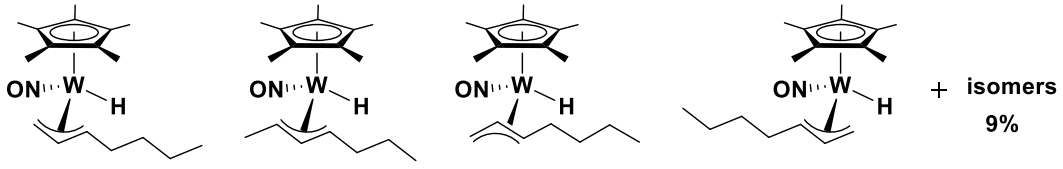

Characterization data for (η^5-C_5Me_5)W(NO)(H)(η^3-C_7H_{13}). IR (cm^{-1}): 1592 (s, υ_{NO}), 1911 (w, υ_{WH}). MS (LREI, *m/z*, probe temperature 150 ºC): 447 [M$^+$, ^{184}W]. HRMS-EI *m/z*: [M$^+$, ^{186}W] Calcd for $C_{17}H_{29}NO^{186}W$ 449.17929. Found 449.17925. Anal. Calcd for $C_{17}H_{29}NOW$: C, 45.65; H, 6.54; N, 3.13. Found: C, 45.38; H, 6.47; N, 3.04. Complete spectroscopic characterization data for four isomers of this complex have recently been reported.[46]

4.4.5 Reaction of 4.1 with *n*-Octane

In a glove box a reaction flask was charged with **4.1** (0.185 g, 0.377 mmol) and *n*-octane (ca. 20 mL) affording a burgundy red reaction mixture. Thermolysis of this reaction mixture for 17 h at 80 ºC produced a brown mixture that was worked up in the manner described in the preceding paragraphs to obtain (η^5-C_5Me_5)W(NO)(H)(η^3-C_8H_{15}) as a dark yellow oil (0.090 g, 0.195 mmol, 52% yield).[64,65]

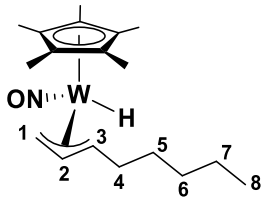

Characterization data for (η^5-C_5Me_5)W(NO)(H)(η^3-C_8H_{15}) containing the *endo* monosubstituted allyl ligand (35%). IR (cm^{-1}): 1596 (s, ν_{NO}). MS (LREI, *m*/*z*, probe temperature 150 °C): 461 [M^+, ^{184}W]. HRMS-EI *m*/*z*: [M^+, ^{186}W] Calcd for $C_{18}H_{31}NO^{186}W$ 463.19494. Found 463.19534. ^{1}H NMR (400 MHz, C_6D_6): δ -1.29 (s, $^1J_{HW}$ = 120.9, 1H, W*H*), 0.21 (d, $^3J_{HH}$ = 10.2, 1H, allyl C1H_2), 0.91 (m, 3H, allyl C8H_3), 1.77 (s, 15H, C_5Me_5), 1.25 – 1.33 (m, 2H, allyl C6H_2), 1.25 – 1.33 (m , 2H, allyl C7H_2), 1.41 – 1.50 (m, 1H, allyl C5H_2), 1.55 – 1.65 (m, 1H, allyl C5H_2), 1.90 (m, 1H, allyl C3*H*), 2.44 (m, 2H, allyl C4H_2), 2.83 (dt, $^3J_{HH}$ = 7.0, $^2J_{HH}$ = 2.5, 1H, allyl C1H_2), 4.63 (ddd, $^3J_{HH}$ = 13.1, $^3J_{HH}$ = 10.0, $^3J_{HH}$ = 7.0, 1H, allyl C2*H*). ^{13}C NMR (100 MHz, C_6D_6): δ 11.0 (C_5Me_5), 14.7 (allyl C8H_3), 23.4 (allyl *C*7H_2), 32.2 (allyl *C*6H_2), 33.8 (allyl *C*5H_2), 35.6 (allyl *C*4H_2), 39.3 (allyl *C*1H_2), 85.9 (allyl *C*3H), 102.6 (allyl *C*2H), 104.9 (C_5Me_5). Anal. Calcd for $C_{18}H_{31}NOW$: C, 46.87; H, 6.77; N, 3.04. Found: C, 47.24; H, 6.89; N, 3.12.

Partial characterization data for (η^5-C_5Me_5)W(NO)(H)(η^3-C_8H_{15}) containing the *endo* 1,3-disubstitued allyl ligand (25%). ^{1}H NMR (400 MHz, C_6D_6): δ -1.44 (s, $^1J_{HW}$ = 121.2, 1H, W*H*), 0.93 (m, 3H, allyl C*H*$_3$), 1.76 (s, 15H, C_5*Me*$_5$), 4.44 (dd, $^3J_{HH}$ = 12.5, $^3J_{HH}$ = 9.4, 1H, allyl C*H*). ^{13}C NMR (100 MHz, C_6D_6): δ 10.8 (C_5*Me*$_5$), 14.4 (allyl *Me*), 104.5 (allyl *C*H), 104.7 (*C*$_5$Me$_5$).

Partial characterization data for (η^5-C_5Me_5)W(NO)(H)(η^3-C_8H_{15}) containing the *endo* 1,3-disubstitued allyl ligand (21%). ^{1}H NMR (400 MHz, C_6D_6): δ -1.40 (s, $^1J_{HW}$ = 122.8, 1H, W*H*), 1.74 (s, 15H, C_5*Me*$_5$), 4.45 (m, 1H, allyl C*H*). ^{13}C NMR (100 MHz, C_6D_6): δ 104.5 (allyl *C*H).

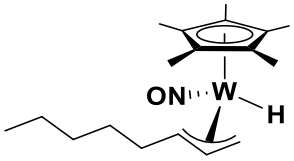

Partial characterization data for (η^5-C_5Me_5)W(NO)(H)(η^3-C_8H_{15}) containing the *endo* monosubstituted allyl ligand (11%). ^{1}H NMR (400 MHz, C_6D_6): δ -1.32 (s, $^1J_{HW}$ = 122.0, 1H, W*H*), 1.65 (s, 15H, C_5*Me*$_5$), 4.36 (ddd, $^3J_{HH}$ = 17.2, $^3J_{HH}$ = 9.8, $^3J_{HH}$ = 7.0, 1H, allyl C*H*). ^{13}C NMR (100 MHz, C_6D_6): δ 104.1 (allyl *C*H).

4.4.6 Thermolysis of Allyl-Hydride Complexes in Various Saturated Hydrocarbons

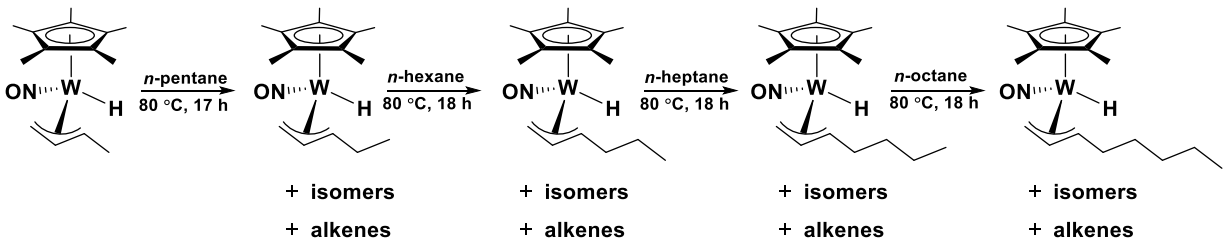

A reaction flask was charged with (η^5-C_5Me_5)W(NO)(H)(η^3-C_4H_7) (0.215 g, 0.531 mmol) and degassed *n*-pentane (ca. 25 mL) to produce a yellow reaction mixture. The flask was sealed with a Kontes greaseless stopcock, and then its stirred contents were maintained at 80 ºC for 17 h to obtain a brown mixture. The ^{1}H NMR spectra of the final reaction mixture and the dark brown residue remaining after solvent removal were recorded in C_6D_6. *n*-Hexane (ca. 25 mL) was next added to the residue in the reaction vessel, and its stirred contents were heated at 80 ºC for 18 h. The ^{1}H NMR spectra of the in situ and crude reaction mixtures were again recorded. The same procedure was repeated with *n*-heptane and then *n*-octane. The final brown reaction mixture was purified by flash chromatography on silica. A yellow band was eluted with a gradient of 0-20% EtOAc in hexanes to obtain a golden yellow eluate. Solvent was removed from the eluate in vacuo to obtain (η^5-C_5Me_5)W(NO)(H)(η^3-C_8H_{15}) as a dark yellow oil (0.025 g, 0.054 mmol, 10% yield). EI-MS spectra of the unpurified product mixtures were also obtained after each step to confirm the presence of the expected (η^5-C_5Me_5)W(NO)(H)(η^3-allyl) complexes.

4.4.7 Reaction of 3.7 with *n*-Pentane

In a glove box a reaction flask was charged with **3.7** (0.299 g, 0.645 mmol) and dried *n*-pentane (ca. 40 mL). The flask was sealed with a Kontes greaseless stopcock, and then its stirred contents were thermalized for 2 d at 60 ºC to produce a brown mixture. Solvent removal in vacuo yielded a dark brown residue that was purified by flash chromatography on silica. A yellow band was eluted with a gradient of 0-20% EtOAc in hexanes, and solvent was removed from the eluate in vacuo to obtain (η^5-$C_5H_4{}^i$Pr)W(NO)(H)(η^3-C_5H_9) as a dark yellow oil (0.043g,

0.11 mmol, 17% yield). In solution three isomers of (η^5-$C_5H_4{}^iPr$)W(NO)(H)(η^3-C_5H_9) (**4.2**) have been identified by ^{1}H and ^{13}C NMR spectroscopy.

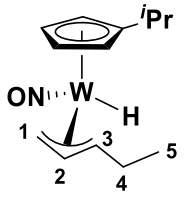

Characterization data for **4.2** containing the *endo* monosubstituted allyl ligand (44%). IR (cm^{-1}): 1610 (s, ν_{NO}). MS (LREI, *m*/*z*, probe temperature 150 °C): 391 [M$^+$, ^{184}W]. ^{1}H NMR (400 MHz, C_6D_6): δ -1.54 (s, $^1J_{HW}$ = 115.6, 1H, W*H*), 0.78 (m, 1H, allyl C1*H*$_2$), 1.08 (d, $^3J_{HH}$ = 6.9, 6H, ^{i}Pr C*H*$_3$), 1.13 (t, $^3J_{HH}$ = 3.7, 3H, allyl C5*H*$_3$), 1.97 – 2.04 (m, 2H, allyl C4*H*$_2$), 2.42 (m, 1H, allyl C3*H*), 2.61 (sept, $^3J_{HH}$ = 6.9, 1H, ^{i}Pr C*H*), 2.84 (dt, $^3J_{HH}$ = 7.0, $^2J_{HH}$ = 2.7, 1H, allyl C1*H*$_2$), 4.44 (m, 1H, allyl C2*H*), 4.61 (m, 1H, $C_5H_4{}^iPr$), 4.83 (m, 1H, $C_5H_4{}^iPr$), 5.01 (m, 1H, $C_5H_4{}^iPr$), 5.15 (m, 1H, $C_5H_4{}^iPr$). ^{13}C NMR (100 MHz, C_6D_6): δ 17.6 (allyl *C*5H$_3$), 24.0 (*i*-Pr *C*H), 32.3 (allyl *C*1H), 80.5 (allyl *C*3H), 90.8 (*C*$_5$H$_4$(*i*-Pr)), 91.7 (*C*$_5$H$_4$(*i*-Pr)), 93.5 (*C*$_5$H$_4$(*i*-Pr)), 93.7 (*C*$_5$H$_4$(*i*-Pr)), 100.7 (allyl *C*2H), 125.0 (*ipso*-*C*$_5$H$_4$(*i*-Pr)).

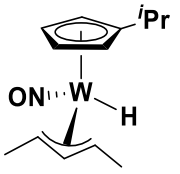

Characterization data for **4.2** containing the *endo* 1,3-disubstituted allyl ligand (44%). ^{1}H NMR (400 MHz, C_6D_6): δ -1.49 (s, $^1J_{HW}$ = 120.9, 1H, W*H*), 1.08 (d, $^3J_{HH}$ = 6.9, 6H, ^{i}Pr C*H*$_3$), 1.45 (m, 1H, allyl C*H*), 2.06 (d, $^3J_{HH}$ = 5.7, 3H, allyl *Me*), 2.19 (m, 1H, allyl C*H*), 2.34 (d, $^3J_{HH}$ = 5.8, 3H, allyl *Me*), 2.45 (sept, $^3J_{HH}$ = 6.9, 1H, ^{i}Pr C*H*), 4.32 (dd, $^3J_{HH}$ = 12.5, $^3J_{HH}$ = 9.9, 1H, allyl *meso* C*H*), 4.55 (m, 1H, $C_5H_4{}^iPr$), 4.74 (m, 1H, $C_5H_4{}^iPr$), 4.96 (m, 1H, $C_5H_4{}^iPr$), 5.18 (m, 1H, $C_5H_4{}^iPr$). ^{13}C NMR (100 MHz, C_6D_6): δ 20.0 (allyl *Me*), 22.1 (allyl *C*H$_3$), 24.1 (*i*-Pr *C*H), 47.7

(allyl *C*H), 66.4 (allyl *C*H), 90.9 (C_5H_4(*i*-Pr)), 91.2 (C_5H_4(*i*-Pr)), 94.0 (C_5H_4(*i*-Pr)), 94.5 (C_5H_4(*i*-Pr)), 107.2 (allyl *meso C*H).

Characterization data for **4.2** containing the *endo* monosubstituted allyl ligand (11%). ^{1}H NMR (400 MHz, C_6D_6): δ -1.34 (s, $^1J_{HW}$ = 122.0, 1H, W*H*), 4.21 (ddd, $^3J_{HH}$ = 13.1, $^3J_{HH}$ = 10.4, $^3J_{HH}$ = 7.4, 1H, allyl C*H*). ^{13}C NMR (100 MHz, C_6D_6): δ 104.1 (allyl *C*H).

Chapter 5: C-C Coupling Reactions by (η^5-C_5Me_5)W(NO)(H)(η^3-allyl) Complexes

5.1 Introduction

Under ambient conditions (η^5-C_5Me_5)W(NO)(CH_2CMe_3)(η^3-CHCHCHMe) loses neopentane, leading to formation of the η^2-diene intermediate.[23] In the presence of acetone, 3-pentanone, or 2-butyne, the coordination of the organic substrate to the metal centre occurs, followed by the coupling of the diene ligand and the substrate at the site of unsaturation of the organic molecule (Scheme 5.1).[23]

Scheme 5.1. C-C coupling reaction of (η^5-C_5Me_5)W(NO)(CH_2CMe_3)(η^3-CHCHCHMe) with ketones and alkyne substrates

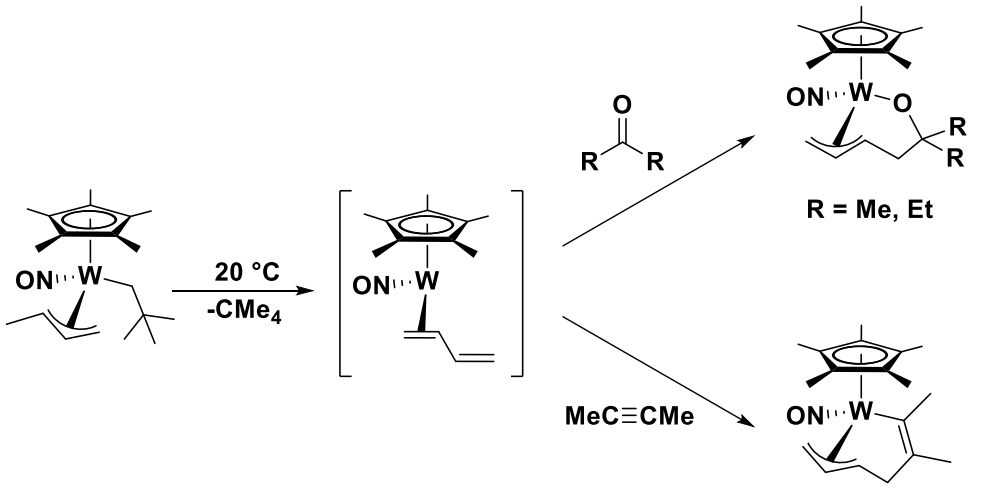

The proposed mechanism of this transformation is based on the thermolysis reaction of (η^5-C_5Me_5)W(NO)(CH_2CMe_3)(η^3-$CHCHCMe_2$) in cyclohexene at 50 ºC, and the analogous reaction of (η^5-C_5Me_5)W(NO)(CH_2CMe_3)(η^3-CHCHCHMe).[23] Thus the coupling reaction proceeds through the following steps: (a) formation of the η^2-diene intermediate upon elimination of neopentane, (b) the coordination of cyclohexene to the metal centre of this

coordinatively unsaturated intermediate, (c) coupling of the two olefin ligands at the sites of unsaturation, (d) $\eta^1 \rightarrow \eta^3$ isomerization of the allylic portion of the ligand (Scheme 5.2).[23]

Scheme 5.2. C-C coupling reaction of (η^5-C_5Me_5)W(NO)(CH_2CMe_3)(η^3-CHCHCHMe) with cyclohexene

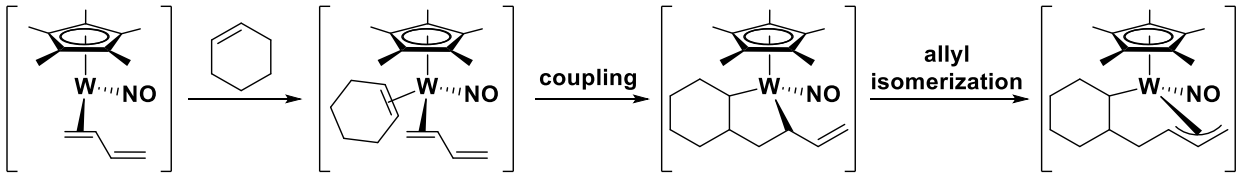

In light of these results the C-C coupling chemistry has been extended to the allyl-hydride systems, which undergo formation of similar reactive η^2-alkene intermediates.[31]

5.2 Results and Discussion

5.2.1 C-C Coupling Reactions of (η^5-C_5Me_5)W(NO)(H)(η^3-allyl) Complexes with Aldehydes

5.2.1.1 Thermolysis of (η^5-C_5Me_5)W(NO)(H)(η^3-allyl) Complexes with Aldehydes

Thermolysis of the reaction mixture of (η^5-C_5Me_5)W(NO)(H)(η^3-CHCHCHMe) and benzaldehyde in deuterated chloroform at 100 °C for 25 min results in a full consumption of the organometallic reagent and formation of the 2-methyl-1-phenylbut-3-en-1-ol and 1-phenylpent-3-en-1-ol coupled organic products (Scheme 5.3). This reaction is carried out under aerobic conditions which lead to the decomposition of the organometallic complex to an intractable

compound, presumably some oxo complex, and the release of the coupled organic product. Analogous reactions have been carried out with (η^5-C_5Me_5)W(NO)(H)(η^3-CHCHCMe$_2$) affording a coupled organic product, namely 2,2-dimethyl-1-phenylbut-3-en-1-ol. The organic products can be obtained from the final reaction mixture by flash column chromatography on silica. These products have been previously obtained by the zinc-mediated crotylation of benzaldehyde.[66]

Scheme 5.3. Thermolysis of (η^5-C_5Me_5)W(NO)(H)(η^3-CHCHCHMe) with benzaldehyde in $CDCl_3$

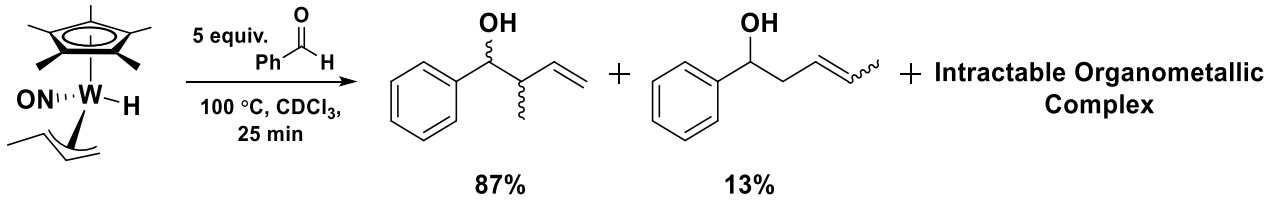

This type of transformation represents a new and facile method for synthesizing unsaturated unsymmetrical alcohols via C-C bond coupling of an allyl ligand and an aldehyde substrate. This reaction is particularly appealing since an allyl ligand can be derived from multiple C-H activations of *n*-alkanes by **4.1**. For instance, (η^5-C_5Me_5)W(NO)(H)(η^3-CHCHCHMe) can be obtained from the reaction of **4.1** with *n*-butane (Scheme 4.1). Therefore, such C-C coupling reactions represent a new synthetic methodology for converting inert *n*-alkanes to value-added chemicals.

5.2.1.2 Mechanistic Considerations

Mechanistic investigation of the C-C coupling reactivity has been carried out by effecting the thermolysis reaction of (η^5-C_5Me_5)W(NO)(H)(η^3-CH_2CHCMe_2) with *p*-tolualdehyde under anaerobic conditions. By avoiding the exposure of the organometallic intermediates to oxygen, which is hypothesized to be responsible for the ultimate release of the coupled product, the organometallic complex formed prior to the release of the alcohol could possibly be detected. To date, attempts to isolate and characterize such organometallic products have been unsuccessful. Numerous attempts to recrystallize this organometallic product have been to date unsuccessful. Purification via column chromatography on various support systems has resulted in a decomposition of these complexes of interest to intractable compounds, accompanied with a release of the alcohol product. The ^{1}H NMR spectrum of the 2,2-dimethyl-1-tolylbut-3-en-1-ol, obtained in the above reaction after purification via chromatography on a basic alumina support, is shown in Figure 5.1. The intermediate complex formed prior to the release of the coupled alcohol product has a signal in the IR spectrum due to a nitrosyl ligand at 1603 cm^{-1}. Upon exposure to oxygen, this signal disappears instantaneously, demonstrating a high sensitivity of this product to oxygen.

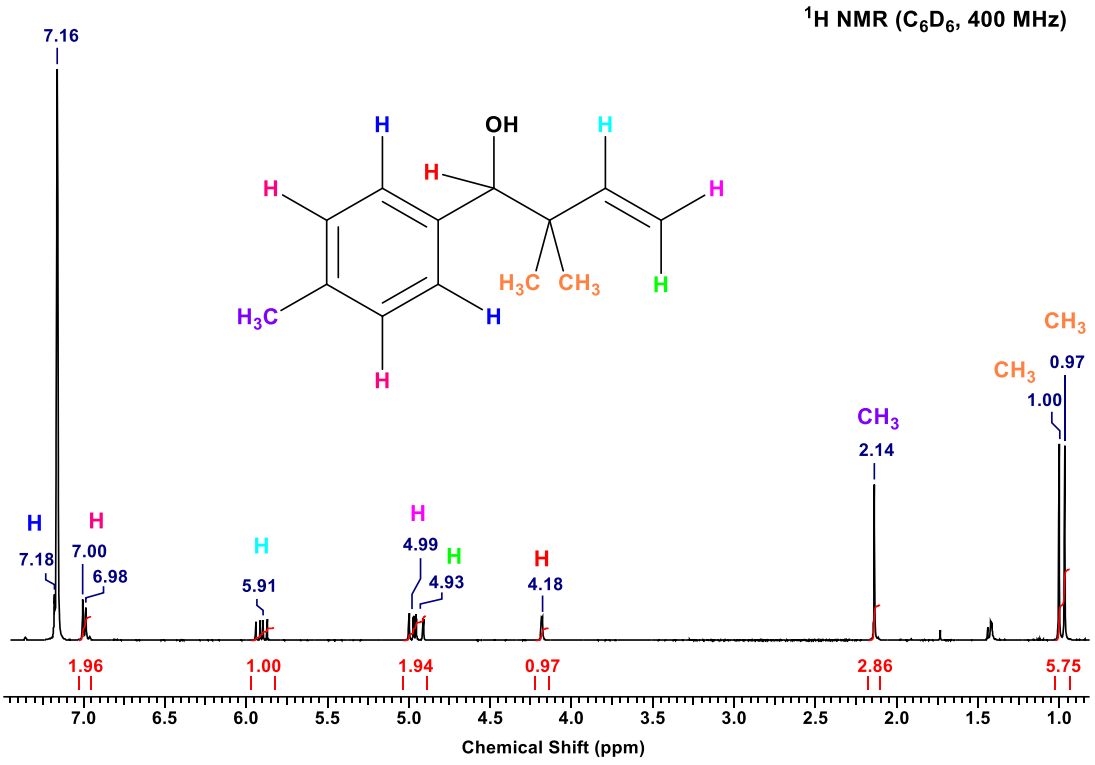

Figure 5.1. ^{1}H NMR spectrum (δ 1.00 to 10.00) of 2,2-dimethyl-1-tolylbut-3-en-1-ol (C_6D_6, 400 MHz).

Reactions of the allyl-hydride complexes with aldehydes require elevated temperatures. Consumption of the starting material occurs at a markedly slower rate when the reactions are carried out at 80 °C instead of 100 °C (even after one week a small residue of starting material remains in the reaction mixture, comparing to a full consumption of the starting material within 25 min at 100 °C). There are two possible thermal-decomposition pathways of the allyl-hydride complexes. They can undergo an intramolecular isomerization to form either the η^1-, or the η^2-alkene intermediates.[31] Previous investigations of the reactivity of these systems with alkanes have shown that the (η^5-C_5Me_5)W(NO)(η^2-alkene) intermediate effects the intermolecular C-H activations of substrates.[46] With that in mind, the proposed mechanism of the C-C coupling

reaction initiated by the (η^5-C_5Me_5)W(NO)(η^2-CH_2=$CHCH_2Me$) intermediate is outlined in Scheme 5.4.

Scheme 5.4. Proposed mechanism for the C-C coupling reaction initiated by the η^2-alkene intermediate

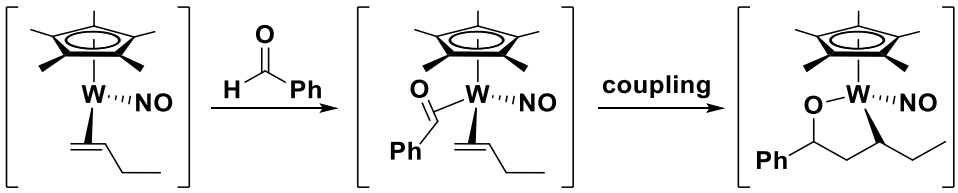

The coupled product produced via this route would be fully saturated. Nevertheless, there is no evidence for the formation of the saturated alcohol products. For instance, 2,2-dimethyl-1-tolylbut-3-en-1-ol is obtained from the reaction of (η^5-C_5Me_5)W(NO)(H)(η^3-CH_2CHCMe_2) with *p*-tolualdehyde, with no evidence for the formation of 2,2-dimethyl-1-tolylbutan-1-ol or 4-methyl-1-tolylpentan-1-ol. This observation indicates that the η^2-alkene complex is not the reactive intermediate effecting the desired transformation.

Scheme 5.5. Proposed mechanism for the C-C coupling reactions initiated by two isomers of the η^1-allyl intermediate

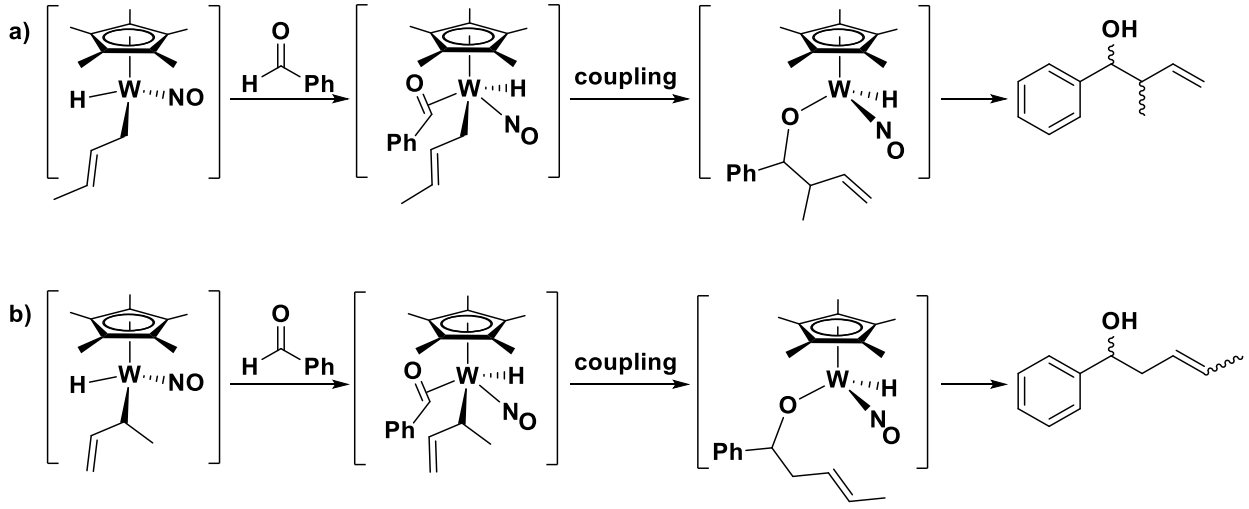

The alternative mechanism involves the η^1-allyl 16e intermediate, which can accommodate the coordination of the C=O bond to the metal centre. The subsequent C-C coupling of the alkene ligand and the aldehyde occurs at the sites of unsaturation, affording a coupled organic fragment which coordinates to the metal centre via the oxygen atom and the alkene part of the ligand (Scheme 5.5). Two isomers of the η^1 intermediate account for the formation of the two organic products isolated upon workup of the product mixture obtained from the reaction of $(\eta^5\text{-}C_5Me_5)W(NO)(H)(\eta^3\text{-}CH_2CHCHMe)$ with benzaldehyde. Interestingly, the similar reaction of $(\eta^5\text{-}C_5Me_5)W(NO)(H)(\eta^3\text{-}CH_2CHCMe_2)$ with *p*-toluadehyde affords the exclusive formation of 2,2-dimethyl-1-tolylbut-3-en-1-ol. This observation can be explained by the preferential formation of the $(\eta^5\text{-}C_5Me_5)W(NO)(H)(\eta^1\text{-}CH_2CH{=}CMe_2)$ intermediate due to steric factors, thus the C-C coupling reaction proceeds via the route outlined in Scheme 5.5a. Additionally, the trapping reactions with PMe_3 of the unsaturated η^1-intermediates, generated from $(\eta^5\text{-}C_5Me_5)W(NO)(H)(\eta^3\text{-}CH_2CHCMe_2)$ under thermal conditions, have shown the exclusive formation of $(\eta^5\text{-}C_5Me_5)W(NO)(H)(\eta^1\text{-}CH_2CH{=}CMe_2)(PMe_3)$.[31]

5.2.2 Thermolysis Reactions of (η^5-C_5Me_5)W(NO)(H)(η^3-CH_2CHCMe_2) with Phenylacetylene

Thermolysis of the reaction mixture of (η^5-C_5Me_5)W(NO)(H)(η^3-CH_2CHCMe_2) with 1 equivalent of phenylacetylene in *n*-octane at 80 °C for 18 h results in multiple C-H activations of the linear alkane and the exclusive formation of the coordination isomers of (η^5-C_5Me_5)W(NO)(H)(η^3-C_8H_{15}). Therefore, the following reactions have been carried out in neat phenylacetylene.

Maintaining the reaction mixture of (η^5-C_5Me_5)W(NO)(H)(η^3-CH_2CHCMe_2) in excess phenylacetylene at 80 °C for 18 h results in the formation of two major organometallic products **5.1** and **5.2**. Additionally, the mass spectrum of the crude reaction mixture displays signals at *m/z* 204 and 306 attributable to the products of dimerization and trimerization of phenylacetylene (Scheme 5.6). Other examples of oligomerization and polymerization of phenylacetylene can be found in the literature.[67,68]

Scheme 5.6. Thermolysis reaction of (η^5-C_5Me_5)W(NO)(H)(η^3-CH_2CHCMe_2) in neat phenylacetylene

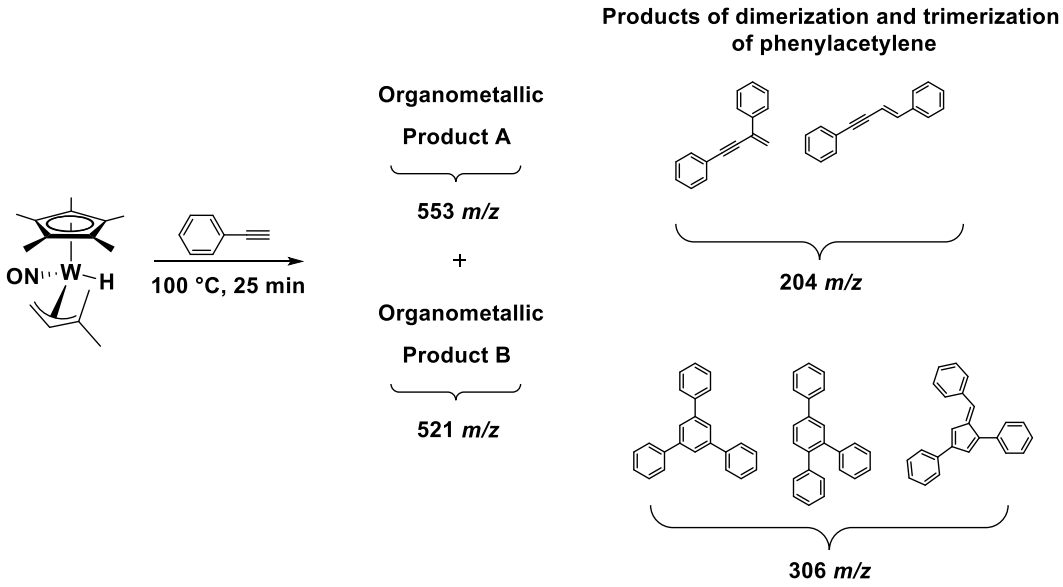

5.2.2.1 Characteristics of the First Isolable Organometallic Product 5.1

The first isolable organometallic complex (**5.1**) has been obtained via column chromatography on basic alumina under anaerobic conditions using 0-15% Et_2O in pentane as an eluant. The mass spectrum of this complex has a signal at *m/z* 553, which could be due to incorporation of two phenylacetylene molecules into the (η^5-C_5Me_5)W(NO) fragment. The IR stretching frequency at 1596 cm^{-1} indicates the presence of the linear NO ligand. The ^1H NMR spectrum of this product has a diagnostic singlet at 9.66 ppm with tungsten-183 satellites having $^2J_{HW}$ = 9.0 Hz (Figure 5.2). The downfield shift of the signal suggests that it is due to an alkylidene proton.

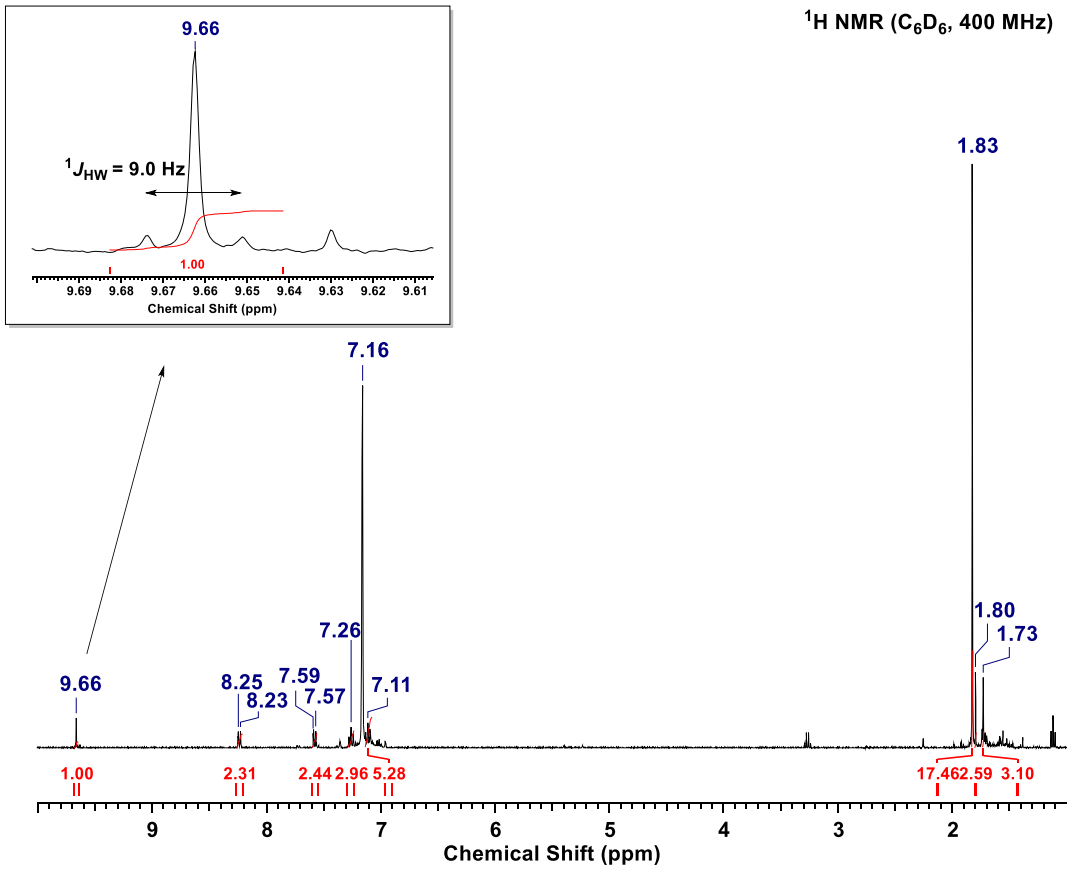

Figure 5.2. Expansion of the ^{1}H NMR spectrum (δ 1.00 to 10.00) of product **5.1** isolated from the thermolysis reaction of (η^5-C_5Me_5)W(NO)(H)(η^3-CH_2CHCMe_2) with phenylacetylene in C_6D_6 (400 MHz).

In order to investigate the origin of the alkylidene proton, a thermolysis reaction of (η^5-C_5Me_5)W(NO)(H)(η^3-CH_2CHCMe_2) in neat phenylacetylene-*d* has been attempted. Interestingly, the ^{1}H NMR spectrum of the final reaction mixture does not have the characteristic alkylidene signal. This observation suggests that the alkylidene signal in the ^{1}H NMR spectrum of **5.1** arises from the incorporated hydrogen atom of the phenylacetylene substrate. Furthermore, the mass spectrum of the product mixture has a signal at *m/z* 555, which supports

the hypothesis of incorporation of two phenylacetylene-*d* molecules onto the (η^5-C_5Me_5)W(NO) fragment.

5.2.2.2 Characteristics of the Second Isolable Organometallic Product 5.2

The second isolable organometallic **5.2** has been obtained via column chromatography on basic alumina under anaerobic conditions as a yellow gold powder using 20-30% Et_2O in pentane as eluant. The mass spectrum of this complex has a signal at *m/z* 521, which accounts for all atoms of the reagents combined. The ^{1}H NMR spectrum of **5.2** also indicates the presence of all hydrogen atoms of the organometallic reagent and of the phenylacetylene substrate, nevertheless the atom connectivity remains unclear. The most unexpected feature of this complex is the presence of what appears to be two hydride ligands.[69] Doublets at -0.41 ppm and 0.65 ppm with tungsten-183 satellites with $^1J_{HW}$ = 6.8 Hz (Figure 5.3) do not correlate to any carbon atoms on the HSQC{^{1}H, ^{13}C} NMR spectrum, suggesting that these signals are due to hydride ligands on the metal centre. The IR spectrum of this "dihydride" product has a nitrosyl-stretching-frequency at 1588 cm^{-1}, suggesting that the final product contains a linear NO ligand.

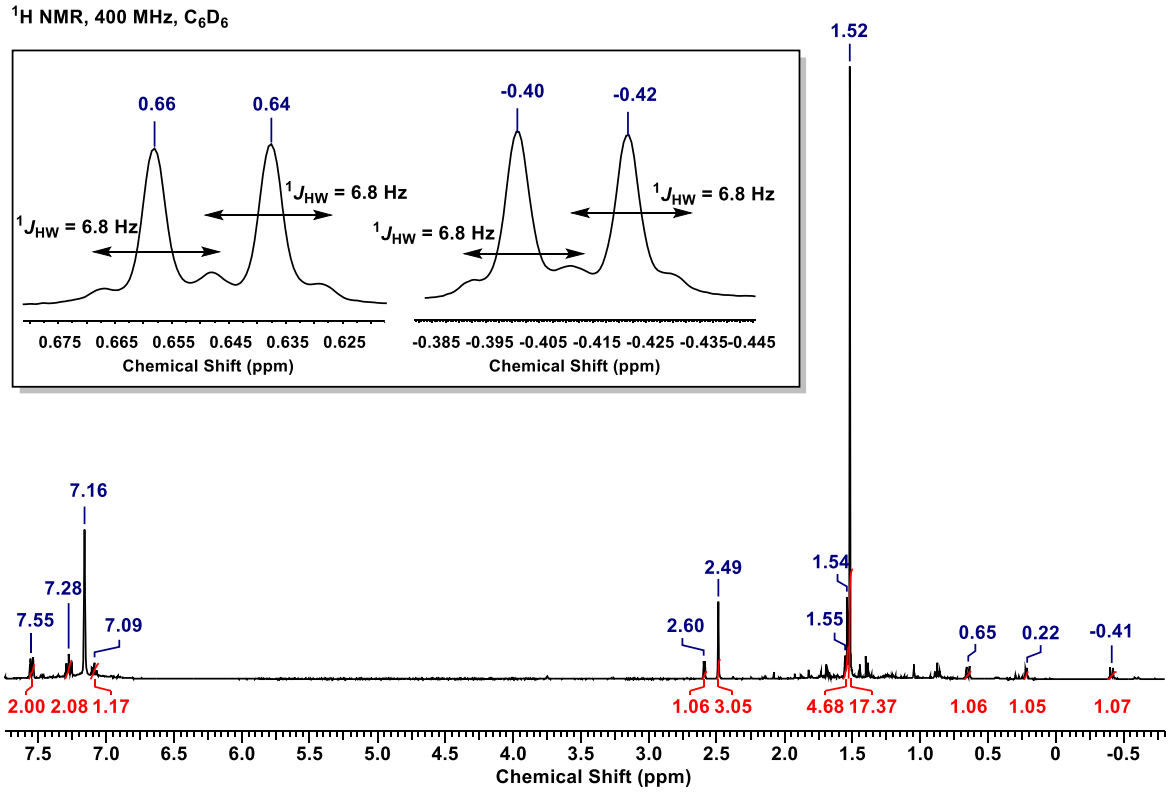

Figure 5.3. Expansion of the ^{1}H NMR spectrum of **5.2** isolated in the thermolysis reaction of (η^5-C_5Me_5)W(NO)(H)(η^3-CH_2CHCMe_2) with phenylacetylene in C_6D_6 (400 MHz).

Thermolysis of this complex in C_6D_6 at 60-100 °C for various durations results in no C-H activation, and a minor decomposition of the starting material into intractable NMR-silent products. Another characteristic of this complex is its air- and moisture-stability, suggesting it might be an 18e organometallic complex.

The thermolysis reaction of (η^5-C_5Me_5)W(NO)(H)(η^3-CH_2CHCMe_2) in neat phenylacetylene-*d* has been attempted in order to investigate the origin of the two hydride ligands. The final product mixture has been subjected to column chromatography purification on basic alumina using 0-30% Et_2O in pentane as an eluant. This method of purification resulted in a complete separation of **5.2**. The ^{1}H NMR spectrum of this product reveals that both hydride

ligands are present on the metal centre. This observation suggests that these ligands do not originate from the C-H (or C-D in this case) activation of the phenylacetylene (or phenylacetylene-*d*). The only difference in the ^{1}H NMR spectra of the products, obtained from thermolysis reactions of (η^5-C_5Me_5)W(NO)(H)(η^3-CH_2CHCMe_2) in deuterated and non-deuterated substrate, is the absence of the signal at 1.54 ppm (Figure 5.4). The mass spectrum of this complex has a signal at *m/z* 522, which again accounts for all atoms of the reagents combined. Unfortunately, the definitive answer about the structure of this complex still remains unclear.

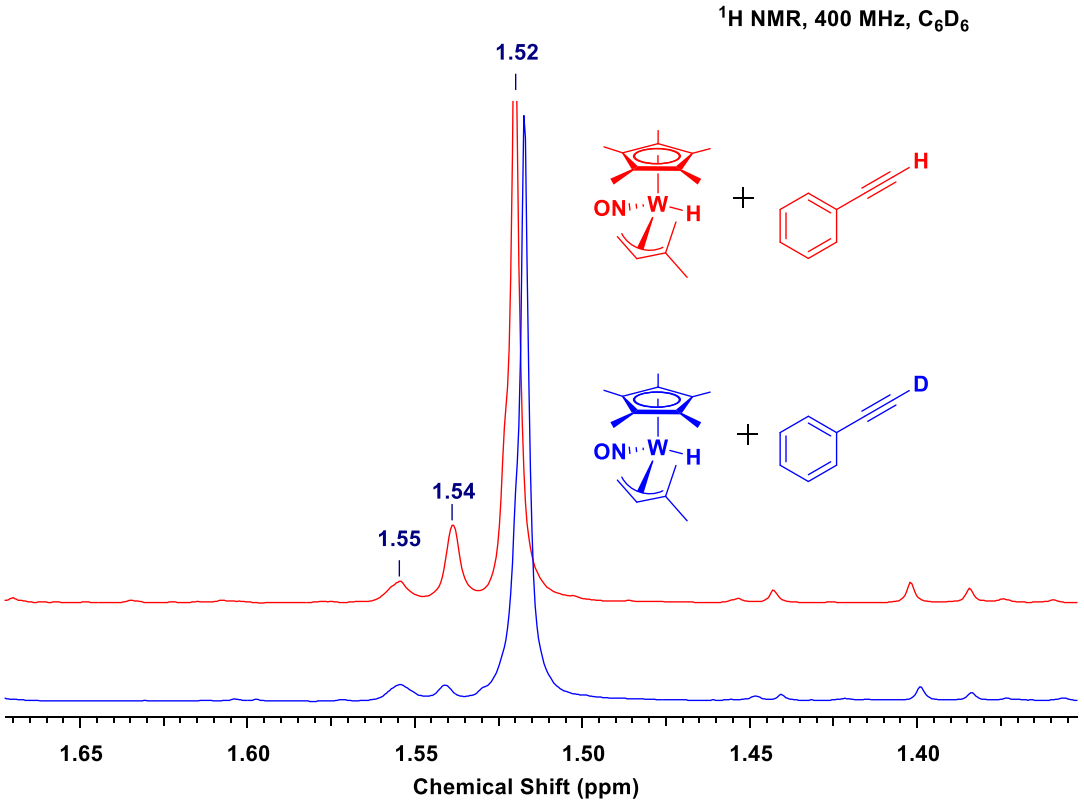

Figure 5.4. Expansion of the overlaid ^{1}H NMR spectra (δ 1.35 to 1.65 ppm) of the products obtained in thermolysis reaction of (η^5-C_5Me_5)W(NO)(H)(η^3-CH_2CHCMe_2) with phenylacetylene (blue) and phenylacetylene-*d* (red) in C_6D_6 (400 MHz).

5.3 Experimental Section

Reactions described in this section were performed following the general experimental procedures outline in section 2.4.1.

5.3.1 Thermolysis Reaction of (η^5-C_5Me_5)W(NO)(H)(η^3-$CH_2CHCHMe$) in Benzaldehyde

A small reaction flask was charged with (η^5-C_5Me_5)W(NO)(H)(η^3-$CH_2CHCHMe$) (0.189 g, 0.466 mmol), benzaldehyde (238 µL, 2.34 mmol), and $CDCl_3$ (ca. 10 mL). The reaction flask was then sealed with a Kontes greaseless stopcock and placed in an ethylene-glycol bath maintained at 100 ºC for 25 min. After heating, the colour of the reaction solution changed from light yellow to a dark brown. Then chloroform was removed in vacuo, and the final reaction mixture was purified by flash chromatography on silica. A faint yellow band was eluted with a gradient of 0-5% EtOAc in hexanes affording a faint yellow eluate. Solvent was removed from the eluate in vacuo to obtain 2-methyl-1-phenylbut-3-en-1-ol and 1-phenylpent-3-en-1-ol as a clear oil (0.044 g, 0.271 mmol, 58% yield).[70]

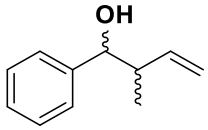

Partial characterization data for 2-methyl-1-phenylbut-3-en-1-ol (74%). MS (LREI, *m*/*z*, probe temperature 150 °C): 162. ^{1}H NMR (400 MHz, $CDCl_3$): δ 0.81 (s, $^3J_{HH}$ = 6.9, 3H, CH*Me*CH=CH_2), 2.22 (broad s, 1H, CH(O*H*)), 2.42 (m, 1H, C*H*MeCH=CH_2), 4.30 (d, $^3J_{HH}$ = 7.8, 1H, C*H*(OH)), 5.11 (d, $^3J_{HH}$ = 10.2, 1H, CHMeCH=C*H*$_2$), 5.15 (d, $^3J_{HH}$ = 17.2, 1H, CHMeCH=C*H*$_2$), 5.75 (ddd, $^3J_{HH}$ = 17.2, $^3J_{HH}$ = 10.2, $^3J_{HH}$ = 7.9, 1H, CHMeC*H*=CH_2), 7.27-

7.38 (m, 5H, aryl *H*). ^{13}C NMR (100 MHz, $CDCl_3$): δ 16.5 (CH*Me*CH=CH_2), 46.2 (*C*HMeCH=CH_2), 77.8 (*C*H(OH)), 116.7 (CHMeCH=*C*H_2), 125.7-129.7 (5C, aryl *C*), 140.6 (CHMeC*H*=CH_2).

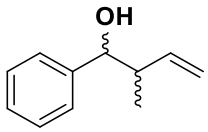

Partial characterization data for 2-methyl-1-phenylbut-3-en-1-ol (13%). ^{1}H NMR (400 MHz, $CDCl_3$): δ 0.95 (s, $^{3}J_{HH}$ = 6.9, 3H, CH*Me*CH=CH_2), 2.51 (m, 1H, C*H*MeCH=CH_2), 4.53 (d, $^{3}J_{HH}$ = 5.5, 1H, C*H*(OH)), 4.97 (m, 1H, CHMeCH=C*H*$_2$), 5.00 (m, 1H, CHMeCH=C*H*$_2$), 5.67 (m, 1H, CHMeC*H*=CH_2), 7.27-7.38 (m, 5H, aryl *H*). ^{13}C NMR (100 MHz, $CDCl_3$): δ 14.0 (CH*Me*CH=CH_2), 44.6 (*C*HMeCH=CH_2), 77.2 (*C*H(OH)), 115.5 (CHMeCH=*C*H_2), 125.7-129.7 (5C, aryl *C*), 140.3 (CHMeC*H*=CH_2).

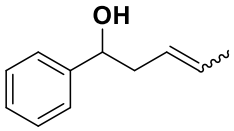

Partial characterization data for 1-phenylpent-3-en-1-ol (13%). ^{1}H NMR (400 MHz, $CDCl_3$): δ 1.63 (s, $^{3}J_{HH}$ = 6.5, 3H, CH_2CH=CH*Me*), 2.35 (m, 2H, C*H*$_2$CH=CHMe), 4.61 (dd, $^{3}J_{HH}$ = 8.0, $^{3}J_{HH}$ = 8.0, 1H, C*H*(OH)), 5.36 (m, 1H, CH_2C*H*=CHMe), 5.53 (m, 1H, CH_2CH=C*H*Me), 7.27-7.38 (m, 5H, aryl *H*). ^{13}C NMR (100 MHz, $CDCl_3$): δ 18.0 (CH_2CH=CH*Me*), 42.7 (*C*H_2CH=CHMe), 73.4 (*C*H(OH)), 126.7 (CH_2*C*H=CHMe), 129.7 (CH_2CH=*C*HMe), 125.7-129.7 (5C, aryl *C*).

5.3.2 Thermolysis Reaction of (η^5-C_5Me_5)W(NO)(H)(η^3-CH_2CHCMe_2) in Benzaldehyde

A small reaction flask was charged with (η^5-C_5Me_5)W(NO)(H)(η^3-CH_2CHCMe_2) (0.298 g, 0.711 mmol), benzaldehyde (260 µL, 3.53 mmol), and $CDCl_3$ (ca 10 mL). The reaction flask was then sealed with a Kontes greaseless stopcock and placed in an ethylene-glycol bath maintained at 100 ºC for 30 min. After heating, the colour of the reaction solution changed from light yellow to a dark brown. Then chloroform was removed in vacuo, and the final reaction mixture was purified by flash chromatography on silica. A faint yellow band was eluted with a gradient of 0-5% EtOAc in hexanes affording a faint yellow eluate. Solvent was removed from the eluate in vacuo to obtain a clear oil identified as 2,2-dimethyl-1-phenylbut-3-en-1-ol (0.020 g, 0.114 mmol, 16% yield).[71]

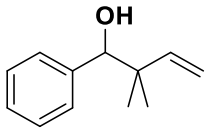

Partial characterization data for 2,2-dimethyl-1-phenylbut-3-en-1-ol which agrees with published data.[72] ^{1}H NMR (400 MHz, $CDCl_3$): δ 0.97 (s, 3H, C*Me*$_2$CH=CH$_2$), 1.02 (s, 3H, C*Me*$_2$CH=CH$_2$), 4.44 (s, 1H, C*H*(OH)), 5.10 (dd, $^3J_{HH}$ = 17.6, $^2J_{HH}$ = 1.4, 1H, CMe$_2$CH=C*H*$_2$), 5.16 (dd, $^3J_{HH}$ = 10.8, $^2J_{HH}$ = 1.4, 1H, CMe$_2$CH=C*H*$_2$), 5.93 (dd, $^3J_{HH}$ = 17.6, $^3J_{HH}$ = 10.8, 1H, CMe$_2$C*H*=CH$_2$), 7.27-7.38 (m, 5H, aryl *H*).

5.3.3 Thermolysis Reaction of (η^5-C_5Me_5)W(NO)(H)(η^3-CH_2CHCMe_2) in *p*-Tolualdehyde

In a glove box, a small reaction flask was charged with (η^5-C_5Me_5)W(NO)(H)(η^3-CH_2CHCMe_2) (0.113 g, 0.270 mmol), and *p*-tolualdehyde (30 µL, 0.254 mmol). On the double

manifold, $CHCl_3$ (ca 20 mL) was cannulated into the vessel. The reaction flask was then sealed with a Kontes greaseless stopcock and placed in an ethylene-glycol bath maintained at 90 ºC for 17 h. After heating, the colour of the reaction solution changed from light yellow to a dark brown. Then chloroform was removed in vacuo, and the final reaction mixture was purified by flash chromatography on basic alumina. A faint yellow band was eluted with a gradient of 0-15% EtOAc in hexanes affording a faint yellow eluate. Solvent was removed from the eluate in vacuo to obtain 2,2-dimethyl-1-tolylbut-3-en-1-ol as a faint yellow oil (0.29 g, 57% yield).

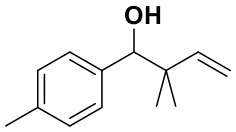

Characterization data for 2,2-dimethyl-1-tolylbut-3-en-1-ol. MS (LREI, *m*/*z*, probe temperature 120 °C): 190. HRMS-EI *m*/*z*: [M^+, ^{186}W] Calcd for $C_{13}H_{18}O$ 190.13577. Found 190.13566. ^1H NMR (400 MHz, C_6D_6): δ 0.97 (s, 3H, C*Me*$_2$CH=CH$_2$), 1.00 (s, 3H, C*Me*$_2$CH=CH$_2$), 2.14 (s, 3H, *p*-*Me*Ph), 4.18 (d, $^3J_{HH}$ = 2.0, 1H, C*H*(OH)), 4.93 (dd, $^3J_{HH}$ = 17.6, $^2J_{HH}$ = 1.4, 1H, CMe$_2$CH=C*H*$_2$), 4.99 (dd, $^3J_{HH}$ = 10.8, $^2J_{HH}$ = 1.4, 1H, CMe$_2$CH=C*H*$_2$), 5.91 (dd, $^3J_{HH}$ = 17.6, $^3J_{HH}$ = 10.8, 1H, CMe$_2$C*H*=CH$_2$), 6.99 (d, $^3J_{HH}$ = 7.8, 2H, *p*-Me*Ph*), 7.17 (m, 2H, *p*-Me*Ph*). ^{13}C NMR (100 MHz, C_6D_6): δ 21.5 (*p*-*Me*Ph), 22.3 (C*Me*$_2$CH=CH$_2$), 24.6 (C*Me*$_2$CH=CH$_2$), 42.8 (*C*Me$_2$CH=CH$_2$), 81.2 (*C*H(OH)), 113.5 (CMe$_2$CH=*C*H$_2$), 128.7 (*p*-Me*Ph*), 137.2 (*p*-Me*Ph*), 139.4 (*p*-Me*Ph*), 145.9 (CMe$_2$*C*H=CH$_2$).

5.3.4 Thermolysis Reaction of (η^5-C_5Me_5)W(NO)(H)(η^3-CH_2CHCMe_2) in Phenylacetylene

In a glove box, a small reaction flask was charged with (η^5-C_5Me_5)W(NO)(H)(η^3-CH_2CHCMe_2) (0.178 g, 0.425 mmol) and phenylacetylene (ca 2 mL) and sealed with a Kontes greaseless stopcock. The contents of the reaction flask were heated at 80 ºC for 18 h. After heating, the colour of the reaction solution changed from light yellow to a dark brown. The final reaction mixture was purified by chromatography on basic alumina in a glove box. A yellow band was eluted with a gradient of 0-15% Et_2O in pentane affording a faint yellow eluate. Solvent was removed from the eluate in vacuo to obtain the organometallic **5.1** as a gold yellow powder (0.016 g, 0.029 mmol, 7% yield). Another yellow band was eluted with a gradient of 20-30% Et_2O in pentane affording a faint yellow eluate. Solvent was removed from the eluate in vacuo to obtain the **5.2** as a gold yellow powder (0.022 g, 0.042 mmol, 10% yield).

Partial characterization data for **5.1**. IR (cm^{-1}): 1596 (s, υ_{NO}). MS (LREI, *m*/*z*, probe temperature 120 °C): 553 [M^+, ^{184}W]. ^1H NMR (400 MHz, C_6D_6): δ 1.73 (s, 3H), 1.80 (s, 3H), 1.83 (s, 15H, (η^5-C_5Me_5)), 7.11 (t, $^3J_{HH}$ = 7.5, 2H), 7.27 (t, $^3J_{HH}$ = 7.5, 2H), 7.58 (t, $^3J_{HH}$ = 8.2, 2H), 8.24 (d, $^3J_{HH}$ = 8.2, 2H).

Partial characterization data for **5.2**. IR (cm^{-1}): 1587 (s, υ_{NO}). MS (LREI, *m*/*z*, probe temperature 120 °C): 521 [M^+, ^{184}W]. ^1H NMR (400 MHz, C_6D_6): δ -0.41 (d, $^2J_{HH}$ = 6.8, 1H, W-*H*), 0.22 (d, J_{HH} = 4.3, 1H, C*H*$_2$), 0.65 (d, $^2J_{HH}$ = 6.8, 1H, W-*H*), 1.52 (s, 15H, (η^5-C_5Me_5)), 1.52 (s, 3H, *Me*), 1.55 (m, 1H), 2.49 (s, 3H. *Me*), 2.60 (d, J_{HH} = 4.3, 1H, C*H*$_2$), 7.09 (m, 1H, *Ph*), 7.28 (m, 2H, *Ph*), 7.55 (d, $^3J_{HH}$ = 8.2, 2H, *Ph*). ^{13}C NMR (100 MHz, C_6D_6): 10.4 (η^5-C_5Me_5), 19.3

(*Me*), 30.9 (*Me*), 51.9 (*C*H_2), 58.5, 106.8 (η^5-*C*$_5$Me$_5$), 113.2, 125.7 (*Ph*), 126.3 (*Ph*), 128.8 (*Ph*), 140.6, 158.2 (*Ph*), 287.7.

5.3.5 Thermolysis Reaction of (η^5-C_5Me_5)W(NO)(H)(η^3-CH_2CHCMe_2) in Phenylacetylene-*d*

This reaction was performed by employing the same procedure as used in the reaction of (η^5-C_5Me_5)W(NO)(H)(η^3-CH_2CHCMe_2) with phenylacetylene. A reaction flask was charged with (η^5-C_5Me_5)W(NO)(H)(η^3-CH_2CHCMe_2) (0.064 g, 0.15 mmol) and phenylacetylene-*d* (ca. 2 mL), and then the solution was maintained at 80 ºC for 18 h. Following the same purification method outlined in the previous section, analogues of **5.1** and **5.2** were isolated.

Partial characterization data for analogues of **5.1** and **5.2**. MS (LREI, *m*/*z*, probe temperature 120 °C): 522 [M^+, ^{184}W (**5.2**)], 555[M^+, ^{184}W (**5.1**)]. Analogue of **5.2**: ^{1}H NMR (400 MHz, C_6D_6): δ -0.42 (d, $^2J_{HH}$ = 6.8, 1H, W-*H*), 0.22 (d, J_{HH} = 4.3, 1H, C*H*$_2$), 0.65 (d, $^2J_{HH}$ = 6.8, 1H, W-*H*), 1.52 (s, 15H, (η^5-C$_5$*Me*$_5$)), 1.52n (s), 1.55 (m, 1H), 2.49 (s, 3H. *Me*), 2.60 (d, J_{HH} = 4.3, 1H, C*H*$_2$), 7.09 (m, 1H, *Ph*), 7.28 (m, 2H, *Ph*), 7.55 (d, $^3J_{HH}$ = 8.2, 2H, *Ph*).

Chapter 6: Conclusions and Future Work

6.1 Summary and Conclusions

A new synthetic methodology for obtaining **2.3** has been developed due to unprecedented effects imparted by the η^5-$C_5H_4{}^iPr$ ligand on the physical and chemical properties of its precursors. Specifically, the reaction of **2.1** with PCl_5 results in the formation of the PCl_3 adduct of the (η^5-$C_5H_4{}^iPr$)W(NO)Cl_2 complex. Moreover, the subsequent metathesis reaction with $Mg(CH_2CH{=}CMe_2)_2$ binary reagent occurs at the P-Cl bond of the adduct affording complex **2.4**.

Displacement of the $PCl_2CMe_2CH{=}CH_2$ ligand in **2.4** has been attempted by addition of excess PMe_3. The solid-state molecular structure of one of the products of this reaction has been obtained (**2.5**). Complex **2.5** is an 18e tungsten complex with a capped trigonal antiprismatic coordination geometry with the 3 chloro and 3 PMe_3 ligands in the staggered conformation with respect to each other, and a linear NO ligand at the crown of the structure. Thus, the reaction of **2.4** with PMe_3 has resulted in a loss of the original cyclopentadienyl ligand. Displacement of the cyclopentadienyl ligand is not typical for reactions of tungsten-nitrosyl complexes with Lewis bases.[26,31]

Novel complexes **3.1**, **3.7**, and **3.9** have been synthesized, and their chemistry investigated in hopes that the η^5-$C_5H_4{}^iPr$ ligand would exert similar beneficial kinetic effects on the C-H activation reactivity of these complexes, as it has shown previously with **2.3**.[25] Trapping reactions of the coordinatively unsaturated reactive intermediates, formed via an intramolecular isomerization of **3.1**, with a Lewis base have been attempted. Detailed analysis of these reactions has demonstrated that **3.1** shows a preferential isomerization to the η^1 intermediate (η^5-$C_5H_4{}^iPr$)W(NO)(H)(η^1-$CH_2CH{=}CMe_2$), isolable as its PMe_3 adduct **3.2**, rather than the formation of the reactive η^2 intermediates (η^5-$C_5H_4{}^iPr$)W(NO)(H)(η^2-$CH_2{=}CHCHMe_2$) and (η^5-

$C_5H_4{}^iPr)W(NO)(H)(\eta^2$-MeCH=$CMe_2$), isolable as their PMe_3 adducts **3.4** and **3.5**. Increasing the temperature facilitates the intramolecular rearrangement to the desired η^2-alkene intermediate, but unfortunately due to the thermal instability of the starting material the C-H activation of alkanes cannot be carried out at very high temperatures.

Alternatively, replacement of η^5-C_5Me_5 with the η^5-$C_5H_4{}^iPr$ ligand in the reaction of **3.7** with hydrogen gas and PPh_3, rather than simply accelerating the intramolecular C-H activation and formation of the reactive *cis*-(η^5-$C_5H_4{}^iPr)W(NO)(H)(\kappa^2$-$PPh_2C_6H_4$) complex, increases the rate of *cis* to *trans* isomerization of the ortho-metallated complex to form **3.9**. In this case, faster rate of *cis* to *trans* isomerization hinders the C-H activation potential of the ortho-metallated complex.

The multiple C-H activations of linear alkanes effected by the transient (η^5-$C_5Me_5)W(NO)(=CHCMe_3$) complex, which is generated from **4.1** under thermal conditions, have been investigated. The corresponding (η^5-$C_5Me_5)W(NO)(H)(\eta^3$-allyl) complexes obtained from reactions with various *n*-alkanes have been isolated and characterized. These thermolysis reactions are accompanied by the generation of alkenes. Attempts to improve production of olefins by varying different experimental conditions have not resulted in a significant improvement of the dehydrogenation reactivity. Reaction of **3.7** with *n*-pentane has also been investigated, but has not shown significant improvement of olefin production.

Finally, the C-C coupling reactivity of (η^5-$C_5Me_5)W(NO)(H)(\eta^3$-allyl) complexes with aldehydes and phenylacetylene has been investigated. Thermolysis reactions of (η^5-$C_5Me_5)W(NO)(H)(\eta^3$-allyl) complexes with aldehydes under aerobic conditions result in the formation of the corresponding coupled alcohol product. Attempts to isolate the organometallic intermediate prior to the alcohol release by carrying out the reaction under anaerobic conditions

to date have been unsuccessful. Numerous attempts to crystallize this complex, and obtain its solid-state molecular structure also have not been successful.

The analysis of the organometallic products, formed in the reaction of (η^5-C_5Me_5)W(NO)(H)(η^3-CH_2CHCMe_2) with phenylacetylene, by mass spectrometry indicates that two phenylacetylene molecules have been incorporated into the (η^5-C_5Me_5)W(NO) fragment in **5.1**, and one phenylacetylene molecule has been incorporated into the (η^5-C_5Me_5)W(NO)(H)(η^3-CH_2CHCMe_2) complex in **5.2**. The solid-state molecular structures of both isolable organometallic products would be essential for gaining insights about this transformation since the exact atom connectivity in these complexes remains unclear.

6.2 Future Directions

Dehydrogenation of *n*-alkanes via the route outlined in Scheme 4.2 offers a new methodology of hydrocarbon functionalization. The fundamental problem with this process appears to be a relatively slow rate of C-H activation of alkanes and decomposition of the organometallic intermediates under thermal conditions. One way of avoiding this obstacle is to introduce a cyclopentadienyl ligand that could be attached onto a heterogeneous surface. In this way, the highly reactive 14e (η^5-C_5Me_5)W(NO) fragments would not be in a close proximity to each other, thus eliminating a potential dimerization and resulting degradation of the catalyst.

The C-C coupling reactivity of the (η^5-C_5Me_5)W(NO)(H)(η^3-allyl) complexes with aldehydes represents a new and facile method for synthesizing unsaturated unsymmetrical alcohols. This reaction is particularly appealing since an allyl ligand can be derived by multiple C-H activation of *n*-alkanes by **4.1**. Thus, such C-C coupling reactions offer a new synthetic

methodology for converting inert *n*-alkanes into value-added chemicals. Nevertheless, regeneration of the organometallic complex upon the release of the coupled product is of paramount importance in order to close a synthetic cycle, and potentially attain a new catalytic system.

One way of achieving the recovery of the organometallic reagent would be by carrying out the reaction under anaerobic conditions, and then exposing the organometallic intermediates formed prior to alcohol release to CO pressure to obtain $(\eta^5\text{-}C_5Me_5)W(NO)(CO)_2$ and the coupled organic product. A similar approach has been implemented during the synthesis of unsaturated unsymmetrical ketones.[45] $(\eta^5\text{-}C_5Me_5)W(NO)(CO)_2$ complex can be then converted to $(\eta^5\text{-}C_5Me_5)W(NO)Cl_2$ by reaction with PCl_5.[30] **4.1** can be synthesized via a metathesis reaction with 1 equivalent of $Mg(CH_2CMe_3)_2$ binary reagent. This bis-alkyl complex can subsequently effect multiple C-H activations of *n*-alkanes, thereby closing a synthetic cycle (Scheme 6.1).

Scheme 6.1. Proposed synthetic cycle of C-C coupling reactions of (η^5-C_5Me_5)W(NO)(H)(η^3-$CH_2CHCHMe$) with benzaldehyde

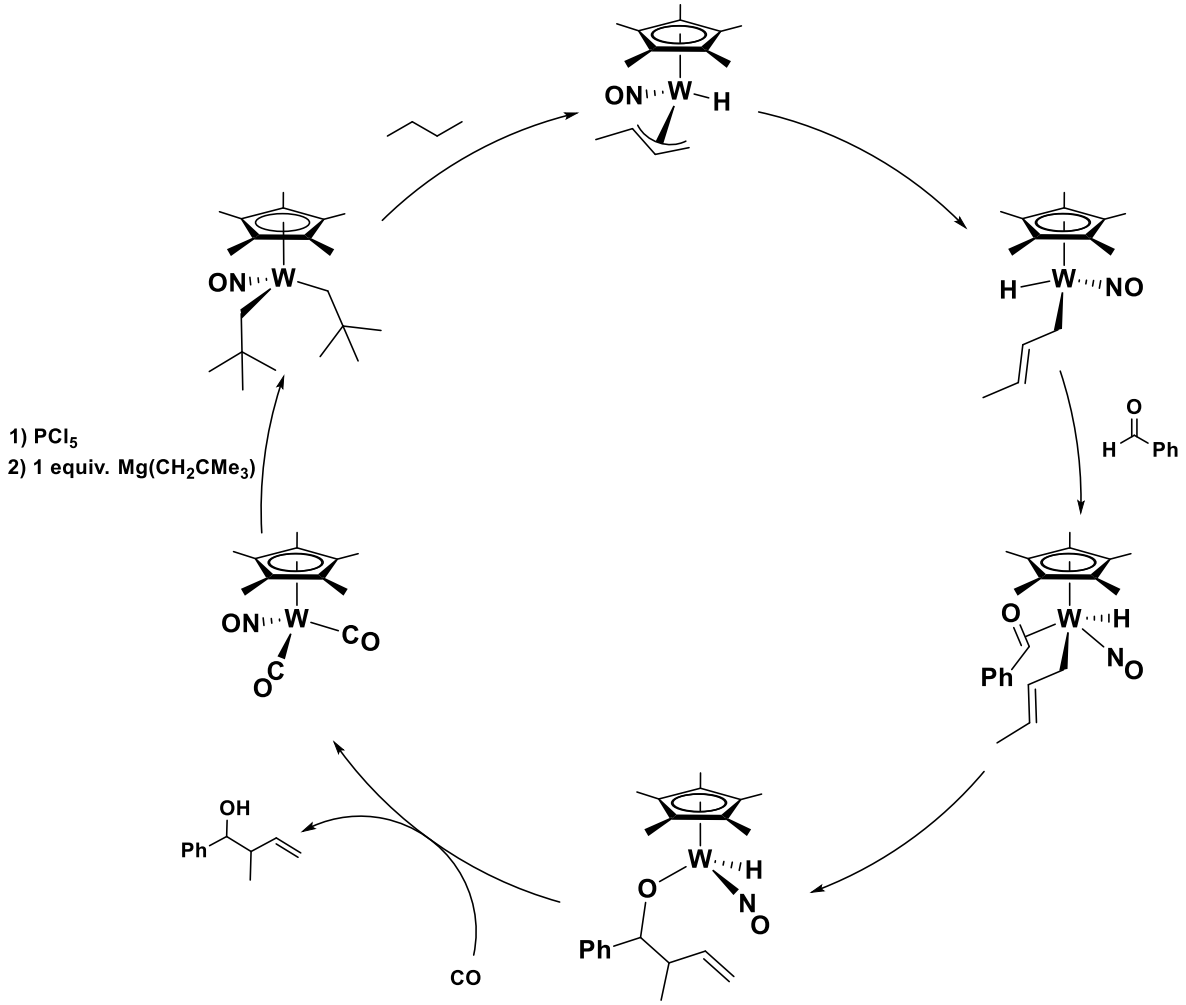

The C-C coupling reactions of (η^5-C_5Me_5)W(NO)(H)(η^3-allyl) complexes with phenylacetylene also represent a new method of functionalization of *n*-alkanes. Analysis of the products formed during the reaction of (η^5-C_5Me_5)W(NO)(H)(η^3-CH_2CHCMe_2) with phenylacetylene provides evidence of incorporation of the phenylacetylene molecules into the metal's coordination sphere. Nevertheless, the exact atom connectivity in the resulting organometallic products is difficult to determine based on the spectroscopic techniques utilized.

The solid-state molecular structures of both isolable organometallic products **5.1** and **5.2** would be essential to gain an understanding of this transformation. To date, numerous attempts to obtain this information have been unsuccessful. The possibility of facilitating the release of the coupled product via exposure to CO gas would also be an interesting methodology to explore in order to close a synthetic cycle in a manner similar to that outlined in Scheme 6.1.

References

1. Bergman, R. G. *Nature* **2007**, *446*, 391-393.

2. Labinger, J. A.; Bercaw, J. E. *Nature* **2002**, *417*, 507-514.

3. Crabtree, R. H. *Chem. Rev.* **1985**, *85*, 245-269.

4. Shilov, A. E.; Shul'pin, G. B. *Chem. Rev.* **1997**, *97*, 2879-2932.

5. Sattler, J. J. H. B.; Ruiz-Martinez, J.; Santillan-Jimenez, E.; Weckhuysen, B. M. *Chem. Rev.* **2014**, *114*, 10613-10653.

6. Torres Galvis, H. M.; de Jong, K. P. *ACS Catal.* **2013**, *3*, 2130-2149.

7. Janowicz, A. H.; Bergman, R. G. *J. Am. Chem. Soc.* **1982**, *104*, 352-354.

8. Hoyano, J. K.; Graham, W. A. G. *J. Am. Chem. Soc.* **1982**, *104*, 3723-3725.

9. Khan, M. S.; Haque, A.; Al-Suti, M. K.; Raithby, P. R. *J. Organomet. Chem.* **2015**, *793*, 114-133.

10. Crabtree, R. H.; Mihelcic, J. M.; Quirk, J. M. *J. Am. Chem. Soc.* **1979**, *101*, 7738-7740.

11. Haibach, M. C.; Kundu, S.; Brookhart, M.; Goldman, A. S. *Acc. Chem. Res.* **2012**, *45*, 947-958.

12. Gupta, M.; Hagen, C.; Flesher, R. J.; Kaska, W. C.; Jensen, C. M. *Chem. Commun.* **1996**, 2083-2084.

13. Kumar, A.; Zhou, T.; Emge, T. J.; Mironov, O.; Saxton, R. J.; Krogh-Jespersen, K.; Goldman, A. S. *J. Am. Chem. Soc.* **2015**, *137*, 9894-9911.

14. Ascoop, I.; Galvita, V. V.; Alexopoulos, K.; Reyniers, M.-F.; Van Der Voort, P.; Bliznuk, V.; Marin, G. B. *J. Catal.* **2016**, *335*, 1-10.

15. Schrock, R. R. *J. Am. Chem. Soc.* **1974**, *96*, 6796-6797.

16. Tran, E.; Legzdins, P. *J. Am. Chem. Soc.* **1997**, *119*, 5071-5072.

17. Bailey, B. C.; Fan, H.; Baum, E. W.; Huffman, J. C.; Baik, M.-H.; Mindiola, D. J. *J. Am. Chem. Soc.* **2005**, *127*, 16016-16017.

18. Bailey, B. C.; Fan, H.; Huffman, J. C.; Baik, M.-H.; Mindiola, D. J. *J. Am. Chem. Soc.* **2007**, *129*, 8781-8793.

19. Crestani, M. G.; Hickey, A. K.; Gao, X.; Pinter, B.; Cavaliere, V. N.; Ito, J.-I.; Chen, C.-H.; Mindiola, D. J. *J. Am. Chem. Soc.* **2013**, *135*, 14754-14767.

20. Kamitani, M.; Pinter, B.; Searles, K.; Crestani, M. G.; Hickey, A.; Manor, B. C.; Carroll, P. J.; Mindiola, D. J. *J. Am. Chem. Soc.* **2015**, *137*, 11872-11875.

21. Ng, S. H. K.; Adams, C. S.; Hayton, T. W.; Legzdins, P.; Patrick, B. O. *J. Am. Chem. Soc.* **2003**, *125*, 15210-15223.

22. Baillie, R. A.; Tran, T.; Lalonde, K. M.; Tsang, J. Y. K.; Thibault, M. E.; Patrick, B. O.; Legzdins, P. *Organometallics* **2012**, *31*, 1055-1067.

23. Tsang, J. Y. K.; Buschhaus, M. S. A.; Graham, P. M.; Semiao, C. J.; Semproni, S. P.; Kim, S. J.; Legzdins, P. *J. Am. Chem. Soc.* **2008**, *130*, 3652-3663.

24. Baillie, R. A.; Legzdins, P. *Coord. Chem. Rev.* **2016**, *309*, 1-20.

25. Fabulyak, D.; Baillie, R. A.; Patrick, B. O.; Legzdins, P.; Rosenfeld, D. C. *Inorg. Chem.* **2016**, *55*, 1883-1893.

26. Lefèvre, G. P.; Baillie, R. A.; Fabulyak, D.; Legzdins, P. *Organometallics* **2013**, *32*, 5561-5572.

27. Adams, C. S.; Legzdins, P.; Tran, E. *J. Am. Chem. Soc.* **2001**, *123*, 612-624.

28. Chin, T. T.; Hoyano, J. K.; Legzdins, P.; Malito, J. T.; Arnold, T.; Swanson, B. I. Dicarbonyl(η5-Cyclopentadienyl)Nitrosyl Complexes of Chromium, Molybdenum, and Tungsten. In *Inorganic Syntheses*, John Wiley & Sons, Inc.: 1990; pp 196-198.

29. Dryden, N. H.; Legzdins, P.; Einstein, F. W. B.; Jones, R. H., *Can. J. Chem.* **1988**, *66*, 2100-2103.

30. Dryden, N. H.; Legzdins, P.; Batchelor, R. J.; Einstein, F. W. B. *Organometallics* **1991**, *10*, 2077-2081.

31. Baillie, R. A.; Holmes, A. S.; Lefèvre, G. P.; Patrick, B. O.; Shree, M. V.; Wakeham, R. J.; Legzdins, P.; Rosenfeld, D. C. *Inorg. Chem.* **2015**, *54*, 5915-5929.

32. Ng, S. H. K.; Adams, C. S.; Legzdins, P. *J. Am. Chem. Soc.* **2002**, *124*, 9380-9381.

33. Doskocz, M.; Malinowska, B.; Młynarz, P.; Lejczak, B.; Kafarski, P. *Tetrahedron Lett.* **2010**, *51*, 3406-3411.

34. Armarego, W. L. F.; Chai, C. C. L. *Purification of Laboratory Chemicals*. 5 ed.; Elsevier: Amsterdam, 2003.

35. Pamplin, C. B.; Legzdins, P. *Acc. Chem. Res.* **2003**, *36*, 223-233.

36. Debad, J. D.; Legzdins, P.; Rettig, S. J.; Veltheer, J. E. *Organometallics* **1993**, *12*, 2714-2725.

37. Altomare, A.; Cascarano, G.; Giacovazzo, C.; Guagliardi, A. *J. Appl. Crystallogr.* **1993**, *26*, 343-350.

38. Altomare, A.; Burla, M. C.; Camalli, M.; Cascarano, G. L.; Giacovazzo, C.; Guagliardi, A.; Moliterni, A. G. G.; Polidori, G.; Spagna, R. *J. Appl. Crystallogr.* **1999**, *32*, 115-119.

39. Cromer, D. T.; Waber, J. T. *International Tables for X-ray Crystallography*. The Kynoch Press: Birmingham, England. 1974; Vol. IV, Table 2.2A.

40. Ibers, J. A.; Hamilton, W. C. *Acta Crystallogr.* **1964**, *17*, 781-782.

41. Creagh, D. C.; McAuley, W. J. *International Tables for Crystallography*. A. J. C. Wilson ed.; Kluwer Academic Publishers: Boston, 1992; Vol. C., Table 4.2.6.8.

42. Creagh, D. C.; Hubbell, J. H. *International Tables for Crystallography*. A. J. C. Wilson ed.; Kluwer Academic Publishers: Boston, 1992; Vol. C., Table 4.2.4.3.

43. XL: Sheldrick, G. M. *Acta Crystallogr.* **2015**, *71*, 3-8.

44. OLEX2-V1.2.6: Dolomanov O. V.; Bourhis L. J.; Gildea R. J.; Howard J. A. K.; Puschmann H. *J. Appl. Cryst.* **2009**, *42*, 339-341.

45. Baillie, R. A.; Lefèvre, G. P.; Wakeham, R. J.; Holmes, A. S.; Legzdins, P. *Organometallics* **2015**, *34*, 4085-4092.

46. Baillie, R. A.; Wakeham, R. J.; Lefèvre, G. P.; Béthegnies, A.; Patrick, B. O.; Legzdins, P.; Rosenfeld, D. C. *Organometallics* **2015**, *34*, 3428-3441.

47. Blackmore, I. J.; Semiao, C. J.; Buschhaus, M. S. A.; Patrick, B. O.; Legzdins, P. *Organometallics* **2007**, *26*, 4881-4889.

48. Fabulyak, D.; Handford, R. C.; Holmes, A. S.; Levesque, T. M.; Wakeham, R. J.; Patrick, B. O.; Legzdins, P.; Rosenfeld, D. C. *Inorg. Chem.* **2017**, *56*, 573-582.

49. Burkey, D. J.; Debad, J. D.; Legzdins, P. *J. Am. Chem. Soc.* **1997**, *119*, 1139-1140.

50. Fabulyak, D., *The Beneficial Kinetic Effect of the The η^5-$C_5H_4^{i\text{-}}$Pr Ligand on the C-H Activation Chemistry Inititated by CpW(NO)(η^3-allyl)(alkyl) and CpW(NO)(alkyl)$_2$ Complexes*. Chem 449 Undergraduate Thesis Project, The University of British Columbia, Vancouver. **2014**.

51. Legzdins, P.; Phillips, E. C.; Sanchez, L. *Organometallics* **1989**, *8*, 940-949.

52. Shree, M. V.; Fabulyak, D.; Baillie, R. A.; Lefèvre, G. P.; Béthegnies, A.; Dettelbach, K.; Patrick, B. O.; Legzdins, P.; Rosenfeld, D. C. *Organometallics* **2017**. (Manuscript submitted for publication)

53. Legzdins, P.; Martin, D. T. *Inorg. Chem.* **1979**, *18*, 1250-1254.

54. Welch, K. D.; Harrison, D. P.; Lis, E. C.; Liu, W.; Salomon, R. J.; Harman, W. D.; Myers, W. H. *Organometallics* **2007**, *26*, 2791-2794.

55. Renkema, K. B.; Kissin, Y. V.; Goldman, A. S. *J. Am. Chem. Soc.* **2003**, *125*, 7770-7771.

56. See Appendix Figure A.1.

57. See Appendix Figure A.2.

58. See Appendix Figure A.3.

59. See Appendix Figure A.4.

60. See Appendix Figure A.5.

61. See Appendix Figure A.6.

62. See Appendix Figure A.7.

63. See Appendix Figure A.8.

64. See Appendix Figure A.9.

65. See Appendix Figure A.10.

66. Zhao, L.-M.; Wan, L.-J.; Jin, H.-S.; Zhang, S.-Q. *Eur. J. Org. Chem.* **2012**, 2579-2584.

67. Ardizzoia, G. A.; Brenna, S.; Cenini, S.; LaMonica, G.; Masciocchi, N.; Maspero, A. *J. Mol. Catal. A: Chem.* **2003**, *204-205*, 333-340.

68. Hilt, G.; Vogler, T.; Hess, W.; Galbiati, F. *Chem. Commun.* **2005**, 1474-1475.

69. See Appendix Figure B.2.

70. Shibahara, F.; Bower, J. F.; Krische, M. J. *J. Am. Chem. Soc.* **2008,** *130*, 6338-6339.

71. See Appendix Figure B.1.

72. Tokuda, M.; Satoh, S.; Suginome, H. *J. Org. Chem.* **1989**, *54*, 5608-5613.

Appendices

Appendix A Supplementary Materials for Chapter 4

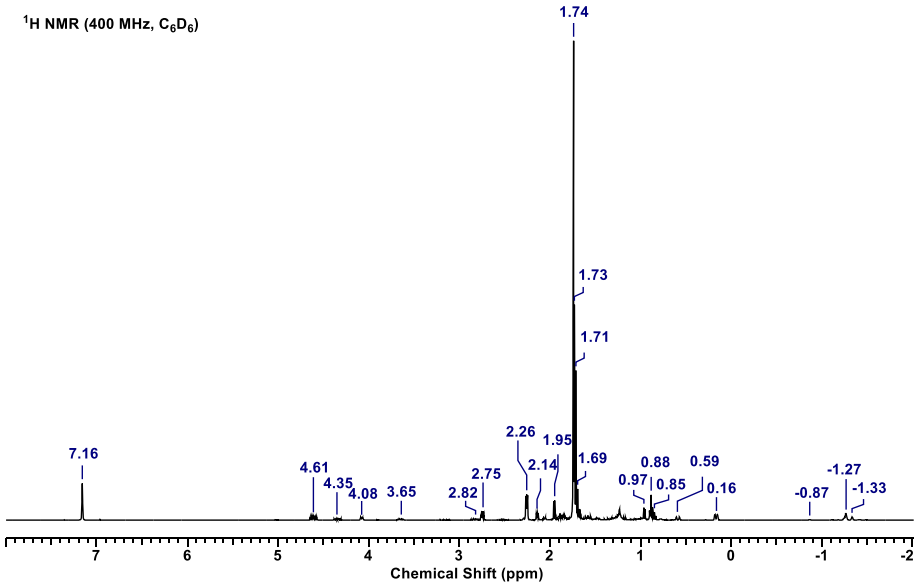

Figure A.1. The ^{1}H NMR spectrum of (η^5-C_5Me_5)W(NO)(H)(η^3-C_4H_7) in C_6D_6 (400 MHz).

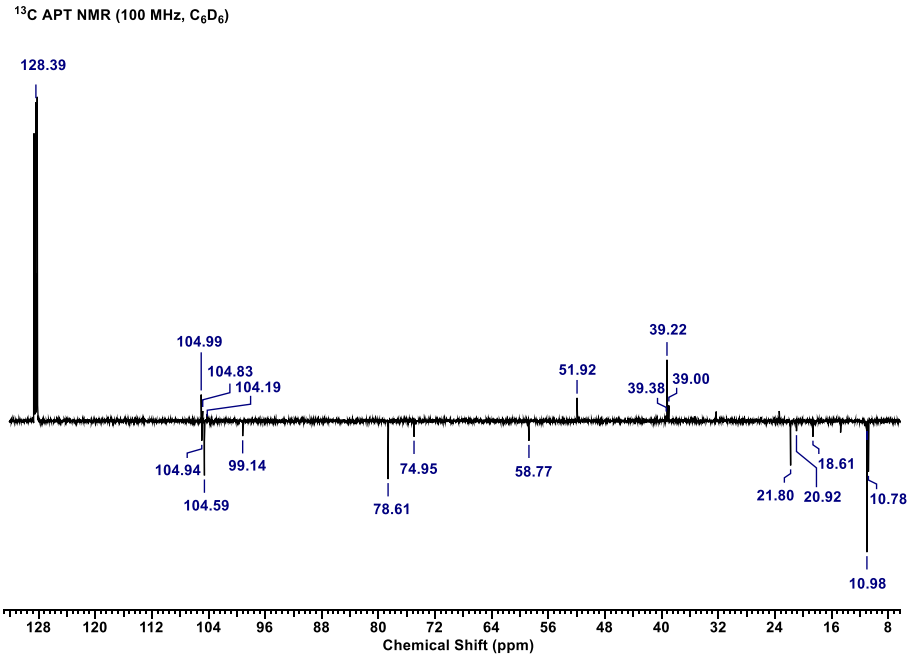

Figure A.2. The ^{13}C APT NMR spectrum of (η^5-C_5Me_5)W(NO)(H)(η^3-C_4H_7) in C_6D_6 (100 MHz)**.**

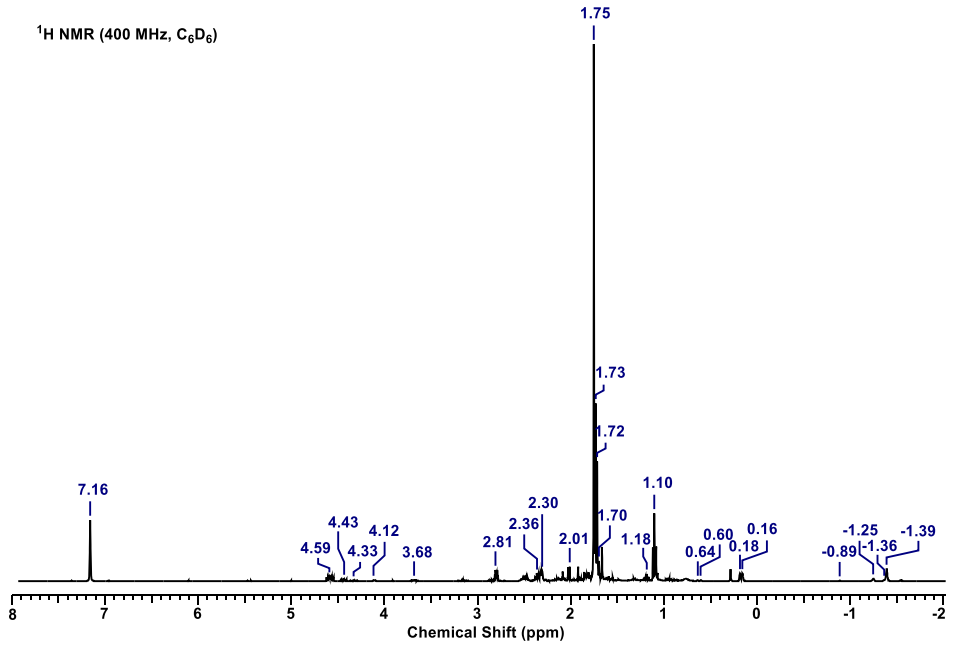

Figure A.3. The ^{1}H NMR spectrum of (η^5-C_5Me_5)W(NO)(H)(η^3-C_5H_9) in C_6D_6 (400 MHz).

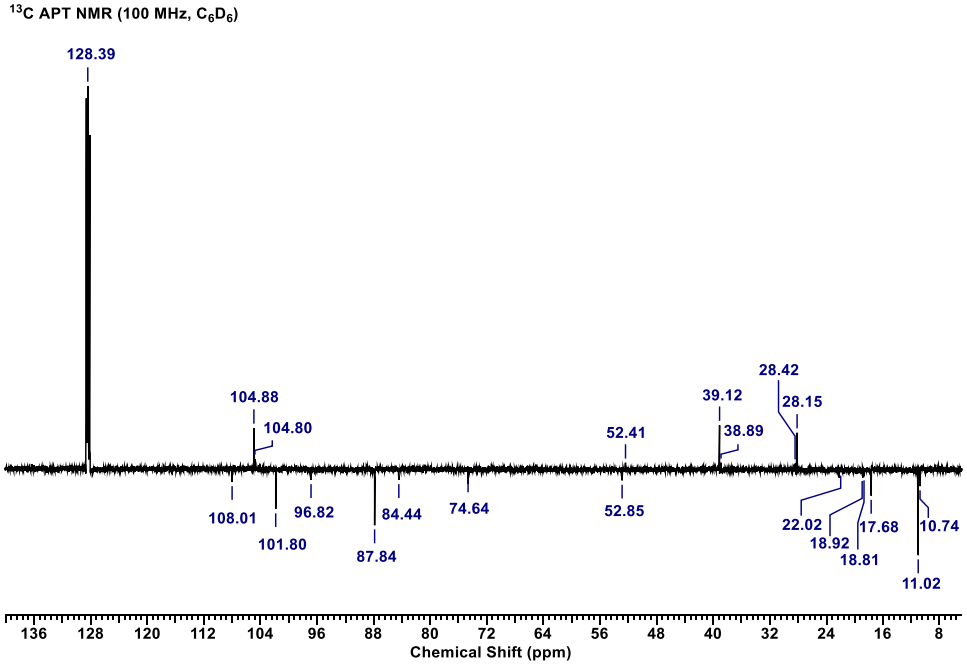

Figure A.4. The ^{13}C APT NMR spectrum of (η^5-C_5Me_5)W(NO)(H)(η^3-C_5H_9) in C_6D_6 (100 MHz).

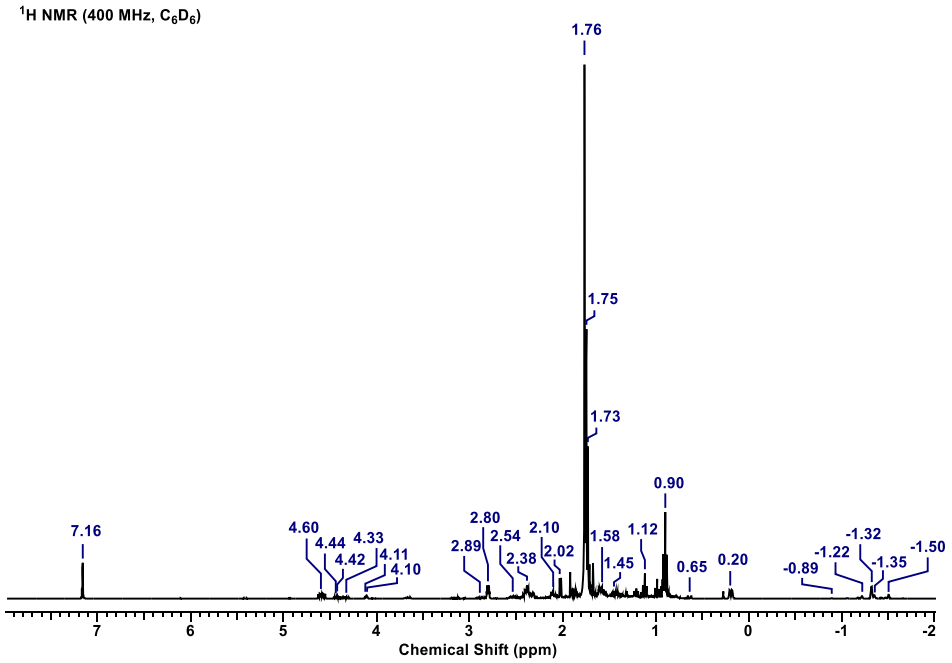

Figure A.5. The ^{1}H NMR spectrum of $(\eta^5\text{-}C_5Me_5)W(NO)(H)(\eta^3\text{-}C_6H_{11})$ in C_6D_6 (400 MHz).

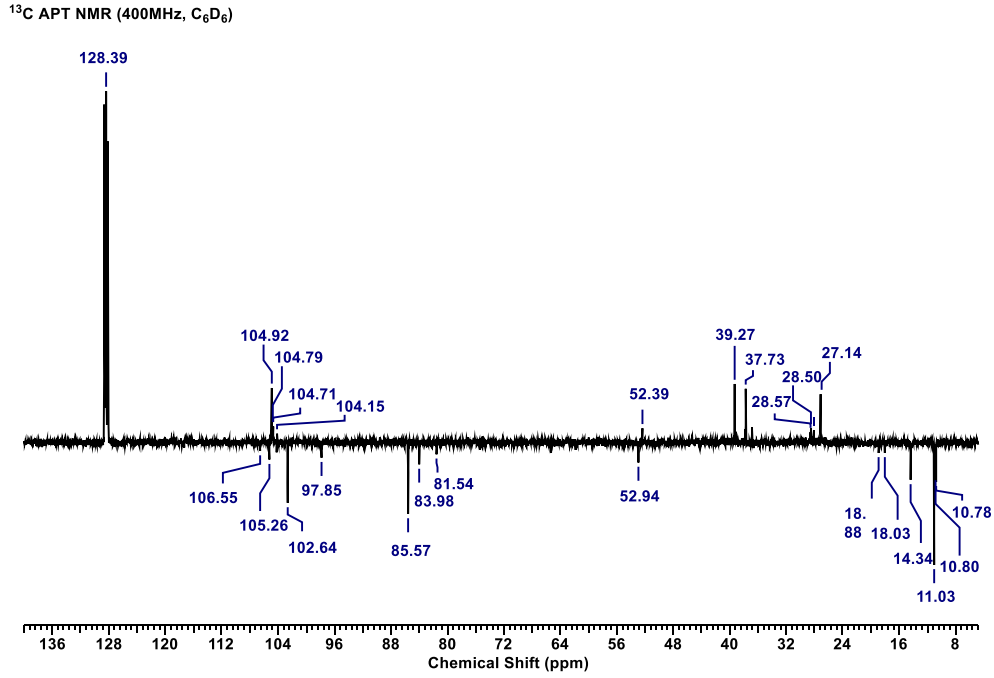

Figure A.6. The ^{13}C APT NMR spectrum of $(\eta^5\text{-}C_5Me_5)W(NO)(H)(\eta^3\text{-}C_6H_{11})$ in C_6D_6 (100 MHz).

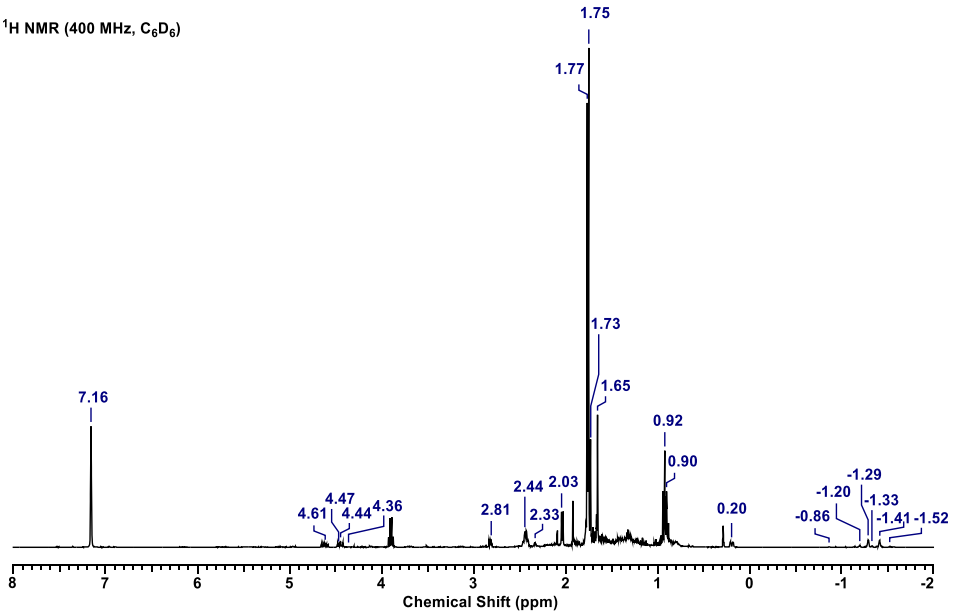

Figure A.7. The ^{1}H NMR spectrum of $(\eta^5\text{-}C_5Me_5)W(NO)(H)(\eta^3\text{-}C_7H_{13})$ in C_6D_6 (400 MHz).

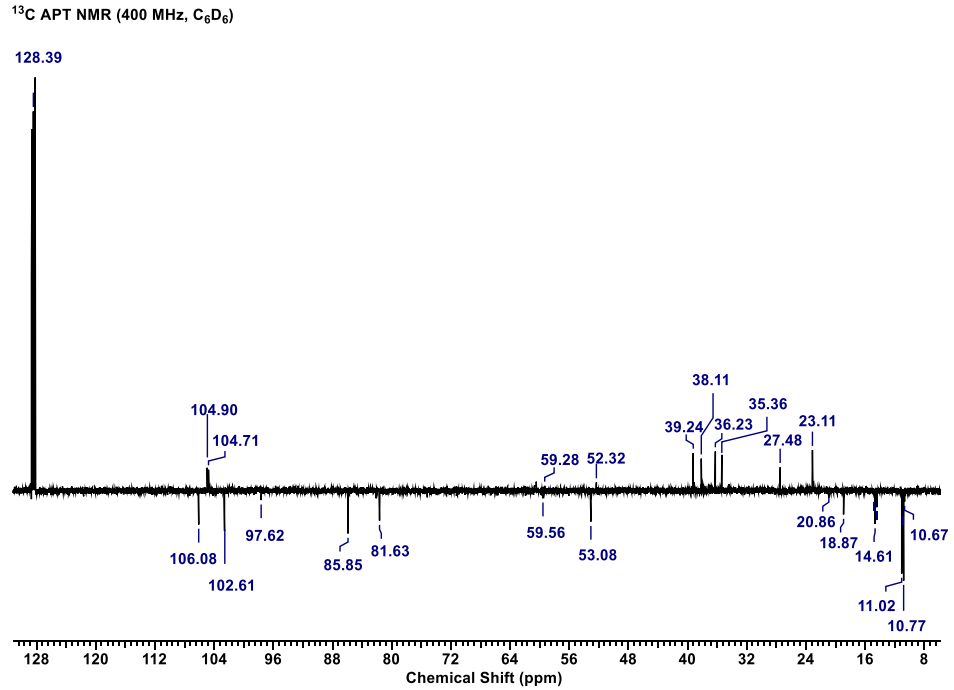

Figure A.8. The ^{13}C APT NMR spectrum of $(\eta^5\text{-}C_5Me_5)W(NO)(H)(\eta^3\text{-}C_7H_{13})$ in C_6D_6 (100 MHz).

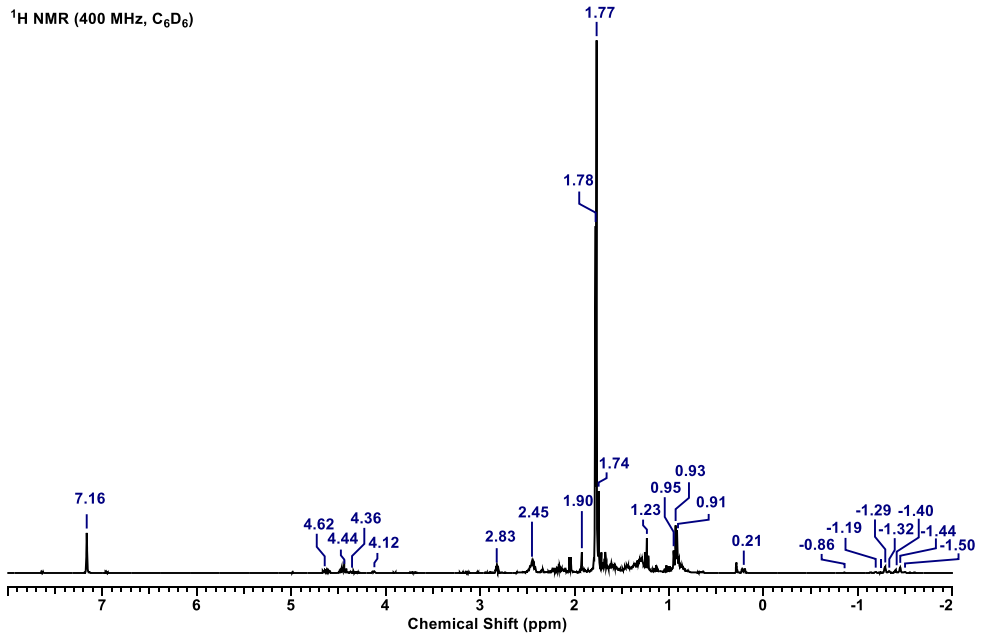

Figure A.9. The ^{1}H NMR spectrum of $(\eta^5\text{-}C_5Me_5)W(NO)(H)(\eta^3\text{-}C_8H_{15})$ in C_6D_6 (400 MHz).

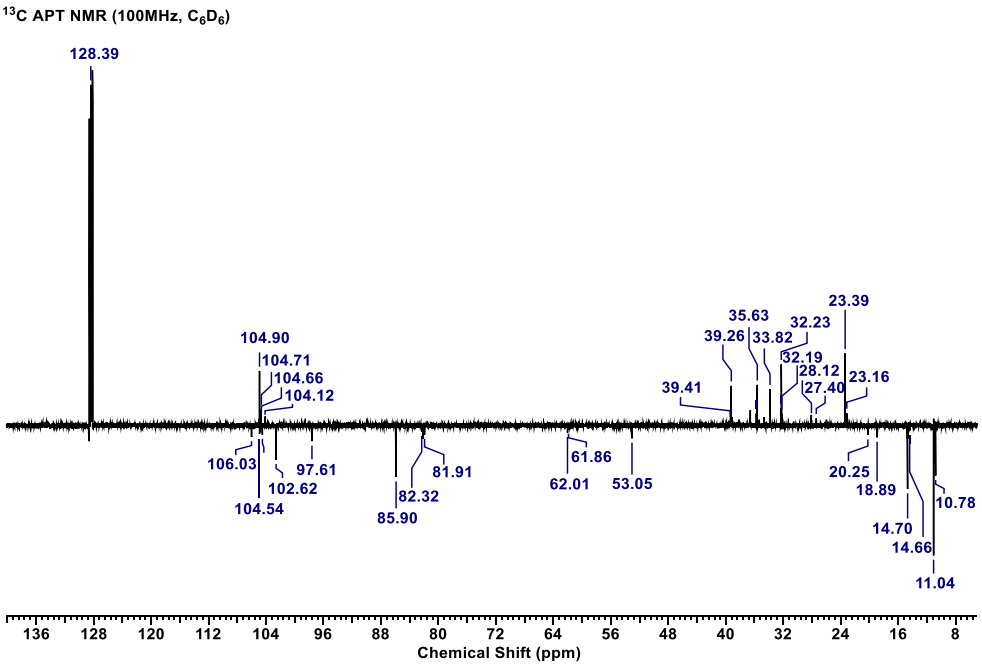

Figure A.10. The ^{13}C APT NMR spectrum of $(\eta^5\text{-}C_5Me_5)W(NO)(H)(\eta^3\text{-}C_8H_{15})$ in C_6D_6 (100 MHz).

Appendix B Supplementary Materials for Chapter 5

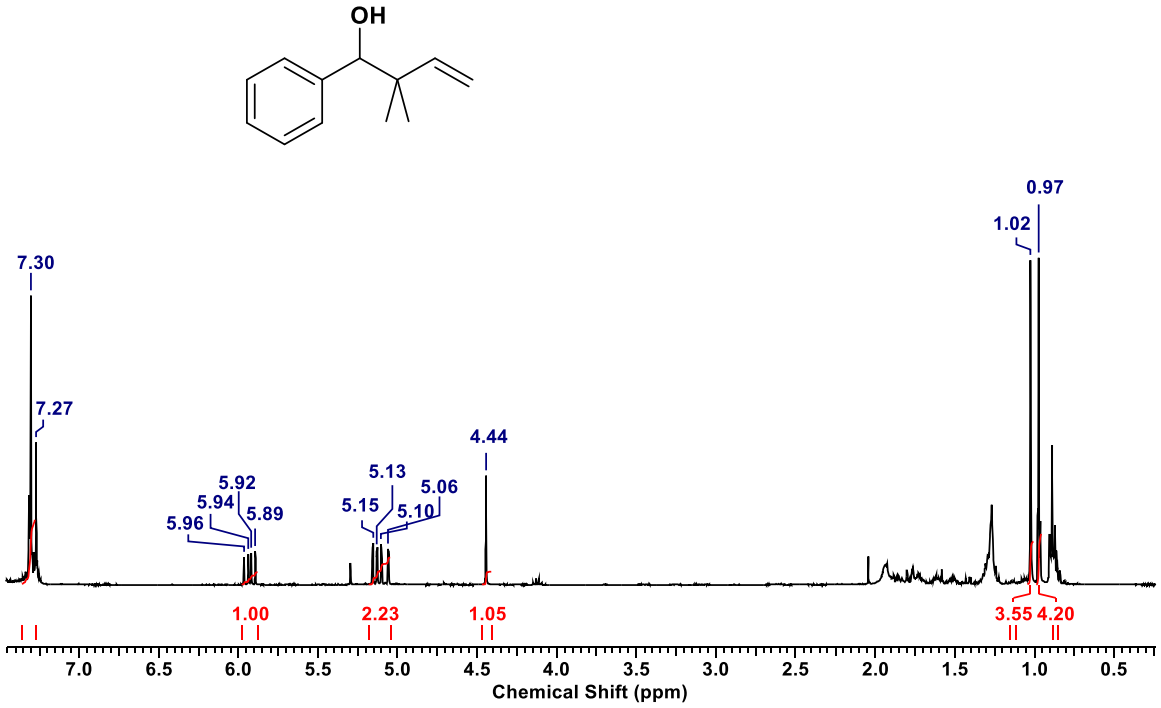

Figure B.1. The ^{1}H NMR Spectrum of 2,2-dimethyl-1-phenylbut-3-en-1-ol in $CDCl_3$ (400 Hz).

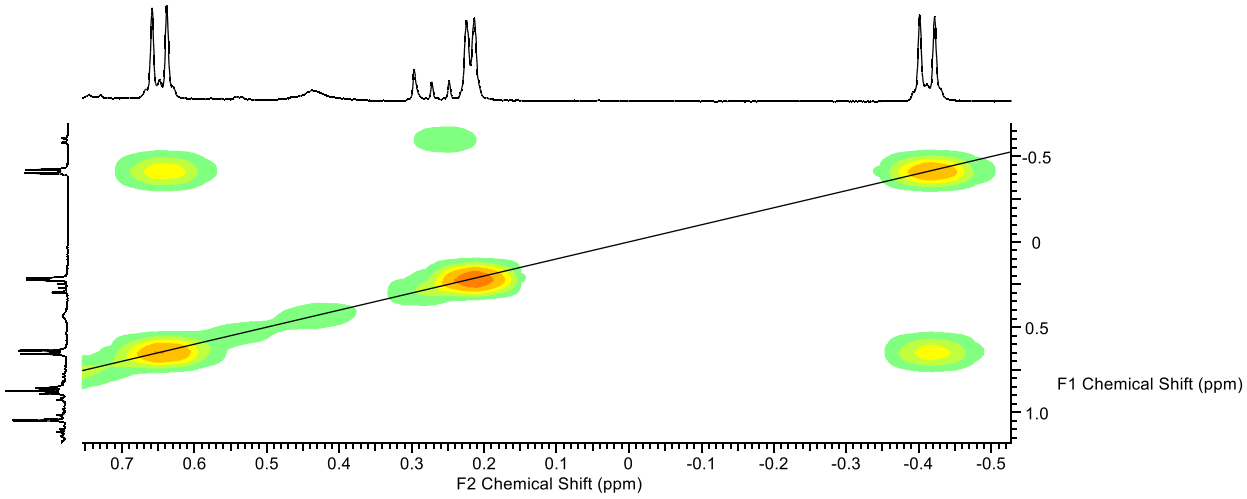

Figure B.2. The $\{^{1}H/^{1}H\}$ COSY NMR (C_6D_6, 400 MHz) spectrum of **5.2** showing a correlation between two hydride ligands.